# Development of New Fluorogenic OligoDNA Probes Utilizing Silylated Fluorescent Material

**THESIS**

*Submitted to Gunma University*

*for the Degree of*

***Doctor of Philosophy in Engineering***

**2015**

Student ID: 12802171

**Jakir Ahmed Chowdhury**

Division of Molecular Science

Graduate School of Science and Technology

Gunma University

Japan

# Contents


## Chapter 1
**General Introduction** 1

1.1 Fundamentals of nucleic acid 2
1.2 Hybridization probe 4
1.3 Principle of fluorescence generation 8
1.4 Fluorescence signal transduction 9
1.5 Fluorescence resonance energy transfer 10
1.6 Fluorescence nucleic acid hybridization probes 10
1.6.1 Adjacent probes or Light Cycler™ hybridization probe 11
1.6.2 *TaqMan*® Probe or 5'-Nuclease probes 13
1.6.3 Strand-displacement probes or Yin-Yang probe 14
1.6.4 Molecular beacon probes 15
1.7 Fundamentals of molecular beacon and its spectroscopic principles 17
1.7.1 Loop sequence 17
1.7.2 Stem sequence 17
1.7.3 Fluorophore 18
1.7.4 Quencher 23
1.8 Applications of molecular beacon probes 24
1.8.1 Biosensor and biochip development 24
1.8.2 Genetic analysis 25
1.8.3 Real-time monitoring of DNA/RNA amplification during PCR 26
1.8.4 In-vivo imaging of cancer cells 26
1.8.5 In-vivo RNA detection 28
1.9 Problems of molecular beacon probes and recent solution 29
1.9.1 Signal-to-noise (S/N) ratio 29
1.9.2 Loop and stem nucleotides 32
1.9.3 Complexity of living environments 34
References

# Chapter 2

## Synthesis of Novel Stem-Loop type Molecular Beacon Probes Possessing Polyamine-connected Deoxyuridine and Silylated Pyrene and Its Fluorescence Properties


2.1 Abstract 46

2.2 Introduction 46

2.3 Results and Discussion 52

2.3.1 Synthesis of [1-(Pyrenyl)dimethylsilylmethyl]-(2-cyanoethyl) -*N*,*N*-diisopropylphosphoramidite 52

2.3.2 Synthesis of 5´-*O*-(4,4´-Dimethoxytrityl)-5-[*N*-[2-*N*,*N*-bis(2-trifluoro-acetamidethyl) amino]ethyl]carbamoylmethyl-2´-deoxyuridine-3´-*O*-yl(2-cyanoethyl)-*N*,*N*-diisopropylphosphoramidite 54

2.3.3 Synthesis of modified oligoDNA possessing polyamine-connected deoxyuridine and silylated pyrene 56

2.3.4 Duplex forming ability of new MB probes 61

2.3.5 Fluorescence properties of new molecular beacon probes 62

2.3.6 The effect of mismatch in the target DNA to the fluorescence signal of the probe 67

2.3.7 Thermal stability of new molecular beacon probes 68

2.4 Conclusion 69

2.5 Experimental 70

2.5.1 General Information 70

2.5.2 Synthesis of 1-(Chloromethyldimethylsilyl) pyrene 71

2.5.3 Synthesis of 1-(Acetoxymethyldimethylsilyl) pyrene 72

2.5.4 Synthesis of 1-(Hydroxymethyldimethylsilyl) pyrene 73

2.5.5 Synthesis of [1-(Pyrenyl)dimethylsilylmethyl]-(2-cyanoethyl)-N,N-diisopropylphosphoramidite 74

2.5.6 Synthesis of 3´, 5´-*O*-Diacetyl-5-methoxycarbonylmethyl-2´ -bromo-2´-deoxyuridine 75

2.5.7 Synthesis of 3´, 5´-*O*-Diacetyl-5-methoxycarbonylmethyl-2´ -deoxyuridine 77

2.5.8 Synthesis of 5-[*N*-[*N*,*N*-Bis(2-trifluoroacetamidethyl)amino]ethyl] -carbamoylmethyl-2´-deoxyuridine 77

2.5.9 Synthesis of 5´-*O*-(4,4´-Dimethoxytrityl)-5-[*N*-[2-*N*,*N*-bis(2-trifluoro-acetamidethyl)amino]ethyl]carbamoylmethyl-2´-deoxyuridine 79
2.5.10 Synthesis of 5´-*O*-(4,4´-Dimethoxytrityl)-5-[*N*-[2-*N*,*N*-bis(2-trifluoroacetamid-ethyl)amino]ethyl]carbamoylmethyl-2´-deoxyuridine -3´-*O*-yl(2-cyanoethyl)-*N*,*N*-diisopropylphosphoramidite 80
2.5.11 Oligonucleotides Synthesis 81
2.5.12 Melting Temperature Analysis 81
2.5.13 Fluorescence Measurements 82
References

# Chapter 3

## Synthesis and Fluorescence Properties of Pseudo-Dumbbell Type of Molecular Beacon Probes bearing a Modified Deoxyuridine and a Silylated Pyrene as a Fluorophore

3.1 Abstract 87
3.2 Introduction 87
3.3 Results and Discussion 92
3.3.1 Synthesis of [1-(Pyrenyl)dimethylsilylmethyl]-(2-cyanoethyl) -N,N-diisopropylphosphoramidite 92
3.3.2 Synthesis of 5-methoxycarbamoylmethyl-3´, 5´-di-*O*-acetyl-2´-bromodeoxyuridine 92
3.3.3 Synthesis of 1-(2-Aminoethylamino) anthraquinone 93
3.3.4 Synthesis of 5-hydroxycarbamoyl methyl-5´-*O*-DMTr -2´-deoxyuridine 93
3.3.5 Introduction of anthraquinone moiety to the C-5 position of deoxyuridine 94
3.3.6 Synthesis of modified oligoDNA possessing C-5 modified deoxyuridine and silylated pyrene 96
3.3.7 Duplex forming ability of new MB probes 107
3.3.8 Fluorescence properties of the probes 109
3.3.9 The effect of mismatch in the target DNA to the fluorescence signal of the probes 115
3.3.10 The effect of deoxyinosine to the fluorescence signal of Probe 4 118
3.3.11 Hybridization abilities of molecular beacon type probe 119

3.4 Conclusion 122
3.5 Experimental 123
3.5.1 General Information 123
3.5.2 Synthesis of 1-(2-Aminoethylamino)anthraquinone 123
3.5.3 Synthesis of 5-Methoxycarbonylmethyl-2´-deoxyuridine (17) 124
3.5.4 Synthesis of 5-Methoxycarbonyl methyl-5´-*O*-DMTr-2´-deoxyuridine 125
3.5.5 Synthesis of 5-Carboxy methyl-5´-*O*-DMTr-2´-deoxyuridine 126
3.5.6 Synthesis of 5´-*O*-(4,4´-dimethoxytrityl)-5-[*N*-[2-[*N*-(anthraquinon -1-yl)amino]ethyl]carbamoylmethyl]-2´-deoxyuridine 127
3.5.7 Synthesis of 5´-*O*-(4,4´-dimethoxytrityl)-5-[*N*-[2-[*N*-(anthraquinon-1 -yl)amino]ethyl]carbamoylmethyl]-2´-deoxyuridine-3´-*O*-yl(2 -cyanoethyl)-*N*,*N*-diisopropylphosphoramidite 128
3.5.8 Oligonucleotides Synthesis 129
2.5.12 Melting Temperature Analysis 129
2.5.13 Fluorescence Measurements 130
References

# Chapter 1

# General Introduction

## 1.1 Fundamentals of Nucleic Acid

Deoxyribonucleic acid, DNA is one of the most important molecules for every living life on earth. DNA was first identified and isolated as a distinct acidic substance stored inside nuclei in 1869 by Friedrich Miescher [1]. Thereafter, it took another 70 years to demonstrate [2] that this DNA molecule carried genetic information. Another important step in the DNA study was made in 1953 by Watson and Crick [3]. They proposed a three-dimensional, right handed double helical B-DNA model of the DNA structure. A further advanced experimental studies revealed that DNA has other double-helical forms such as A-DNA and also many other three-dimensional firms, including triple [4] and quadruple helices [5-10]. On the other hand, ribonucleic acid, RNA which is closely related to DNA and also biologically very important molecule only forms A-type double helical structure.

The primary structures of DNA and RNA consist of phosphodiester-linked nucleotide units that contain a 2′-deoxy–D-ribose or D-ribose sugar ring in DNA and RNA respectively and an aromatic nucleobases (Figure 1.1). The major bases are monocyclic pyrimidines or bicyclic purines. The major purines found in both DNA and RNA are adenine (A) and guanine (G). The major pyrimidines are cytosine (C), thymine (T) and uracil (U) in case of RNA. The resulting polynucleotide chain has a consistent 5′→3′ polarity with both a negatively charged sugar-phosphate backbone and an array relatively hydrophobic nucleobases, amphiphilic features which ultimately drive the assembly and maintenance of secondary and tertiary nucleic acid structures.

In nature, DNA does not usually exist as a single molecule, but instead as a pair of molecules that are held tightly together [3, 11]. These two long strands entwine like vines, in the shape

of a double helix. The nucleotide repeats contain both the segment of the backbone of the molecule, which holds the chain together, and a nucleobase, which interacts with the other DNA strand in the helix. A nucleobase linked to a sugar is called a nucleoside and a base linked to a sugar and one or more phosphate groups is called a nucleotide. A polymer comprising multiple linked nucleotides (as in DNA) is called a polynucleotide. The DNA double helix is stabilized primarily by two forces: hydrogen bonds between nucleobases in horizontal direction and base-stacking interactions among aromatic nucleobases in perpendicular direction [3].

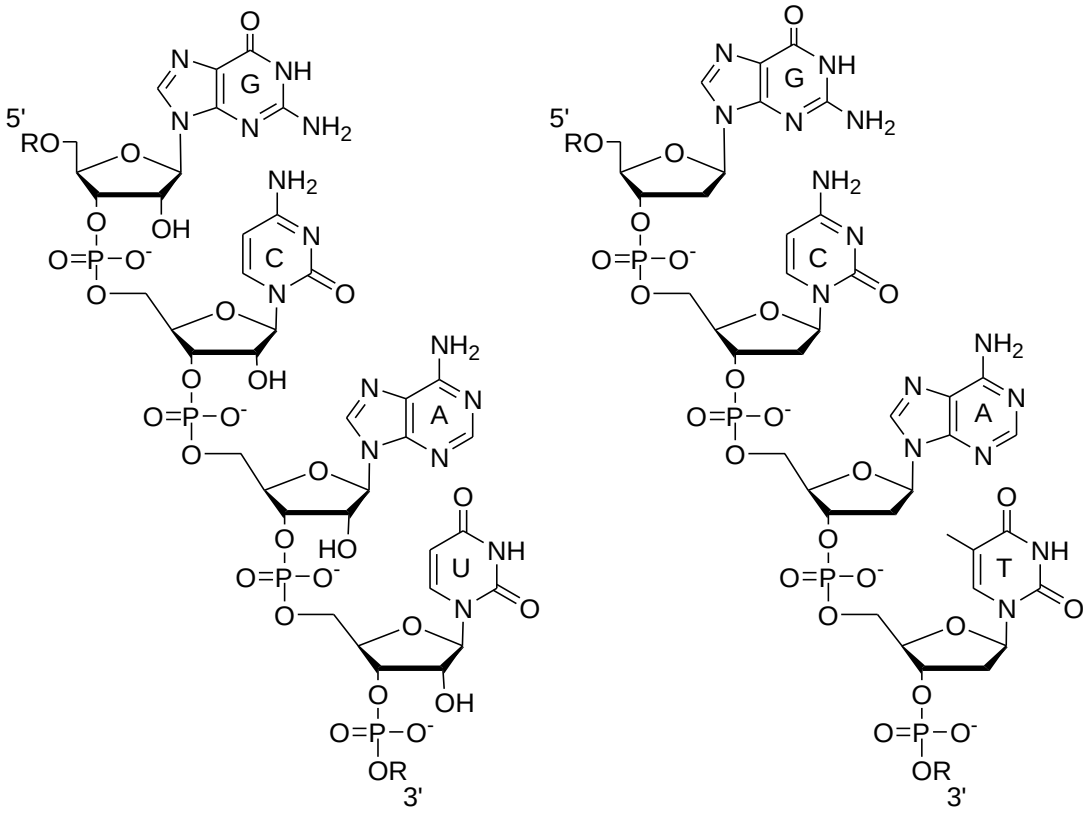


**Figure 1.1:** The primary structures of DNA and RNA

## 1.2 Hybridization Probe

A hybridization probe is a fragment of DNA or RNA of variable length (usually 15-100 bases long) which is used in DNA or RNA samples to detect the presence of specific sequences that are complementary to the sequence in the probe. The probe thereby hybridizes to single-stranded nucleic acid (DNA or RNA) whose base sequence allows probe-target base pairing due to complementarity between the probe and target. The probe-target base pairing usually occurs by its hydrogen-bonding capability where the probe itself hybridize to the target sequence. Protein probes interact with their specific target through a blend of forces such as hydrophobic, ionic and hydrogen bonding at only a few specific sites. Whereas, nucleic acid probes interact with their complements through hydrogen-bonding (Figure1.2), at tens, hundreds or thousands of sites, depending on the length of the hybrid [12]

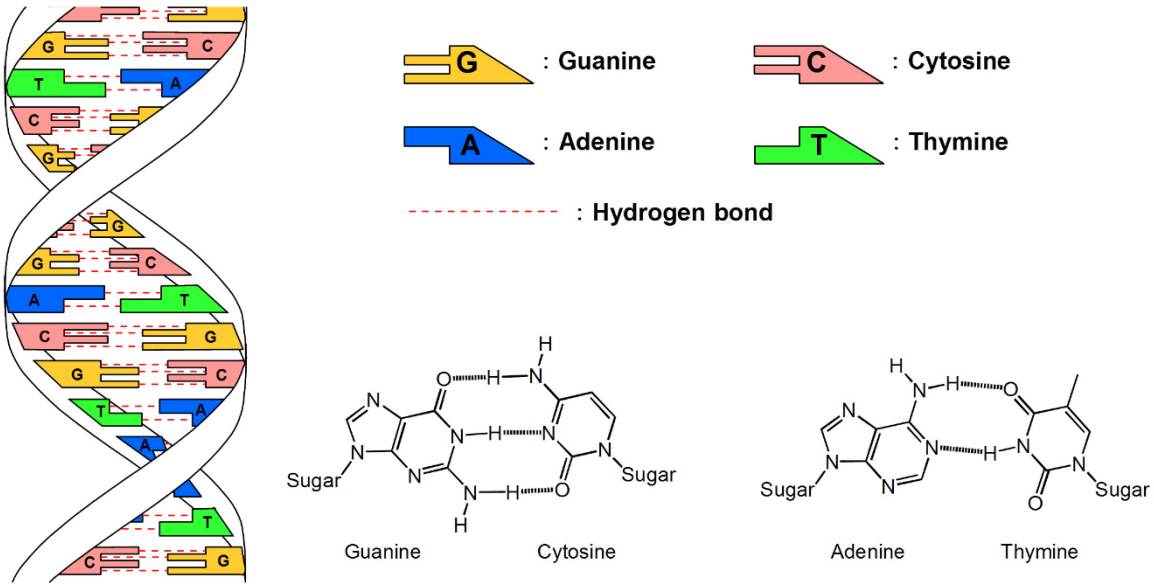


**Figure 1.2:** Sequence specificity of nucleic acid

The probe is tagged or labeled with a molecular marker of either radioactive or non-radioactive fluorescent molecules. The commonly used radioactive markers are $^{32}P$ [13-15] and non-radioactive marker digoxigenin [16-17]. The probes whose fluorescence signal changes upon hybridization with a target sequence is referred as fluorogenic hybridization probe [18]. In an electrochemical DNA hybridization detector, a short ssODN (a single-stranded DNA probe with 15–20 nucleotides long) is usually immobilized on a transducer (electrode) to create a DNA recognition element. The probe-modified electrode is then immersed into a solution of target DNA. When the target DNA contains a sequence that exactly matches that of the probe DNA, a hybrid duplex is formed at the electrode surface. In the absence of a complementarity between the probe and target, no duplex is formed. Hybrid formation is then translated into an electrical, analytically useful signal. Partial complementary binding of these DNAs may result, however, in a weak interaction that is more difficult to recognize.

Utilizing fluorescent dyes, meanwhile, several types of fluorogenic hybridization probes have been developed until date [19-26]. In general, we can divide them in two groups: dual-labeled and single-labeled probes.

The dual labeled probe utilizes an alteration of dye-dye interactions. The probe alone gives quenching effect by the close contact of the dye molecules. On the other hand, upon hybridization with a target sequence, the dyes are spatially separated which results in a significant fluorescence increase. These include either simplest linear probe or stem-loop structures probe (Figure 1.3). The fluorescence quenching in stem less dual labelled single stranded probe occurs by random probe coiling (Figure 1.4). A measurable change in

fluorescent intensity is accompanied by forming a duplex with the target. The energy transfer from the donor to the acceptor dye is the major mechanism of signal generation of

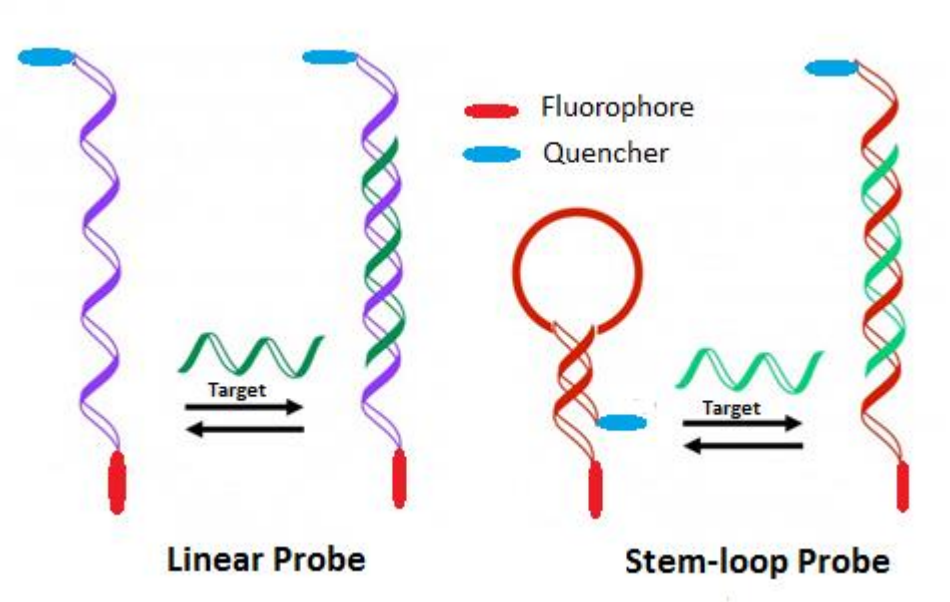


**Figure 1.3:** Schematic diagram of linear and stem-loop probe [cited from ref. 27]

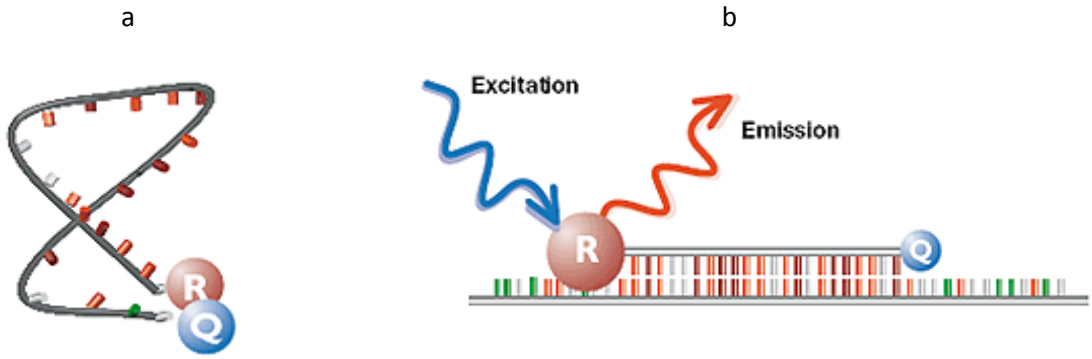


**Figure 1.4:** Dual labelled single stranded linear probe. **(a)** In absence of target, fluorescence quenching occur through random coiling of the probe **(b)** In presence of target, probe hybridize with its target and give an intense fluorescence signal. [cited from ref. 28]

this type of probe [19]. The donor dye is fluorescent, while the acceptor dye can be fluorescent [19] or non-fluorescent [20-21]. On the other hand, stem-loop type dual labeled probe has a sequence recognition region located in the loop and the stem has fluorescent dye and non-fluorescent dye which ensures quenching property by making a close contact of the dyes [29].

The single labeled probe utilizes the alteration of fluorescence efficiency of a single dye that takes place due to the hybridization event. This probe exploits the ability of the dyes to enhance fluorescence upon intercalation into double-stranded DNA. One example of such probe is hybeacon probes [22]. They are single-labeled oligonucleotides that increase their fluorescence upon hybridization. The inherent quenching ability of deoxyguanosine nucleotides has also been used to design single labeled probe formats (Figure 1.5) [23-26].

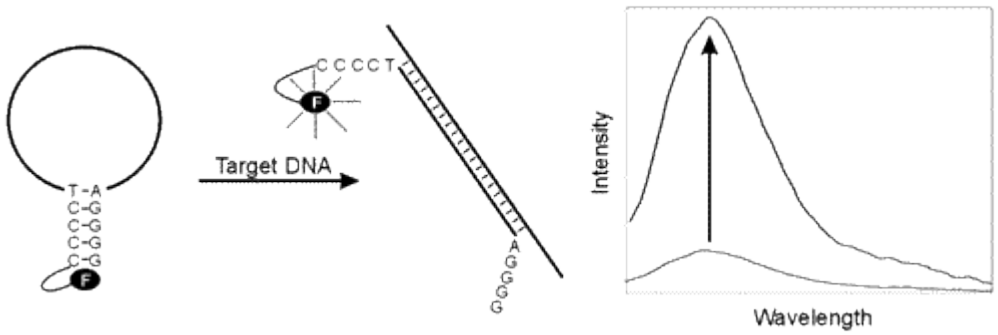


**Figure 1.5:** Schematic operation of singly labeled DNA-hairpins: The fluorophore is attached to the 5´-end of the oligonucleotide and quenched by guanosine residues in the complementary stem via photoinduced intramolecular electron transfer. (cited from ref. 26)

## 1.3 Principles of Fluorescence Generation [30]

In the last few years, there have been a tremendous growth in utilization of fluorescence in the field of biological sciences [31]. Fluorescence is a kind of luminescence which is resulted from the emission of light from a substance. This phenomenon is extensively used in biotechnology, medical diagnostic, DNA sequencing and other disciplines. The pattern of fluorescence emission is varied depending on the types of hybridization probes. It needs to have at least one fluorophore in the probes which has the capability to absorb energy from light and by transferring this energy internally emit this energy as light of a characteristic wavelength. A fluorophore is usually raised from its ground state to higher vibrational level of an excited singlet state by absorbing energy. Then, it loses some of its energy as heat and come back once again to a relatively stable lowest vibrational level of excited singlet state. Thereafter, it return to the ground state from this excited singlet state by the emission of light. This emitted light is usually termed as fluorescence. The process is depicted in the Figure 1.6.

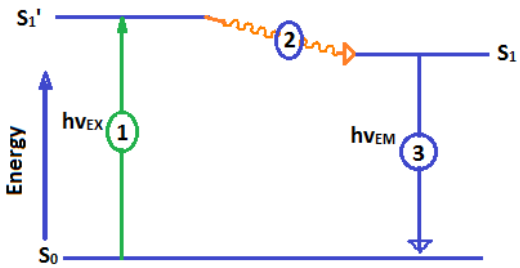


**Figure 1.6:** Different energy state of Jablonski diagram by absorbing energy and subsequent emission of fluorescence. 1, 2 and 3 express the stage of excitation, lifetime of excited state and fluorescence emission respectively [cited from ref. 31].

## 1.4 Fluorescence Signal Transduction

Different types of fluorescent dyes like pyerene, perylene, FAM, TET, HEX, Cy dyes, TMR, ROX, Texas red, JOE, Oregon green, Rhodamine, Coumarin and others are used to design fluorescent probes. In addition to fluorophore, some quencher molecules are also used in the fluorescent oligonucleotide probes like DDQ-I, DABCYL, Eclipse, Iowa Black RQ, BHQ-1 and others. In case of single labeled probes, the signal transduction occurs by binding with nucleic acids. Fluorescent properties change by dye-nucleotide interaction due to the photo induced electron transfer between them. Crockett *et al.* reported the quenching properties of fluorescein oligonucleotide by interaction with deoxyguanosine nucleotide [24]. The dynamical behavior of electron transfer reaction between guanosine containing oligonucleotides and the covalently bonded Oxazine dye is also reported [32]. On the other hand, the transduction process of dual-labeled probes depends on the fluorescence quenching, fluorescence resonance energy transfer (FRET) and monomer-excimer emission switching with fluorophore. Energy transfer, quenching and excimer formation depend on the design of the probes. These three processes are mainly distance dependent. An alteration of fluorescence properties resulted due to the structural rearrangement occurred under the presence of targets.

## 1.5 Fluorescence Resonance Energy Transfer

Fluorescence resonance energy transfer (FRET) is a dipole-dipole interaction that happen when two fluorophores come in close proximity and the emission spectrum of one overlaps with the excitation spectrum of others. The excitation of the acceptor fluorophore occurs due to the emission energy transfer from donor fluorophore [33, 34]. This is first described by Forster in the year of 1948 as Forster type energy transfer [35]. This non-radiative process is a process of energy transfer between a donor and acceptor molecule. This process is mainly a distance dependent energy transfer mechanism. Generally the donor molecule and acceptor molecule are covalently attached at different location of a probe. At the same time, it is also necessary to overlap the absorption of excited acceptor partially with the emission of donor. Acceptor may be a fluorescent or non-fluorescent molecule. The transferred energy is usually emitted as fluorescence in case of fluorescent acceptor. While it lost the absorbed energy as heat in case of a non-fluorescent acceptor.

## 1.6 Fluorescence Nucleic Acid Hybridization Probes

Fluorogenic nucleic acid hybridization probes are newly developed probe that generate a characteristics fluorescence signal upon hybridization with complementary target nucleic acid sequence [36]. This is a highly useful and selective probes for analysis of many bioanalytes [37]. With inclusion of potent and relatively low cost fluorescent labelling agent (Figure 1.7), it has become a very attractive research field because it has numerous applications in detection and visualization of target oligonucleotides. It is also utilized to detect non-nucleic acid analytes like protein, metal ion and other small molecules. Several fluorescent hybridization probes have been used in the detection of nucleic acid. A brief

discussion on different types of fluorescent hybridization probes are discussed in the following which are cited from SAE Marras - Fluorescent Energy Transfer Nucleic Acid Probes, 2006 [30].

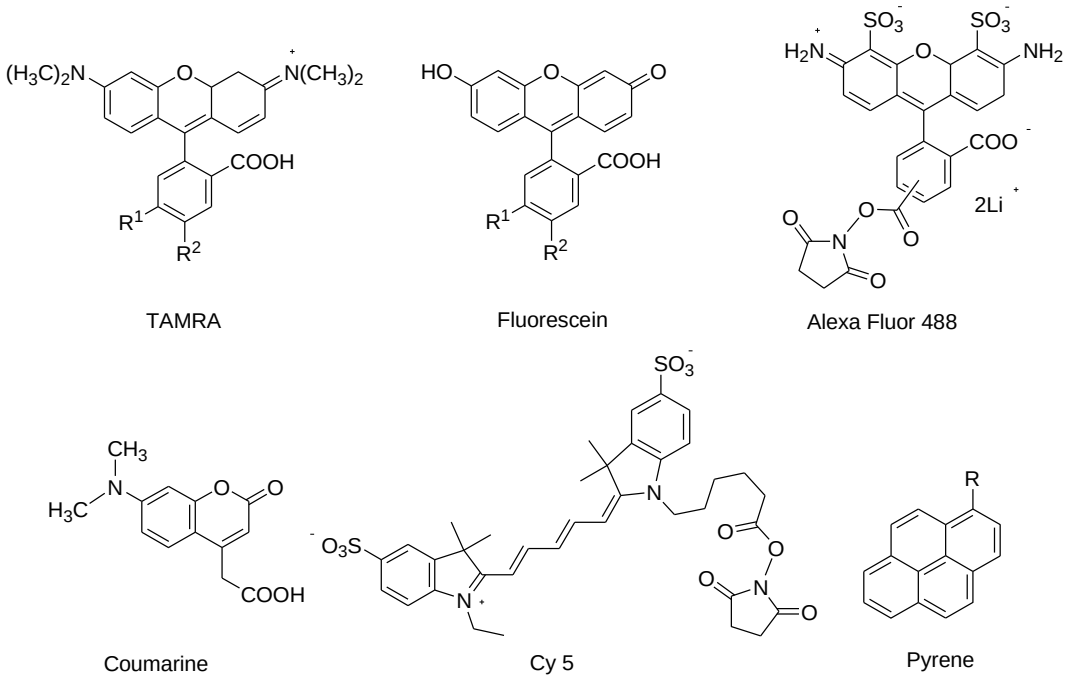


**Figure 1.7:** Frequently used fluorescent labelling agent for designing fluorogenic probes

### 1.6.1 *Adjacent probes or LightCycler™ hybridization probes*

Adjacent probe is a type of fluorescent hybridization probes that utilize two single stranded probes. One probe is labelled with a donor fluorophore molecule at one end of nucleic acid and the other is labeled with acceptor molecule at the other end. Usually the donor molecule is attached to the 3´-end, whereas, the acceptor molecule is attached to the 5´-end of the respective single stranded probe. There is no energy transfer between them while they stayed free condition in solution without target. However, these probes bind to the neighboring

sites on a target nucleic acid when they come in contact with their targets [38]. In the presence of target nucleic acid, the hybridization of the probe with target DNA is measured either by decreasing the donor fluorescence signal or by increasing the acceptor fluorescence signal through the fluorescence energy transfer from the donor to the acceptor. A schematic diagram of this kind of probes is shown in Figure 1.8.

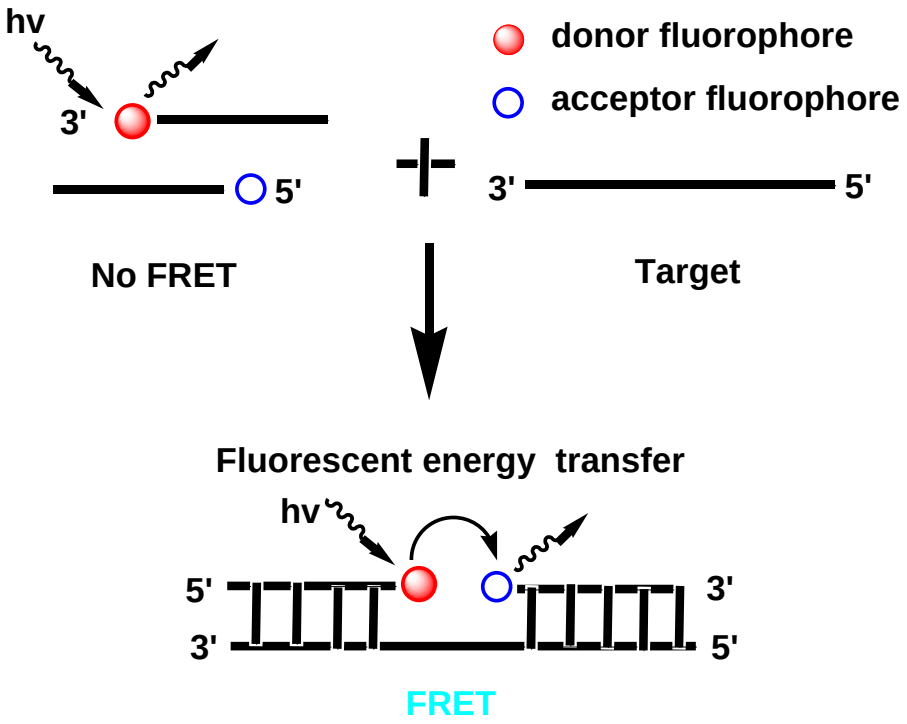


**Figure 1.8:** Schematic overview of energy transfer and fluorescence signal generation in adjacent probes.

### 1.6.2 *TaqMan® probe or 5´-Nuclease probes*

5´-Nuclease probe (Figure 1.9) is a single stranded hybridization probes simultaneously labelled with a fluorophore acts as the donor and a quencher acts as the acceptor molecules in one strand that utilizes the inherent endonucleolytic activity of *Taq* DNA polymerase to

generate a fluorescence signal [19]. The *Taqman* probes and the primers, designed to hybridize within the target DNA sequences, are introduced into a PCR assay. The fluorescence signal of the fluorophore is quenched by the quencher molecule via FRET. Annealing of the probes start synthesis of the complementary strands from the primer, the *Taq* DNA polymerase extends the primer and reached to the probe binding downstream of the primer. Then the enzyme degrades the probe and releases the fluorophore from it which results the separation of the fluorophore from the quencher molecules. Thus an increased fluorescent signal is resulted. After completion of each cycle, a new cycle of hybridization takes place. As a result, more fluorophores are separated from the probes (quencher), resulting in increased fluorescence signal which indicates the accumulation of target DNA molecules. A schematic overview of fluorescent signal generation is shown below.

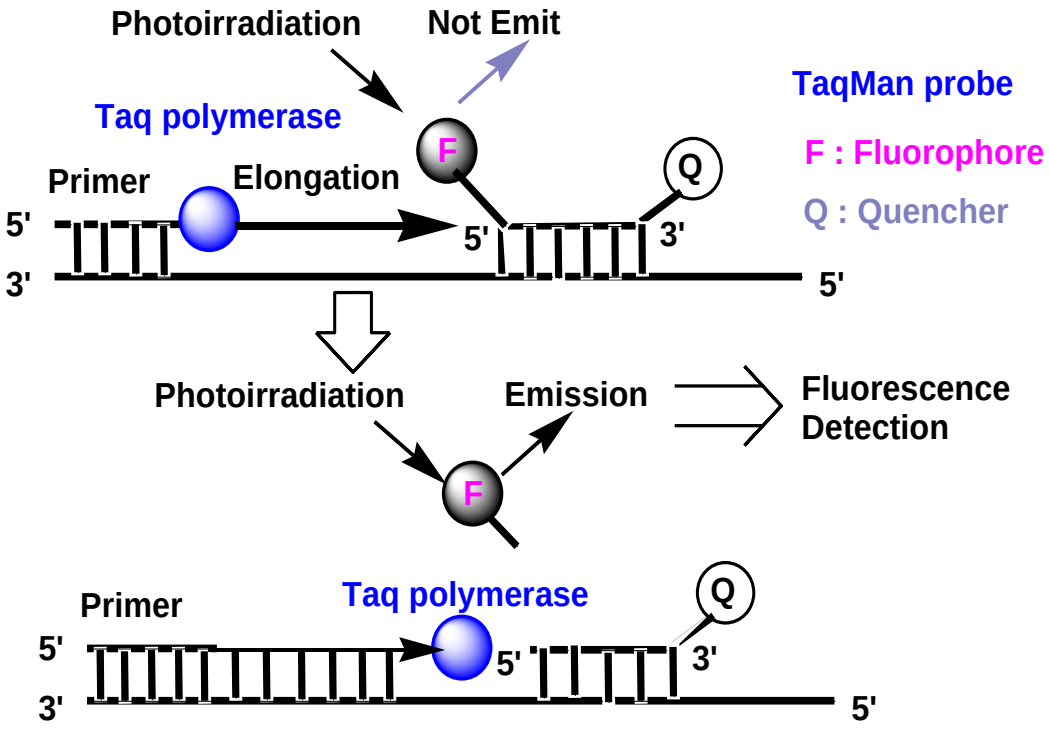


**Figure 1.9:** Schematic overview of energy transfer and fluorescence signal generation in 5´-Nuclease probes.

### 1.6.3 *Strand-displacement probes or Yin-Yang probe*

This probe is designed by utilizing two complementary nucleic acid probes. One of the probe is designed by labeling with fluorophore. On the other hand, the other probe is labeled with a non-fluorescent quencher molecule [39]. Fluorophore and quencher molecules come in close proximity while the probes hybridize each other and as a result it gives a very low fluorescence emission i.e. contact quenching property. By the addition of the probes into the solution of target, one of the probe forms a more stable probe-target hybrid than the other, thus two probes are being separates from each other. Due to this displacement, the fluorophore is no longer in the close contact of the quencher and an increased fluorescence signal is generated. The schematic diagram of the mechanism of this kind of probe is shown in Figure 1.10.

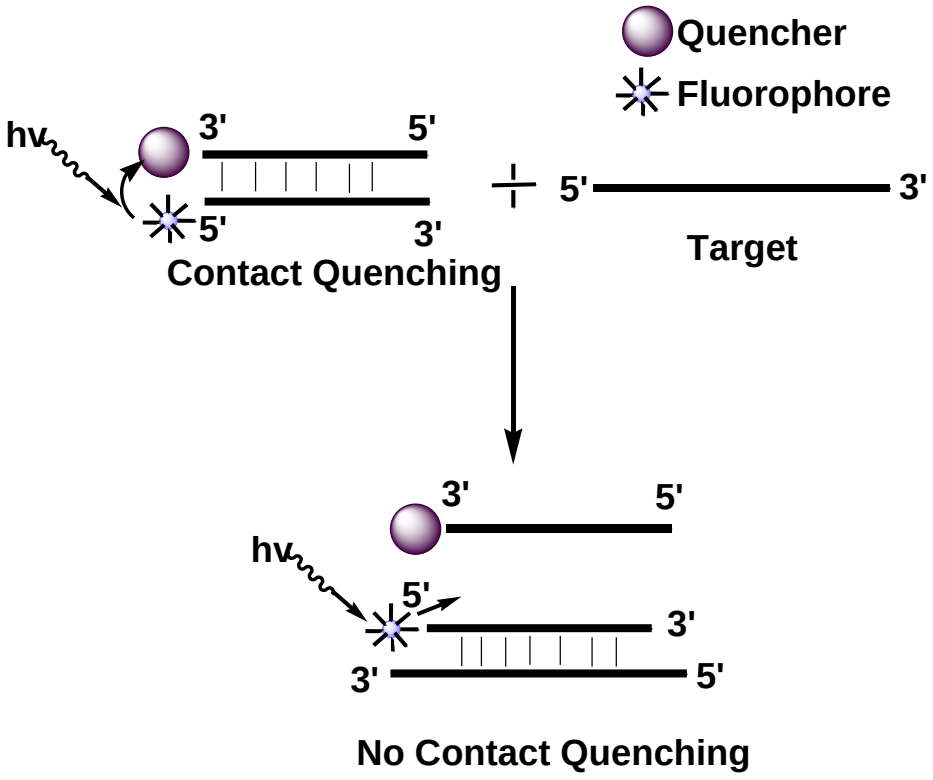


**Figure 1.10:** Schematic overview of energy transfer and fluorescence signal generation in Strand-displacement probes.

### 1.6.4 *Molecular beacon probes*

Since the first report in 1996 [29], molecular beacon probes have attracted great interests as FRET based DNA and RNA probes. Molecular beacon is a single stranded hybridization probe that forms stem-loop structure (Figure 1.11). The loop portion is complementary to the target oligonucleotide and, therefore, acts as the binding portion to the target. The loop portion is inserted between two stem sequences which are complementary to each other and, therefore, ultimately forms the double-stranded stem portion of the probe. At the same time, the probe is connected to both a fluorophore and a quencher molecule. While it stays alone (means absence of the target), it forms a stem-loop (hairpin) type of structure. In this

structure, the fluorophore and quencher molecules come in close proximity and thus the probe gives a low fluorescence emission due to the FRET occurs between the fluorophore and the quencher. Upon addition of target oligonucleotide, the loop-portion binds to the target to form a stable probe-target hybrid with the dissociation of the stem-portion. (Figure 1.11). As a result, the fluorophore is placed in a distant position from the quencher causing the recovery of fluorescence signal.

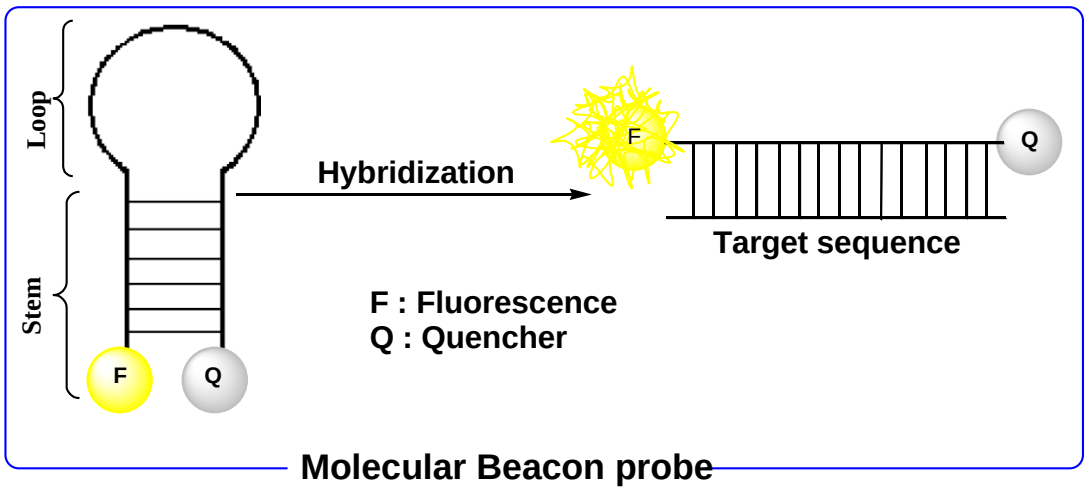


**Figure 1.11:** Schematic overview of energy transfer and fluorescence signal generation in molecular beacon probes.

## 1.7 Fundamentals of Molecular Beacon and its Spectroscopic Principles

### 1.7.1 *Loop sequence*

The loop sequence of molecular beacon is generally consisting of 15 to 30 nucleotide units and should not form any kind of secondary structure by themselves [29, 40-41]. Their sequences are usually complementary to a part of target oligonucleotides. This part of molecular beacon probe is also termed as sequence recognition part. Upon mixing of target and the molecular beacon probe, the loop portion binds with the target molecule in a sequence specific manner. To ensure the binding of molecular beacon probe with target oligonucleotide, the thermal stability (melting temperature) of the duplex formed by the loop portion and the target should be higher than that of stem portion. It means the stability of probe-target duplex should be sufficiently stronger than the intermediate duplex formation by molecular beacon alone. In general, the stability can be increased by increasing the length of the sequence recognition part (loop-portion).

### 1.7.2 *Stem sequence*

The stem is typically consisting of 5 to 8 base pairs which dissociates during the hybridization of molecular beacon probe with a target oligonucleotide. The thermal stability of stem depends on their length as well as its GC content. In order to ensure the stem-loop type of structure of the MB probe in the free form, the melting temperature of the stem should be 7-10 °C higher than the detection temperature [42]. The thermal stability of the complex consisting of target and molecular beacon probe with 15-25 base pairs is thought to be sufficiently higher than that of the stem [29, 40-41]. When the stem length is short, the

probe would have a faster hybridization kinetics to the target compared with the probe having longer length stem. However, the signal to background ratio would decreases because of undesired dissociation of the stem-portion even under the absence of the target. On the other hand, if the stem length is too long (too stable), then the probe hardly binds to the target and the signal to background ratio would decrease too. In addition to these, the neighboring nucleotide of the fluorophore in the probe would exhibit quenching properties of the molecular beacon probe. Drake *et al.* recently reported that the neighboring nucleotide showed a variable degree of quenching in order of G>A>C>T [43]. Thus, one should be careful to decide about the length as well as the sequence and the neighboring nucleotide to the fluorophore in the design of stem-potion in molecular beacon type probes.

### 1.7.3 *Fluorophore*

Fluorophores, a fluorescent materials, have been used extensively in many days in material sciences as well as in biomedical sciences. Moreover, it is still focused by many researchers to find out novel fluorescent small molecules as well as making alternation in their physiochemical properties, such as absorption, excitation and emission wavelength, quantum yield and so forth. The majority of commercially available fluorescent materials are usually made from the small synthetic fluorophore. A few of genetically encoded proteins come from natural animal origin are considered as naturally occurring fluorophores. Different types of fluorophores have been tested for their feasibility to make fluorescent oligonucleotide probes. Their emission spectra vary from near UV to near IR wavelength. A few of the commonly used fluorophores and their analogs are discussed in the following.

**Pyrene derivaties**

Pyrene, a poly aromatic hydrocarbon of four fused benzene ring, has attracted much attention due to their unique properties. This is a chromophore of choice in fundamental and applied photochemical research. Laurent was first isolated pyrene from the residue of the destructive distillation of coal tar in the year of 1837 [44]. Initially, the synthetic dye industries used pyrene for preparing several derivatives like pyranthrone [45]. In the year of 1954, Forster and Kasper was first found the intermolecular emission (excimer emission) property of pyrene [46]. This excimer showed high quantum yield [47]. Due to these attractive properties, pyrene has become a subject of extensive research for its photophysical properties.

For the last 50 years, the fluorescence properties of pyrene have been mostly used in investigation of water soluble polymer and making dye for fluorogenic probes [48-49]. It is widely used as a probe to investigate the surfactant micelles properties, aggregates of surfactant/polymers and phospholipid vesicles. As a labelling agent, pyrene has been utilized to investigate protein and peptide structural features [50-53], lipid membrane [54-61] and also oligonucleotide recognition [62-66]. In addition, many researchers observed the red-shift of absorption and emission wavelength and increased quantum yield by incorporation of certain functional groups [67-69]. Figure 1.12 shows the possible position of incorporation of such functional groups in the structure of pyrene for improvement of quantum yield.

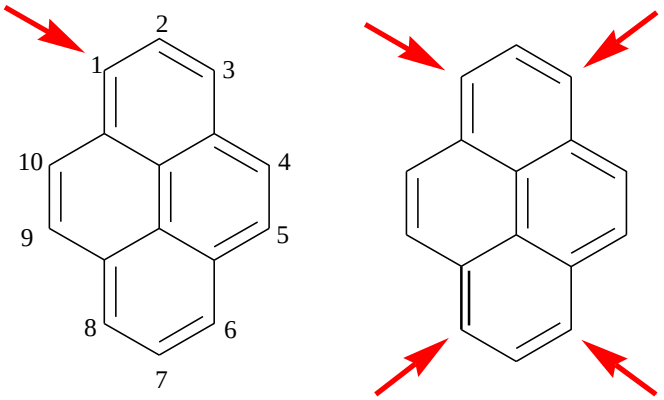


**Figure 1.12:** Representative structure of 1-substituted pyrene and 1, 3, 6, 8-tetrasubstituted pyrene derivatives.

**Anthracene derivatives**

Anthracenes have been utilized in many practical applications as a core material for preparing potential therapeutics [70-73], polymeric material [74-75] and optical devices [76-77]. Though anthracene derivatives are well known for many days [78-81], a few studies have been done to characterize their emission wavelengths of its derivatives.

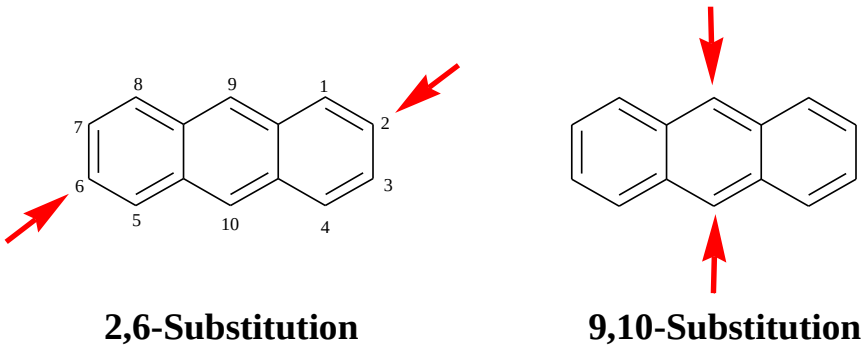


**Figure 1.13:** General structure of 2, 6-disubstituted anthracene and 9, 10-disubstituted anthracene derivatives.

The general structure and substitution position in the anthracene are shown in Figure 1.13. The substitutions in 2, 6 position of the anthracene by trifluoromethylphenyl and thiophene have significant influence on their emission wavelength [82]. It is also possible to alter the emission wavelengths of anthracene 2, 6-disulfonic acid by varying organic salts in the solid state [83-84]. Kyushin and co-workers reported recently the synthesis of 9,10-disilylanthracene and they observed an intense quantum yield of this anthracene derivative ($\Phi_f > 0.9$ ) [85].

**Fluorescein derivatives**

Fluorescein is a main dye of choice in medicine and science for more than 100 years due to its high quantum yield, ease of handling and also for non-toxicity. It was first developed by A. Beyer in 1871 [86]. It gives an emission with reasonably long wavelength (500 to 600 nm) with relatively high quantum yield ($\Phi_f$=0.85-0.97) upon excitation in aqueous media [87]. Fluorescein is used as fluorescent material for labeling and sensing many biomolecules [88-90]. A huge number of novel fluorescein based fluorescent materials have been synthesized by many researchers [91-95]. For example, the photophysical properties of the fluorescein improved by making modification at the aryl moiety attached to the xathene core framework [96-97]. Some structures and substituted derivatives of fluorescein with their quantum yields are presented in Figure 1.14.

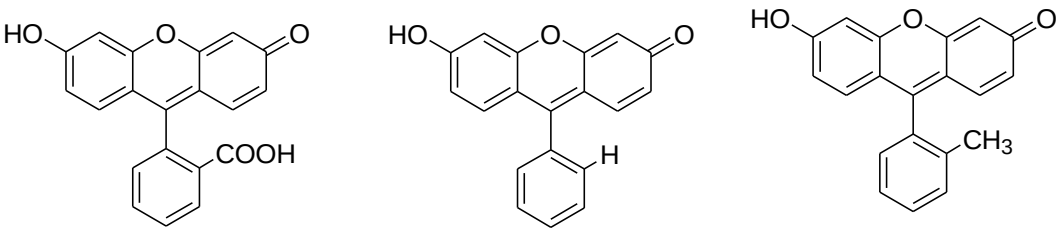


**Fluorescein**
Φ = 0.85

**Hydroxyphenylflurone**
Φ= 0.20

**2-Me Tokyo Green**
Φ = 0.85

**Figure 1.14:** Structure of Fluorescein and its substituted derivatives with quantum yield [cited from ref. 91]

**BODIPY derivatives**

BODIPY, 4,4-Difluoro-4-bora-3a,4a-diaza-*s*-indacene, is a molecule which was first discovered in 1968 by Treibs and Kreuzer [98]. Upon excitation, it emits sharp fluorescent peak with high quantum yield due to their tendency to strongly absorb of UV radiation. As a continuation, efficient fluorescent materials were synthesized by making a simple modification in its structure. For example, Wael *et al.* prepared an alkylated BODIPYs by symmetrical di-substitution with methyl function. The derivative showed a quantum yield 0.81 in ethanol. At the same time, they also prepared unsymmetrical di-substituted alkylated BODIPYs which showed a quantum yield 0.70 [99]. However, the symmetrical tetra, hexa and hepta-alkylated BODIPYs showed quantum yield 0.80, 0.56, and 0.70 respectively [99-100]. Kim *et al.* also recently developed some new analogs of BODIPY which have high quantum yield ($\Phi_f$=0.56-0.98) (Figure 1.15) [101].

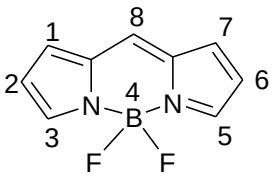


**BODIPY CORE**

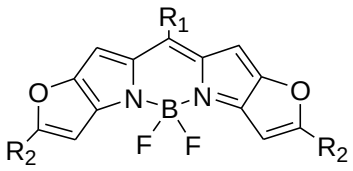


| | |
|---|---|
| $R_1$=H, $R_2$=Me, | Φ=0.96 |
| $R_1$=$CF_3$, $R_2$=Me, | Φ=0.98 |
| $R_1$=H, $R_2$=4-methoxyphenyl, | Φ=0.86 |
| $R_1$=$CF_3$, $R_2$=4-methoxyphenyl, | Φ=0.56 |
| $R_1$=H, $R_2$=Phenyl, | Φ=0.90 |
| $R_1$=H, $R_2$=2-methoxyphenyl, | Φ=0.91 |
| $R_1$=H, $R_2$=4-isopropylphenyl, | Φ=0.97 |

**Figure 1.15:** Basic Structure of BODIPY and some of their analogs having high quantum yield [cited from ref. 101]

### 1.7.4 *Quencher*

Quencher is a molecule which decreases the emission intensity of a fluorescence substances. The process is usually taking place when emission spectra of fluorescent donors have sufficiently overlap with absorption spectra of the quencher molecule (Förster Mechanism, FRET). This is only happened when both molecules come in sufficiently closed position. The quencher molecule is widely used to design FRET based fluorogenic probes for protease activity detection [102-114], nucleic acid hybridization [29, 115], and real-time PCR [116-118]. The natural nucleobase is also used to get the quenching of fluorescence of the fluorophore. For example, the guanosine residue can effectively reduce the fluorescent intensity of the fluorophore depending on the type of fluorophore [119-120]. However, this feature of guanosine has been utilized by others to design quencher free molecular beacon probes [121].

## 1.8 Applications of Molecular Beacon Probes

The development of MB based assay for gene identification has emerged an areas of research that were not possible previously. With time, it has become a powerful tool for many applications in human health aspects. These have included biosensor and biochip development, genetic analysis, real-time monitoring of DNA/RNA amplification during PCR, in vivo imaging of cancer cell as well as in vivo RNA detection.

### 1.8.1 *Biosensor and biochip development*

For the last couple of years, MB probes are popularly used to design highly sensitive and selective biosensors or biochips. Surface-immobilized MB sensors have been reported for various applications including ultra-small optical fiber probes using avidin–biotin binding [122], fiber optic microsphere-based biosensor [123] and microarrays [124-125]. The MB immobilized magnetic nanoparticle or genomagnetic nanocapturers (GMNC) have also designed for detecting the DNA/RNA molecules [126]. This kind of GMNC was made through avidin-biotin interaction by conjugating the probe onto the surface of magnetic nanoparticle. Martinez *et al.* reported a surface-immobilized MB biosensor having 2′,4′-locked nucleic acid (LNA) bases [127]. Due to the high binding affinity and stability of LNA, their biosensor are very stable and robust, and selective and sensitive.

The surface-immobilized MBs have a general configuration where it includes the immobilization of the hairpin onto a surface. The MBs possess a fluorophore and quencher moiety. However, the ‘on’ versus ‘off’ ratios generated by its fluorophore and quencher moieties are important factor in the immobilization of this kind of MB probes. In most cases,

immobilized molecular beacons showed low signal-to-background ratios because of the additional strain of the solid surface to its confirmation which ultimately makes an unstable hairpin structure. For this reason there is an increased number of 'on' molecules than in a homogenous assay. To overcome this problem, attempts have been taken recently by using longer stem which further force the MBs to be isolated from the solid surface [128].

### 1.8.2 *Genetic analysis*

The analysis of genetic discrepancy is an automated procedures like sequencing which requires a high throughput methods. However, the use of MBs is a simple and capable to discriminate single-base mismatches. The probes are also very selective considering the thermal stability. The perfectly matched probe-target hybrids are more stable that usually force the stem portion to open. It was also reported that the detection of mismatched using MB probes have shown their potentiality due to the formation of less stable mismatched MB probes duplexes than mismatched linear probe duplexes [115]. The stability of MB probes is also influenced by many factors like the number of complementary bases participate in the hybridization, GC content, position of the mismatches in the sequence as well as hybridization temperature. The high selectivity of MB probes to discriminate single base alternation makes them a promising probes for analyzing genetic variation [129]. Piatek *et al*. reported a MB which has the ability to analyze 81bp region of the rpoB gene for *Mycobacterium tuberculosis* mutations associated with resistance of isoniazid and rifampin [130]. In another report, Kostrikis *et al.* have designed a molecular beacons to distinguish allele of the β-chemokine receptor 5 gene that determines susceptibility to HIV-I [129].

### 1.8.3 *Real-time monitoring of DNA/RNA amplification during PCR*

MBs are also used for real-time monitoring of nucleic acid amplification during PCR [28, 115]. This kind of analysis should be done at lower temperature because the MBs become dissociated at high temperature. When the annealing of primers ensured at a low temperature, the non-hybridized MB will not emit fluorescence signal because of forming stem loop type of structure. However, it generate a fluorescence signal by binding with the target amplicons. The increase fluorescence signal indicates the degree of amplification at each annealing cycle. Recent reports indicate that real-time PCR monitoring with MBs is better than other conventional methods. For example, MBs have showed better genotyping results than *TaqMan* probes [131]. Moreover, it can process many samples simultaneously and consuming relatively short period of time. Considering the risk of contamination, the confirmation of amplified sample in the same tube is also an additional advantage of this method compare with time-consuming gel electrophoresis and southern blotting methods. This method has been utilized by many researchers in many purposes like development of surface immobilized PNA-DNA hybrid probes for detecting PCR amplicons [132], quantification of viruses [133-134] as well as study of replication of hepatitis virus [135].

### 1.8.4 *In-Vivo imaging of cancer cells*

Specific and sensitive molecular beacon probe development is one of the central challenges in cancer cell imaging. In *in-vivo* imaging of cancer cell, the probes should have faster tissue uptake, shorter residence in the site of action and higher ratio of target accumulation. Shi *et al.* reported one of such novel MB probes (Figure 1.16) [136]. They named it as activated aptamer probe (AAP) which has a fluorophore and quencher moiety attached at its terminus. In the absence of cancer cell, it remained as a hairpin structure where the fluorophore and quencher stayed in a close position resulted in quenching of the fluorescence. However, the

probe gave fluorescence signal upon binding with a specific protein tyrosine kinase (PTK7; CCK4) on the membrane of the target cancer cell due to the conformational change of the probe that displaces the fluorophore from the quencher (Figure 1.16). They observed the fast restoration of fluorescence of AAP by the presence of target cancer cell in tumor site compared with the other areas.

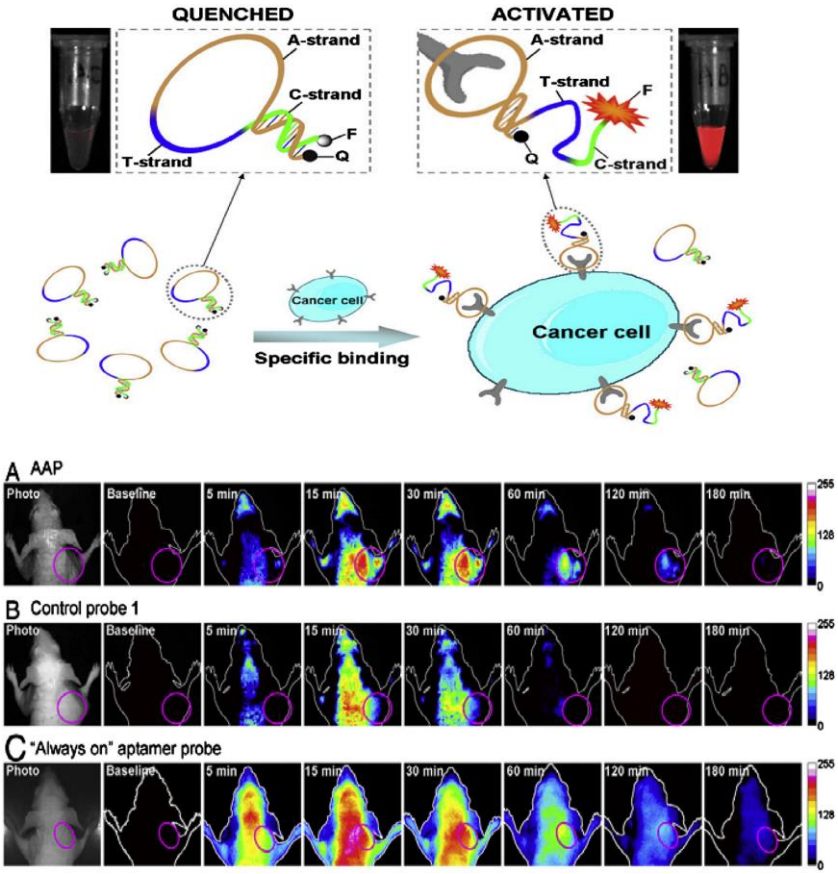


**Figure 1.16:** Schematic presentation of the novel strategy for *in vivo* cancer imaging using AAP. CCRF-CEM tumor-bearing nude mice were intravenously injected with **(a)** the AAP, **(b)** control probe, and **(c)** the ‘‘always-on’’ aptamer probe, respectively. The pink circle in every image locates the tumor site [cited from ref. 136]

### 1.8.5 *In vivo RNA detection*

The success of *in vivo* RNA detection using MB probes depends on the combination of rational sequence design, ability of probe to be inserted in the cell as well as the choice of target mRNA sequence. The molecular beacon has already showed potentiality to decode the message of coded mRNA. A novel way of detecting cancer at very early stage by detecting the mRNA transcripts that comes from the gene in the living cells. Fang *et al.* recently reported a molecular beacons which injected into the living cells for the detection of mRNA using an ICCD based fluorescence imaging process [137]. The cells location determination and background measurements were carried out by taking optical and fluorescence images. After injection, CCD images of the cells were collected. The fluorescence signal of the injected cells increases with time (Figure 1.17). Whereas, no fluorescence observed in the control. It indicates that MBs can be used for the real time detection of mRNA. In 1998, Matsu reported a 15-nucleotide long antisense sequence for human basic fibroblast growth factor for the detection of mRNA [138]. The injection of MB probes into K562 human leukemia cells disclosed the real-time visualization and interaction of mRNA by fluorescence confocal microscopy [138-139].

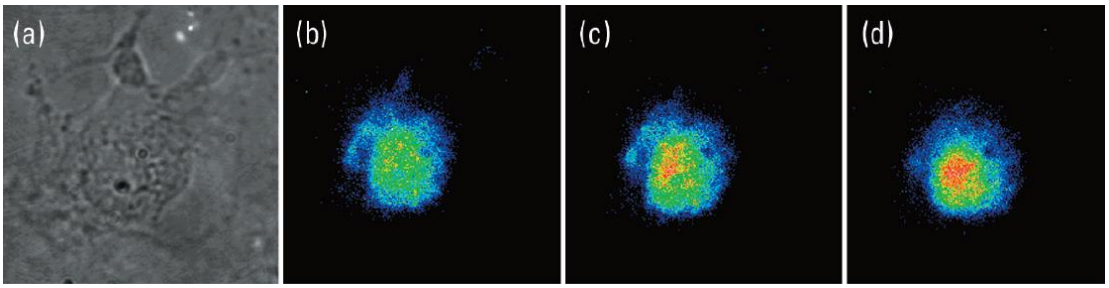


**Figure 1.17:** Hybridization of the MB to mRNA in living cells. **(a)** Optical image of a kangaroo rat kidney cell and the fluorescence images of the cell **(b)** 3 min **(c)** 12 min, and **(d)** 15 min after injecting MB. [cited from ref. 137]

## 1.9 Problems of Molecular Beacon Probes and Recent Solutions

Molecular beacon probe has shown its potentiality in the modern era of genomics and proteomics involving the study of cancer, genetic analysis, DNA-protein interaction, designing biosensors, *in vivo* RNA detection and molecular beacon aptamers etc. as described earlier. However, more improvements can also be achieved in the area like increment of signal-to-noise ratio, selection of loop and stem sequences and also overcoming the complexity of living environment. Some of the problems and their recent solutions are discussed below.

### 1.9.1 *Signal-to-noise (S/N) ratio:*

The fundamental phenomenon of molecular beacon probes is the signal increase upon hybridization to the target (increment in S/N ratio). The lower limit of the detection can only be achieved by the huge increase in fluorescence upon probe-target hybridization. On the other hand, the S/N ratio can be increased either by improving the fluorescent intensity of the fluorophore under the presence of the target or by reducing the background under the absence of the target. Many attempts have been taken until now to increase the fluorescent intensity of fluorophore. Yang *et al.* recently reported a water soluble poly(phenylene ethylene) (PPE) polymeric fluorophore. They conjugated PPE with an oligonucleotide [140]. They reported their synthetic method is efficient, simple, and readily controllable of water soluble PPE with an oligonucleotide. Increasing the fluorescent intensity of the fluorophore was also reported by the silylation of fluorescent aromatic compound like pyrene and anthracene [67, 85]. Recently our lab has also designed many silylated pyrene derivatives possessing dimethylsilyl function with modifiable terminal group for this purposes [69, 141-

143]. The fluorescent quantum yield of such pyrene derivatives showed more than double compare to that of pyerene moiety. Some of these derivatives with their quantum yield are shown in Figure 1.18. Krasnoperov *et al*. also developed a very impressive lanthanide based luminescent complex [144]. They designed a cross linkable lanthanide chelate probes. They showed the detection limit of their probe is 1000 times lower than that of traditional MB probe and 30 times lower than the other lanthanide based probes.

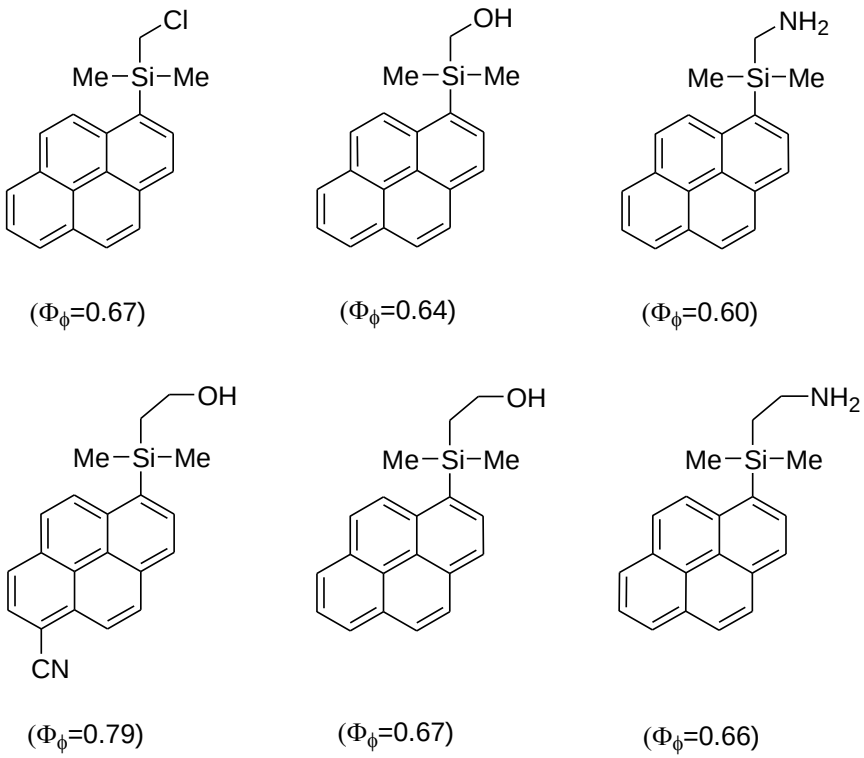


**Figure 1.18:** Structure of pyrene derivatives with their quantum yields

On the other hand, reducing of background fluorescence largely depends on the design of the molecular beacon probes. The design should enable the fluorophore and quencher in a very close proximity which will ultimately ensures the efficient quenching. Yang *et al.* reported an approach of using multiple quencher dyes to design a molecular beacon probes

(Figure 1.17a) and observed an S/N ratio of upto 320 [145]. Kashida and collegues have reported another approach of improving the S/N ratio by placing the fluorophore/quencher pairs in the stem region (Figure 1.17b) and reported an S/N ratio of upto 58 [146]. Dubertret *et al.* used gold nanoparticles for fluorescence quenching of many fluorophore to rise the S/N ratio of the MB probe (Figure 1.17c) [147]. Using this kind of metal, they able to rise S/N ratio upto 100. Though many attempts have already taken to solve the matter of S/N ratio of the molecular beacon probes, it is still a big concern to design a molecular beacon probe with appropriate S/N ratio to ensure the lower limit of detection.

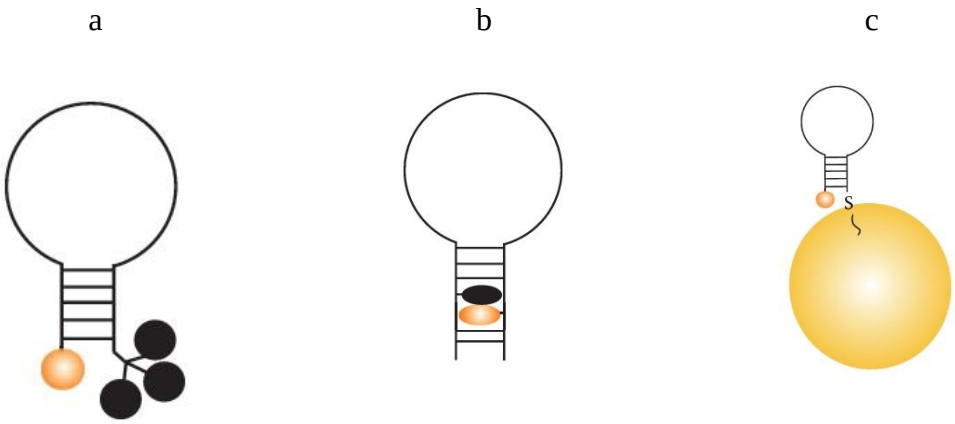


**Figure 1.17:** Strategies to reduce background fluorescence of MB probes **(a)** Superquenched MB probe contains more than one quencher **(b)** In-stem probe takes advantages of stacking interaction of the base pairs with fluorophore and a quencher dye to achieve efficient quenching **(c)** Gold nanoparticles conjugated MB probe takes advantages of super quenching abilities of gold nanoparticles. [cited from ref. 148]

### 1.9.2 *Loop and stem nucleotides*:

The loop and stem nucleotides sequences influence the folding and hybridization of MB probes. Undesired structures of MB probes would be emerged by the interference of the loop as well as stem sequences. For example, the MB probes containing partially self-complementary loop sequence could hybridize each other making a secondary structure (figure 1.18a) which would be more stable and less accessible by the target DNA. Thus, it may reduce the hybridization efficiency of the MB probes with its target DNA. If the stem nucleotides have partial complementary sequence to the loop nucleotides, an alternative structure (Figure 1.18b) of MB probes may be formed. The alternate structure formation thus formed would separate the fluorophore of the MB probes from the quencher resulting in reducing the quenching efficiency of the probes. These are why one should carefully

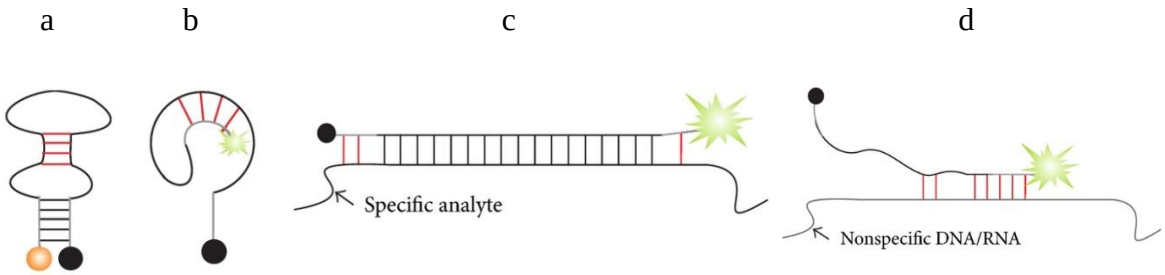


**Figure 1.18:** Examples of loop and stem interferences in MB probe. **(a)** Loop interference. Complementary loop nucleotides hybridize to each other, thus making folded conformation more stable and less accessible by the target DNA. **(b)** Stem hybridizes to loop thus separating the fuorophore from the quencher resulting in elevated background signal. **(c)** Stem nucleotides can partially hybridize to the nucleotides of the targeted DNA. **(d)** Stem and loop nucleotides bind nonspecific nucleic acids present in a sample. Red lines indicate undesired or undersigned base pairs. [cited from ref. 148]

select the stem nucleotides to avoid any kind of complementarity with the loop. Stem invasion is kind of interaction of stem nucleotides with the analyte nucleotide which flank the target site. This may also happen by wrong choice of stem sequences (Figure 1.18 c,d). In these cases, stem nucleotides can partially bind to the complementary target DNA that does not allow the target to bind perfectly with the probes resulting in the flanking of target site. At the same time, both stem and loop nucleotides also bind in a nonspecific site of DNA or RNA which may present in the sample solution.

Many strategies have been adapted by researchers to overcome the aforementioned problems. Kim *et al.* developed a modified MB probes by using unnatural enantiomeric L-DNA in the stem [149]. They showed the incorporation of L-DNA in the stem reduces the intra- and intermolecular stem invasions. An alternate strategy was also developed by Kolpashchikov where he used adaptor strands (A and B strands in Figure 1.19) [150]. Each strand has a complementary part to the MB probe and another complementary part to the analyte nucleic acid. Both strands interact with the target. This complex interaction ensures the open conformation of the MB probes, thus resulting a high fluorescence.

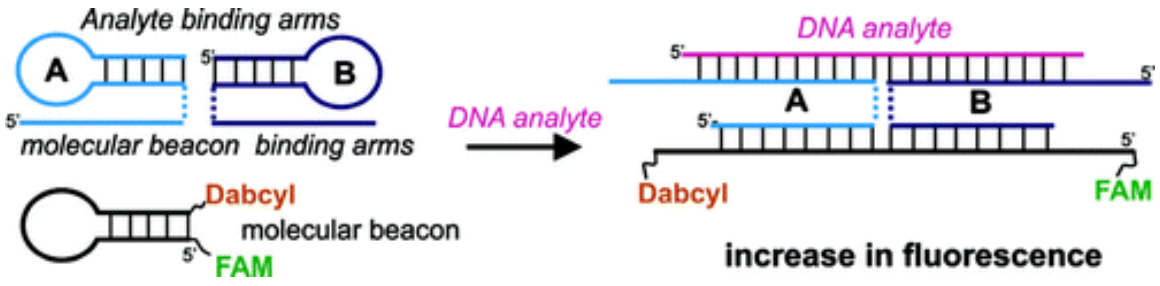


**Figure 1.19:** Adaptor *A* and *B* strands hybridize to both analyzed sequence and MB probe. Triethylene glycol linkers (TEG) that connect the MB-binding arms with the analyte-binding arms are shown as dashed lines. [cited from ref. 150]

### 1.9.3 *Complexity of living environments*:

The utilization of molecular beacon probe for analyzing gene expression can frequently limited by the degradation of the backbone of the oligonucleotides of molecular beacon probes by nuclease [151-153]. In living cell, it was also previously reported that the half-life of unmodified phosphodiester oligonucleotides is very short which may vary from 15 to 20 min [154-156]. That's why, it is necessary to design a nuclease resistant backbone in the molecular beacon probe for example using phosphorothioate backbone in place of phosphodiester backbone [157] for use in living environments. Replacing natural nucleotides of the probes by 2′-OMe-modified RNA, peptide nucleic acid and locked nucleic acid have been employed to overcome these kind of problems [158, 159-160].

## References


1. McCarty, M. *The Transforming Principle*; W. W. Norton, New York, 1985.
2. Avery, O. T.; MacLeod, C. M.; McCarty, M. *J. Exp. Med.*, 1944, **79**, 137.
3. Watson, J. D.; Crick, F. H. C. *Nature,* 1953, **171**, 737.
4. Soyfer, V. N.; Potaman, V. N. *Triple-Helical Nucleic Acids*; Springer: New York, 1996.
5. Gellert, G.; Lipsett, M. N.; Davies, D. R. *Proc. Natl. Acad. Sci., U.S.A.* 1962, **48**, 2013.
6. Zimmerman, S. B.; Cohen, G. H.; Davies, D. R. *J. Mol. Biol.*, 1975, **92**, 181.
7. Tougard, P.; Chantot, J. F.; Guschlbauer, W. *Biochim. Biophys. Acta.*, 1973, **308**, 9.
8. Wang, I.; Patel, D. J. *Biochemistry*, 1992, **31**, 8112.

9. Laughlan, G.; Murchie, A. I. H.; Norman, D. G.; Moore, M. H.; Moody, P. C. E.; Lilley, D. M. J.; Luisi, B. *Science*, 1994, **265**, 520.

10. Phillips, K.; Murchie, A. I. H.; Lilley, D. M. J.; Luisi, B. *J. Mol. Biol.*, 1997, **273**, 171.

11. Yakovchuk, P.; Protozanova, E.; Frank-Kamenetskii, M. D. *Nucleic Acids Res.*, 2006, **34,** 564.

12. Keller, G. H.; Manak, M. M. *DNA Probes*, Stockton Press, New York, **1989**, 1.

13. Tabares, E. *Arch Virol.*, 1987, **92**, 233.

14. Zeph, L. R.; Lin, X.; Stotzky, G. *Current Microbiology*, 1991, **22**, 79.

15. Carey, M. F.; Peterson, C. L.; Smale, S. T. *Cold Spring Harb Protoc*, Cold Spring Harbor Laboratory Press, New York, 2013.

16. Wu, W.; Gong, P.; Li, J.; Yang, J.; Zhang, G.; Li, H.; Yang, Z.; Zhang, X. *RNA*, 2014, **20**, 580.

17. Pardue, M. L. *Cold Spring Harb Protoc*, Cold Spring Harbor Laboratory Press, New York, 2011.

18. Guo, J.; Ju, J.; Turro, N. J. *Anal. Bioanal. Chem.*, 2012, **402**, 3115.

19. Livak, K. J.; Flood, S. J. A.; Mamoro, J.; Giusti, W.; Deetz, K. *PCR Methods Appl.*, 1995, **4**, 357.

20. Livak, K. J.; Flood, S. J. A.; Mamoro, J.; Giusti, W.; Mullah, K. B. Hybridization Assay Using Self-quenching Fluorescence Probe, US Patent, US 6030787 A, 2004.

21. Kuhn, H.; Demidov, V. V.; Coull, J. M.; Fiandaca, M. J.; Gildea, B. D.; Frank-Kamenetskii, M. D. *J. Am. Chem. Soc.*, 2002, **124**, 1097.

22. Marks, A. H.; Bhadra, P. K.; McDowell, D. G.; French, D. J.; Douglas, K. T.; Bichenkova, E. V.; Bryce, R. A. *J. Biomol. Struct. Dyn.*, 2005, **23**, 49.

23. Knemeyer, J. P.; Marme, N.; Sauer, M. *Anal. Chem.*, 2000, **72**, 3717.

24. Crockett, A. O.; Wittwer, C. T. *Anal. Biochem.*, 2001, **290**, 89.

25. Kurata, S.; Kanagawa, T.; Yamada, K.; Torimura, M.; Yokomaku, T.; Kamagata, Y.; Kurane, R. *Nucleic Acids Res.*, 2001, **29**, E34.

26. Heinlein, T.; Knemeyer, J. P.; Piestert, O.; Markus Sauer, M. *J. Phys. Chem. B,* 2003, **107**, 7957.

27. http://chemweb.unl.edu/lai/research-area-one-biosensor-design/

28. http://www.abbottmolecular.com/products/infectious-diseases/realtime-pcr/hepatitis-hcv-assay.html

29. Tyagi, S; Kramer, F. R. *Nat. Biotechnol*., 1996, **14**, 303.

30. Marras, S. A. E. *Fluorescent Energy Transfer Nucleic Acid Probes*, Humana Press, New Jersey, 2006

31. Lakowicz, R. *Principles of Fluorescence Spectroscopy*, 3rd Edition, Springer, New York, 2006.

32. Sauer, M.; Drexhage, K. H.; Liberwirth, U.; Muller, R.; Nord, S.; Zander, C. *Chem. Phys. Lett.*, 1998, **284**, 153.

33. Clegg, R. M. In X. F. Wang and B. Herman (eds), *Fluorescence Imaging Spectroscopy and Microscopy*, Wiley-Interscience Publication, New York, 1996.

34. Herman, B. In D. L. Taylor and Y. L. Wang (eds), *Fluorescence Microscopy of Living Cells in Culture,* Academic Press, San Diego, 1989.

35. Forster, T. *Intermolecular Energy Migration and Fluorescence*. Translated by R. S. Knox. *Ann. Phys. (Leipzig)*, 1948, **2**, 55.

36. Lukhtanov, E. A.; Lokhov, S. G.; Gorn, V. V.; Podyminogin, M. A.; Mahoney, W. *Nucleic Acids Res.*, 2007, **35,** e30.

37. Thompson, M. B. (ed) *Fluorescence Sensors and Biosensors,* Taylor and Francis, Boca Raton, 2006.

38. Witter, C. T.; Herrman, M. G.; Moss, A. A.; Rasmussen, R. P. *Biotechniques*, 1969, **22**, 130.

39. Li, Q.; Luan, G.; Guo, Q.; Liang, J. *Nucleic Acids Res.*, 2002, **30**, e5

40. Kostrikis, L. G.; Tyagi, S.; Mhlanga, M. M.; Ho, D. D.; Kramer, F. R. *Science*, 1998, **279**, 1228.

41. Ortiz, E.; Estrada, G.; Lizardi, P. M. *Mol. Cell Probes*, 1998, **12**, 219.

42. http://www.molecular-beacons.org/MB_SC_design.html.

43. Drake, T. J.; Tan, W. *Appl. Spectro.*, 2004, **58**, 269A.

44. Laurent, A. *Ann. Chim. Phys.*, 1837, **66**, 136.

45. Welham, R. D. *J. Soc. Dyers Color*, 1963, **79**, 98.

46. Forster, T.; Kasper, K. Z. *Elektrochem.*, 1955, **59**, 976.

47. Birks, J. B. *Photophysics of Aromatic Molecules*; Wiley-Interscience, London, 1970.

48. Winnik, M. A.; Winnik, F. M. *Adv. Chem. Ser.*, 1993, 485.

49. Winnik, F. M. *Chem. Rev.*, 1993, **93**, 587.

50. Goedeweeck, R.; Vanderauweraer, M.; Deschryver, F. C. *J. Am.Chem. Soc.*, 1985, **107**, 2334.

51. Hammarstrom, P.; Kalman, B.; Jonsson, B. H.; Carlsson, U. *FEBS Lett.*, 1997, **420**, 63.

52. Sahoo, D.; Weers, P. M. M.; Ryan, R. O.; Narayanaswami, V. *J. Mol. Biol.*, 2002, **321**, 201.

53. Sahoo, D.; Narayanaswami, V.; Kay, C. M.; Ryan, R. O. *Biochemistry*, 2000, **39**, 6594.

54. Ollmann, M.; Schwarzmann, G.; Sandhoff, K.; Galla, H. J. *Biochemistry*, 1987, **26**, 5943.

55. Pap, E. H. W.; Hanicak, A.; Vanhoek, A.; Wirtz, K. W. A.; Visser, A. J. W. G. *Biochemistry*, 1995, **34**, 9118.

56. Kurzchalia, T. V.; Parton, R. G. *Curr. Opin. Cell Biol.*, 1999, **11**, 424.

57. Song, X. D.; Swanson, B. I. *Langmuir*, 1999, **15**, 4710.

58. Smit, J. M.; Bittman, R.; Wilschut, J. *J. Virol.*, 1999, **73**, 8476.

59. Irurzun, A.; Nieva, J. L.; Carrasco, L. *Virology*, 1997, **227**, 488.

60. Pillot, T.; Goethals, M.; Vanloo, B.; Talussot, C.; Brasseur, R.; Vandekerckhove, J.; Rosseneu, M.; Lins, L. *J. Biol. Chem.*, 1996, **271**, 28757.

61. Somerharju, P. *Chem. Phys. Lipids*, 2002, **116**, 57.

62. Paris, P. L.; Langenhan, J. M.; Kool, E. T. *Nucleic Acids Res.*, 1998, **26**, 3789.

63. Lewis, F. D.; Zhang, Y. F.; Letsinger, R. L. *J. Am. Chem. Soc.*, 1997, **119**, 5451.

64. Yamana, K.; Iwai, T.; Ohtani, Y.; Sato, S.; Nakamura, M.; Nakano, H. *Bioconjug. Chem.*, 2002, **13**, 1266.

65. Yamana, K.; Takei, M.; Nakano, H. *Tetrahedron Lett.*, 1997, **38**, 6051.

66. Tong, G.; Lawlor, J. M.; Tregear, G. W.; Haralambidis, J. *J. Am. Chem. Soc.*, 1995, **117**, 12151.

67. Maeda, H; Inoue, Y.; Ishida, H.; Mizuno, K. *Chem. Lett.*, 2001, **30**, 1224.

68. Shinozuka, K.; Moriguchi, T.; *Pyrene: Chemical Properties, Biochemistry Applications and Toxic Effect*, ed. By P. Ruzicka, T. Kral, Nova Science Publishers Inc., New York, 2013.

69. Sekiguchi, T.; Ebara, Y.; Moriguchi, T.; Shinozuka, K. *Bioorg. Med. Chem. Lett.*, 2007, **17**, 6883.

70. Alfred, L. J.; Dipaolo, J. A. *Cancer Res.*, 1968, **28**, 60.

71. Srinivasan, R.; Tan, L. P.; Wu, H.; Yao, S. Q. *Org. Lett.*, 2008, **10**, 2295.

72. Tan, W. B.; Bhambhani, A.; Duff, M. R.; Rodger, A.; Kumar, C. V. *Photochem. Photobiol.*, 2006, **82**, 20.

73. Piao, W. H.; Wong, R.; Bai, X. F.; Huang, J.; Campagnolo, D. I.; Dorr, R. T.; Vollmer, T. L.; Shi, F. D. *J. Immunol.*, 2007, **179**, 7415.

74. Hargreaves, J. S.; Webber, S. E. *Macromolecules*, 1984, **17**, 235.

75. Rameshbabu, K.; Kim, Y.; Kwon, T.; Yoo, J.; Kim, E. *Tetrahedron Lett.*, 2007, **48**, 4755.

76. Hirose, K.; Shiba, Y.; Ishibashi, K.; Doi, Y.; Tobe, Y. *Chem. Eur. J.*, 2008, **14**, 981.

77. Gimenez, R.; Pinol, M.; Serrano, J. L. *Chem. Mater.*, 2004, **16**, 1377.

78. Lee, S. K.; Yang, W. J.; Choi, J. J.; Kim, C. H.; Jeon, S. J.; Cho, B. R. *Org. Lett.*, 2005, **7**, 323.

79. James, T. D.; Sandanayake, K. R. A. S.; Iguchi, R. ; Shinkai, S. *J. Am. Chem. Soc.*, 1995, **117**, 8982.

80. Gunnlaugsson, T.; Davis, A. P.; Glynn, M. *Chem. Commun.*, 2001, 2556.

81. Bouas-Laurent, H.; Castellan, A.; Desvergne, J. P.; Lapouyade, R. *Chem. Soc. Rev.*, 2000, **29**, 43.

82. Ando, S.; Nishida, J. I.; Fujiwara, E.; Tada, H.; Inoue, Y.; Tokito, S.; Yamashita, Y. *Chem. Mater.*, 2005, **17**, 1261.

83. Mizobe, Y.; Tohnai, N.; Miyata, M.; Hasegawa, Y. *Chem. Commun.*, 2005, 1839.

84. Mizobe, Y.; Miyata, M.; Hisaki, I.; Hasegawa, Y.; Tohnai, N. *Org. Lett.*, 2006, **8**, 4295.

85. Kyushin, S.; Ikarugi, M.; Goto, M.; Hiratsuka, H.; Matsumoto, H. *Organometallics*, **1996,** *15*, 1067.

86. Baeyer, A. *Ber. Dtsch. Chem. Ges.*, 1871, **4**, 555.

87. Sun, W.; Gee, K. R.; Klaubert, D. H.; Haugland, R. P. J. *Org. Chem.*, 1997, **62**, 6469.

88. Kojima, H.; Nakatsubo, N.; Kikuchi, K.; Kawahara, S.; Kirino, Y.; Nagoshi, H.; Hirata, Y.; Nagano, T. *Anal. Chem.*, 1998, **70**, 2446.

89. Kojima, H.; Urano, Y.; Kikuchi, K.; Higuchi, T.; Nagano, T. *Angew. Chem., Int. Ed.*, 1999, **38**, 2899.

90. Mizukami, S.; Kikuchi, K.; Higuchi, T.; Urano, Y.; Mashima, T.; Tsuruo, T.; Nagano, T. *FEBS Lett*., 1999, **453**, 356.

91. Urano, Y.; Kamiya, M.; Kanda, K.; Ueno, T.; Hirose, K.; Nagano, T., *J. Am. Chem. Soc.*, 2005, **127**, 4888.

92. Tanaka, K.; Miura, T.; Umezawa, N.; Urano, Y.; Kikuchi, K.; Higuchi, T.; Nagano, T. *J. Am. Chem. Soc*., 2001, **123**, 2530.

93. Umezawa, N.; Tanaka, K.; Urano, Y.; Kikuchi, K.; Higuchi, T.; Nagano, T. *Angew. Chem. Int. Ed.*, 1999, **38**, 2899.

94. Setsukinai, K.; Urano, Y.; Kakinuma, K.; Majima, H. J.; Nagano, T. *J. Biol. Chem*., 2003, **278**, 3170.

95. Hirano, T.; Kikuchi, K.; Urano, Y.; Higuchi, T.; Nagano, T. *J. Am. Chem. Soc*., 2000, **122**, 12399.

96. Ueno, T.; Urano, Y. ; Setsukinai, K. I.; Takakusa, H.; Kojima, H.; Kikuchi, K.; Ohkubo, K.; Fukuzumi, S.; Nagano, T. *J. Am. Chem. Soc*., 2004, **126**, 14079.

97. Miura, T.; Urano, Y.; Tanaka, K.; Nagano, T.; Ohkubo, K.; Fukuzumi, S. *J. Am. Chem. Soc.*, 2003, **125**, 8666.

98. Treibs, A.; Kreuzer, F. H. *Justus Liebigs Ann. Chem*., 1968, **718**, 208.

99. Wael, E. V. D.; Pardoen, J. A.; Koeveringe, J. A. V.; Lugtenburg, J. *Recl. Trav. Chim. Pays-Bas*, 1977, **96**, 306

100. Bandichhor, R.; Thivierge, C.; Bhuvanesh, N. S. P.; Burgess, K. *Acta. Crystallogr. Sect. E: Struct. Rep.*, 2006, E62, o4310.

101. Kim, E.; Park, S. B. *Chem. Asian J.*, 2009, **4**, 1646.

102. Matayoshi, E. D.; Wang, G. T.; Krafft, G. A.; Erickson, J. *Science*, 1990, **247,** 954.

103. Bullok, K. E.; Maxwell, D.; Kesarwala, A. H.; Gammon, S.; Prior, J. L. ; Snow, M. Stanley, S.; Piwnica-Worms, D. *Biochemistry*, 2007, **46**, 4055.

104. Zheng, G.; Chen, J.; Stefflova, K.; Jarvi, M.; Li, H.; Wilson, B. C. *Proc. Natl. Acad. Sci., USA 2007,* **104**, 8989.

105. Blum, G.; Mullins, S. R.; Keren, K.; Fonovic, M.; Jedeszko, C.; Rice, M. J.; Sloane, B. F.; Bogyo, M. *Nat. Chem. Biol.*, 2005, **1**, 203.

106. Blum, G.; Degenfeld, G. V.; Merchant, M. J.; Blau, H. M.; Bogyo, M. *Nat. Chem. Biol.*, 2007, **3**, 668.

107. George, J.; Teear, M. L.; Norey, C. G.; Burns, D. D. *J. Biomol. Screen*, 2003, **8**, 72.

108. Kuo, C. J.; Chi, Y. H.; Hsu, J. T.A.; Liang, P. H. *Biochem. Biophysic. Research Commun.*, 2004, **318**, 862.

109. Grahn, S.; Ullmann, D.; Jakubke, H. *Anal. Biochem.*, 1998, **265**, 225.

110. Taliani, M.; Bianchi, E.; Narjes, F.; Fossatelli, M.; Urbani, A.; Steinkuhler, C.; De Francesco, R.; Pessi, A. *Anal. Biochem.*, 1996, **240**, 60.

111. Wang, G. T.; Chung, C. C.; Holzman, T. F.; Krafft, G. A. *Anal. Biochem.*, 1993, **210**, 351.

112. Cummings, R. T.; Salowe, S. P.; Cunningham, B. R.; Wiltsie, J.; Park, Y. W.; Sonatore, L. M.; Wisniewski, D.; Douglas, C. M.; Hermes, J. D.; Scolnick, E. M. *Proc. Natl. Acad. Sci., USA* 2002, **99**, 6603.

113. Beekman, B.; Van El, B.; Drijfhout, J. W.; Ronday, H. K.; TeKoppele, J. M. *FEBS Lett.*, 1997, **418**, 305.

114. Garcia-Echeverria, C.; Rich, D. H. *FEBS Lett.*, 1992, **297**, 100.

115. Tyagi, S.; Bratu, D. P.; Kramer, F. R. *Nat. Biotechnol.*, 1998, **16**, 49.

116. Swan, D. C.; Tucker, R. A.; Holloway, B. P.; Icenogle, J. P. *J. Clin. Microbiol.*, 1997, **35**, 886.

117. Huang, S.; Salituro, J.; Tang, N.; Luk, K. C.; Hackett Jr., J.; Swanson, P.; Cloherty, G.; Mak, W. B.; Robinson, J.; Abravaya, K. *Nucleic Acids Res.*, 2007, **35**, e101.

118. Bustin, S. A. *J. Mol. Endocrinol.*, 2002, **29**, 23.

119. Nazarenko, I.; Pires, R.; Lowe, B.; Obaidy, M.; Rashtchian, A. *Nucleic Acids Res.*, 2002, **30**, 2089.

120. Seidel, C. A. M.; Schulz, A.; Sauer, M. H. M. *J. Phy. Chem.*, 1996, **100**, 5541.

121. Saito, Y.; Shinohara, Y.; Bag, S. S.; Takeuchi, Y.; Matsumoto, K.; Saito, I. *Nucleic Acids Symp.*, 2008, **52**, 361.

122. Liu, X.; Tan, W. *Anal. Chem.*, 1999, **71**, 5054.

123. Epstein, J. R.; Leung, A. P. K.; Lee, K. H.; Walt, D. R. *Biosens. Bioelectron.*, 2003, **18**, 541.

124. Broude, N. E. *Trends Biotechnol.*, 2002, **20**, 249.

125. Lou, H. J.; Tan, W. *Instrum. Sci. Technol.*, 2002, **30**, 465.

126. Zhao, X.; Tapec-Dytioco, R.; Wang, K.; Tan, W. *Anal. Chem.*, 2003, **75**, 3476.

127. Martinez, K.; Estevez, M.; Wu, Y.; W. Phillips, W.; Medley, D.; Tan, W. *Anal. Chem.*, 2009, **81**, 3448.

128. Yao, G.; Tan, W. *Anal. Biochem.*, 2004, **331** 216.

129. Kostrikis, L.G.; Tyagi, S.; Mhlanga, M.M.; Ho, D.D.; Kramer, F.R. *Science*, 1998, **279**, 1228.

130. Piatek, A. S.; Tyagi, S.; Pol, A. C.; Telenti, A.; Miller, L. P.; Kramer, F. R.; Alland, D. *Nat. Biotechnol.*, 1998, **16**, 359.

131. Tapp, I.; Malmberg, L.; Rennel, E.; Wik, M.; Syvanen, A. C. *Biotechniques*, 2000, **28**, 732.

132. Ortiz, E.; Estrada, G.; Lizardi, P. M. *Mol. Cell Probes*, 1998, **12**, 219.

133. Weusten, J. J.; Carpay, W. M.; Oosterlaken, T. A.; van Zuijlen, M. C.; van de Wiel, P. A. *Nucleic Acids Res.*, 2002, **30**, E26.

134. Yates, S.; Penning, M.; Goudsmit, J.; Frantzen, I.; van de Weijer, B.; van Strijp, D. van Gemen, B. *J. Clin. Microbiol.*, 2001, **39**, 3656.

135. Komurian-Pradel, F.; Perret, M.; Deiman, B.; Sodoyer, M.; Lotteau, V.; Paranhos-Baccala, G.; Andre, P. *J. Virol. Methods*, 2004, **116**, 103.

136. Shi, H.; He, X.; Wang, K.; Wu, X.; Ye, X.; Guo, Q.; Tan, W.; Qing, Z.; Yang, X.; Zhou, B. *Proc. Natl. Acad. Sci., USA 108*, 2011, 3900.

137. Fang, X.; Li, J. J.; Perlette, J.; Tan, W.; Wang, K. *Anal. Chem.*, 2000, **72**, 747.

138. Matsu, T. *BBA-Gen. Subjects*, 1998, **1379**,178.

139. Sokol, D. L.; Zhang, X. L.; Lu, P. Z.; Gewitz, A. M. *Proc. Natl. Acad. Sci., USA* 1998, **95**, 538.

140. Yang, C. J.; Pinto, M.; Schanze, K.; Tan, W. *Angew. Chem. Int. Ed.*, 2005, **44**, 2572.

141. Mogi, M.; Uddin, M. G.; Ichimura, M.; Moriguchi, T.; Shinozuka, K. *Chem. Lett.*, 2010, **39**, 1254.

142. Sato, Y.; Moriguchi, T.; Shinozuka, K. *Chem. Lett.*, 2012, **41**, 420.

143. Moriguchi, T.; Ichimura, M.; Kato, K.; Suzuki, K.; Takahashi, Y.; Shinozuka, K. *Bioorg. Med. Chem. Lett.*, 2014, **24,** 4372.

144. Krasnoperov, L. N.; Marras, S. A. E.; Kozlov, M.; Wirpsza, L.; Mustaev, A. *Bioconjug. Chem.*, 2010, **21**, 319.

145. Yang, C. J.; Lin, H.; Tan, W. *J. Am. Chem. Soc.*, 2005, **127**, 12772.

146. Kashida, H.; Takatsu, T.; Fujii, T., *Angew. Chem. Int. Ed.*, 2009, **48**, 7044.

147. Dubertret, B.; Calame, M.; Libchaber, A. J. *Nat. Biotechnol.*, 2001, **19**, 365.

148. Kolpashchikov, D.M. *Scientifica*, 2012, Article **ID 928783**.

149. Kim, Y.; Yang, C. J.; Tan, W. *Nucleic Acids Res.*, 2007, **35**, 7279.

150. Kolpashchikov, D. M. *J. Am. Chem. Soc.*, 2006, **128**, 10625.

151. Dirks, R. W.; Molenaar, C.; Tanke, H. J. *Histochem. Cell Biol.*, 2001, **115**, 3.

152. Molenaar, C.; Marras,S. A.; Slats, J. C.; Truffert, J. C.; Lemaitre, M.; Raap, A. K.; Dirks, R.W.; Tanke, H. J. *Nucleic Acids Res.*, 2001, **29**, e89.

153. Li, J. J.; Geyer, R.; Tan,W. *Nucleic Acids Res.*, 2000, **28**, e52.

154. Fisher, T. L.; Terhorst, T.; Cao, X.; Wagner, R. W. *Nucleic Acids Res.*, 1993, **21**, 3857.

155. Leonetti, J. P.; Mechti, N.; Degols, G.; Gagnor, C.; Lebleu, B. *Proc. Natl. Acad. Sci., USA* 88, 1991, 2702.

156. Uchiyama, H.; Hirano, K.; Kashiwasake-Jibu, M.; Taira, K. *J. Biol. Chem.*, 1996, **271**, 380.

157. Shah, R; El-Deiry, W. S. *Cancer Biol. Ther.*, 2004, **3**, 871.

158. Fang, X.; Liu, X.; Schuster, S.; Tan, W. *J. Am. Chem. Soc.*, 1999, **121**, 2921.

159. Seitz, O. *Angew. Chem. Int. Ed. Engl.*, 2000, **39**, 3249.

160. Wang, L.; Yang, C. Y. J.; Medley, C. D.; Benner, S. A.; Tan, W. H. *J. Am. Chem. Soc.*, 2005, **127**, 15664

# Chapter 2

# Synthesis of Novel Stem-Loop type Molecular Beacon Probes Possessing Polyamine-connected Deoxyuridine and Silylated Pyrene and Its Fluorescence Properties

## 2.1 Abstract

A novel molecular beacon (MB) type probe possessing polyamine-bearing deoxyuridine and silylated pyrene in a short stem-portion was synthesized. The probe is assumed to form a pseudo dumbbell-type structure in near physiological condition. Fluorescent signal of the probe was efficiently quenched while the probe stays alone. On the other hand, the signal was significantly increased under the presence of the oligoDNA complementary to the loop portion.

## 2.2 Introduction

Since the first report on DNA sequencing by Walter Gilbert and Fred Sanger in the 1970s, it is becoming a subject of intense research for analysis of genetic information [1-2]. However, in the recent years, detection of specific gene through the hybridization of fluorescence-labelled oligoDNA probes to a target gene is a remarkable advancement in this area for their application in medical diagnostics and genetic studies [3-8]. Many kinds of fluorescent oligonucleotide probes have been developed because of their ease of handling and relative inexpensiveness compared to the classical radio-labeling method [9]. In a practical point of view, it is highly desirable that the probe exhibits strong fluorescent signal upon hybridization with its target gene fragment. This would ensure easy detection of the target [10]. In addition, the probe should be capable of recognizing uncomplimentary dissimilarities of the target, including single-nucleotide alterations, to overcome the chance of wrong detection. Until date, there are several reports on specific fluorescent oligioDNA and oligoRNA probes, such as molecular beacon types of probe [11-15] and other

fluorophore-quencher conjugated probes [16-18], for the detection of specific gene through the binding to complementary and uncomplimentary gene fragments.

One recent development in the area of fluorescent oligoDNA probe is molecular beacon probes. They are single stranded hybridization probes forming a stem-loop structure [19-31]. Most importantly, the molecular beacon probes should generate a very strong fluorescence emission in the presence of target. At the same time, absolutely no fluorescence signal in the absence of targets. However, the fulfillment of this features of molecular beacon probes is very limited. It is still worthwhile searching whether such characteristics of MB probes generated by selecting efficient fluorophore as well as their structural modifications. Recently Maeda *et al.* reported that the fluorescence intensity of substituted pyrene derivatives was either lower or higher than the unsubstituted pyrene depending on their type of substitutions [32]. In case of monosilyl substitution in pyrene, the fluorescence intensity was higher than that of unsubstituted pyrene. However, the intensity of germyl and stannyl substituted pyrene derivatives was lower than that of unsubstituted pyrene. At the same time they also reported that the fluorescence intensity was also increased by increasing the number of silyl substitution in pyrene. The structures of substituted pyrene derivatives and their fluorescence spectra are depicted in the Figure 2.1. Moreover, the UV absorption of all substituted pyrene derivatives shifted longer wavelength compared with the un-substituted pyrene (Table 2.1).

**(a)** **(b)** **(c)**

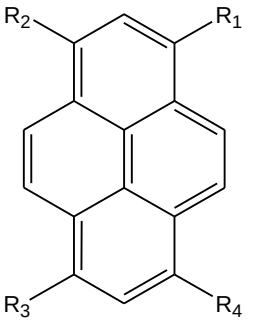


1a: $R_1$= $SiMe_3$, $R_2$=$R_3$=$R_4$=H
1b: $R_1$= $GeMe_3$, $R_2$=$R_3$=$R_4$=H
1c: $R_1$= $SnMe_3$, $R_2$=$R_3$=$R_4$=H
1d: $R_1$= $R_2$=$R_3$=$R_4$=H
1e: $R_1$= $R_3$=$SiMe_3$, $R_2$=$R_4$=H
1f: $R_1$= $R_4$=$SiMe_3$, $R_2$=$R_3$=H
1g: $R_1$= $R_2$= $R_3$=$SiMe_3$, $R_4$=H
1h: $R_1$= $R_2$= $R_3$=$R_4$=$SiMe_3$

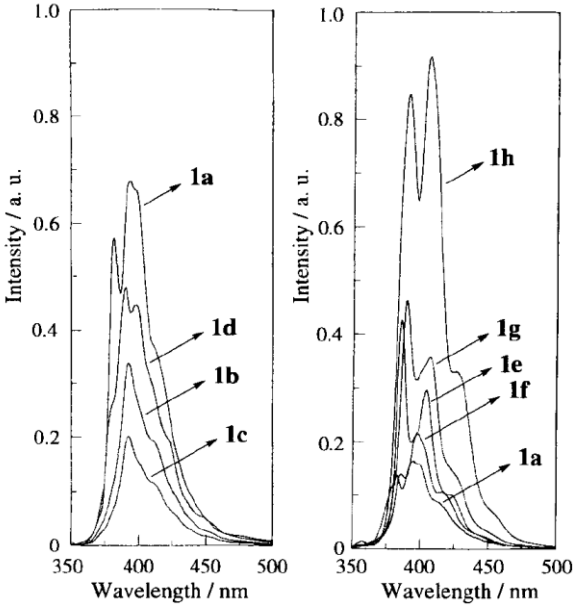


**Figure 2.1: (a)** Structure of substituted pyrene derivatives **(b)** Fluorescence spectra of mono substituted pyrene derivatives **(c)** Fluorescence spectra of multi-substituted pyrene derivatives [cited from ref. 32]

**Table 2.1:** Absorption maximum of substituted pyrene derivatives [cited from ref. 32]

| Compound | 1a | 1b | 1c | 1d | 1e | 1f | 1g | 1h |
|---|---|---|---|---|---|---|---|---|
| Absorption maximum | 344.5 | 343.5 | 344.0 | 334.5 | 354.5 | 355.0 | 365.0 | 375.0 |

Meanwhile, Shinozuka *et al.* reported novel oligoDNA conjugated with dimethylsilyl pyrene moiety at its 5′-terminus showed marked fluorescence emission only upon binding with full match complements [9]. They also reported that the fluorescent emission of the

silylated pyrene connected with oligonucleotides depends on the base composition of the 5′-end nucleotides. They further investigated the influence of neighboring base on the fluorescence property of silylated pyrene by making different monomer nucleotides using the four nucleobases (A, C, T and G). The fluorescent spectra of monomer nucleotides of different base containing silylated pyrene are shown in Figure 2.2. They observed strong fluorescence quenching property of silylated pyrene when the neighboring nucleobase is G, C or T.

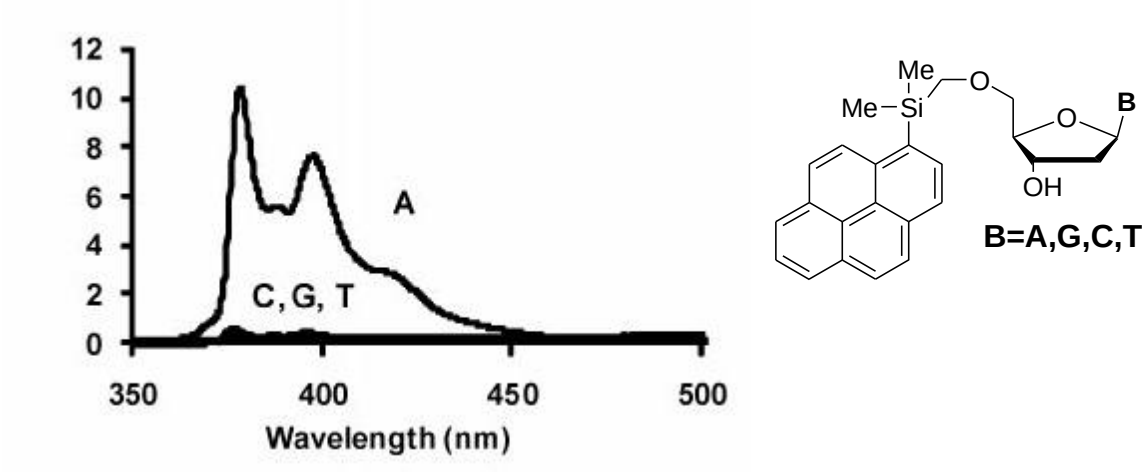


**Figure 2.2:** Fluorescence Spectra of 5′-silylated pyrene nucleotides derivatives [cited from ref. 33].

Whereas, the fluorescence emission of adenosine base was not quenched as much as the G, C and T. They proposed the mechanism of quenching behavior by the presence of neighboring base is due to photo induced electron transfer between the silylated pyrene and the nucleobase [33]. Based on these findings, dimethylsilaylated pyrene is used in this study as a fluorophore for designing the novel stem loop type molecular beacon probes where natural nucleoside residue is expected to function as a quencher.

Significant improvements in the design and development in the structure of molecular beacon have recently been reported [34-39]. A most recent examples of such improvements are the development of quencher free molecular beacon probe [40-44]. There are many types of quencher free MB probe designed until date. One of the way of designing such quencher free MB probe is the introduction of a fluorophore in the stem which has a terminal guanosine (G) base as a quencher at the opposite of the stem terminus (Figure 1.5, chapter 1) [44]. The other researcher designed by placing a fluorophore attached to pyrrolocytidine in the middle of the stem which also has a guanosine base at the opposite of fluorophore bearing pyrrolocytidine (Figure 2.3) [45].

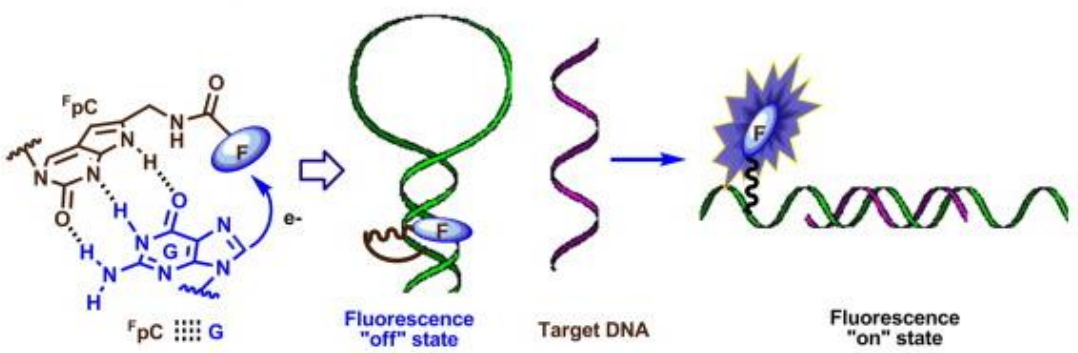


**Figure 2.3:** End free and quenched free MB probes [cited from ref. 45].

Recently, our group synthesized a novel fluorescent oligoDNA probe bearing silylated pyrene derivative at C-2′ position of deoxyuridine. The silylated pyrene derivatives were incorporated into two consecutive positions of the OligoDNA. It showed an excimer emission upon binding with fully matched complementary DNA strand while both the excimer and monomer emission were quenched while staying alone or hybridize to a single base mismatched complementary target [46]. One major problem of using this technique is that the fluorescent strength of the probe after binding to the correct target DNA is only 5-

folds higher compared to that of the probe staying alone. Idealistic probe should give more than 20-folds stronger signal, at least. Our group also reported that an oligoDNA incorporated with modified deoxyuridine residues bearing polyamine group at C-5 position instead of natural thymidine residues exhibited enhanced duplex-forming ability due to the reduction of electronic repulsion between the two strands [47].

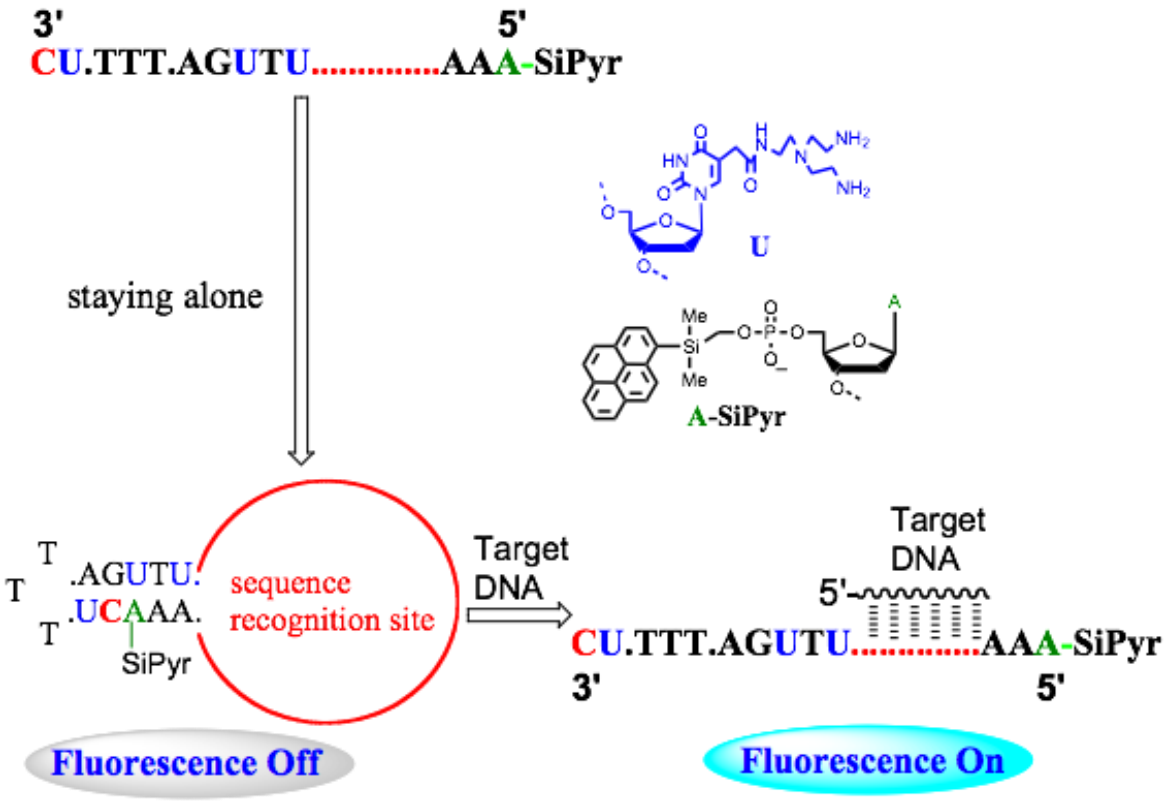


**Figure 2.4:** Schematic diagram of the proposed pseudo dumbbell type molecular beacons and their principle of activity.

Based on the knowledge, described above, I have designed a new molecular beacon type of probe outlined in Figure 2.4. In this probe, silylated pyrene molecule is attached to the 5´-terminus neighboring consecutive dA residues of an oligoDNA. At the same time, the probe has partial self-complementary sequence and, therefore, the probe would form a pseudo

dumbbell type of secondary structure as it is depicted in Figure 2.4. In this form, silylated pyrene connected next to consecutive dA residues will be in a closed proximately position of dC residue at 3′-terminus and the fluorescence signal of the silylated pyrene would be effectively quenched by the action of dC residue. Once the probe meets the complementary DNA in a solution, the secondary structure of the probe will be dissolved and the probe would form normal duplex with the target. In this stage, the fluorescent signal of the silylated pyrene will recovers since it is positioned far away from dC residue at 3′-terminus. In this probe, the modified deoxyuridine residues bearing polyamine at C-5 position described above should be included in certain position of the probe to increase the stability of the dumbbell type of secondary structure to minimize the length of the stem sequence of the probe.

## 2.3 Results and Discussion

### 2.3.1 *Synthesis of [1-(Pyrenyl)dimethylsilylmethyl]-(2-cyanoethyl)-N,N-diisopropyl-phosphoramidite (5)*

Scheme 2.1 shows the synthesis of the phosphoramidite derivative of silylated pyrene derivative. Compound **2** (1-Bromopyrene) was prepared by reaction of pyrene (**1**) with *N*-bromosuccinimide at room temperature in DMF. Resulting 1-Bromopyrene (**2**) was treated with *n*-BuLi in dry THF (-78°C) under $N_2$ atmosphere followed by the addition of chlorodimethylsilyl chloride to give the corresponding silylated pyrene (**2**). The obtained compound **2** was treated with sodium acetate in aqueous DMF at 100°C to make an acetoxy derivative **3**, which was then treated with NaOH in aqueous methanol to produce compound **4** bearing hydroxyl group. The phosphoramidite derivative of dimethylsilylated pyrene

(compound **5**) was prepared by mixing with *N*,*N*-diisopropylethylamine in dry dichloromethane and was stirred under $N_2$ atmosphere at room temperature. Thereafter, the phosphitylating reagent, chloro-(2-cyanoethoxy) diisopropylamino-phosphine was added drop wise to the previous mixture under $N_2$ atmosphere at room temperature. The crude product was purified by silica-gel column chromatography.

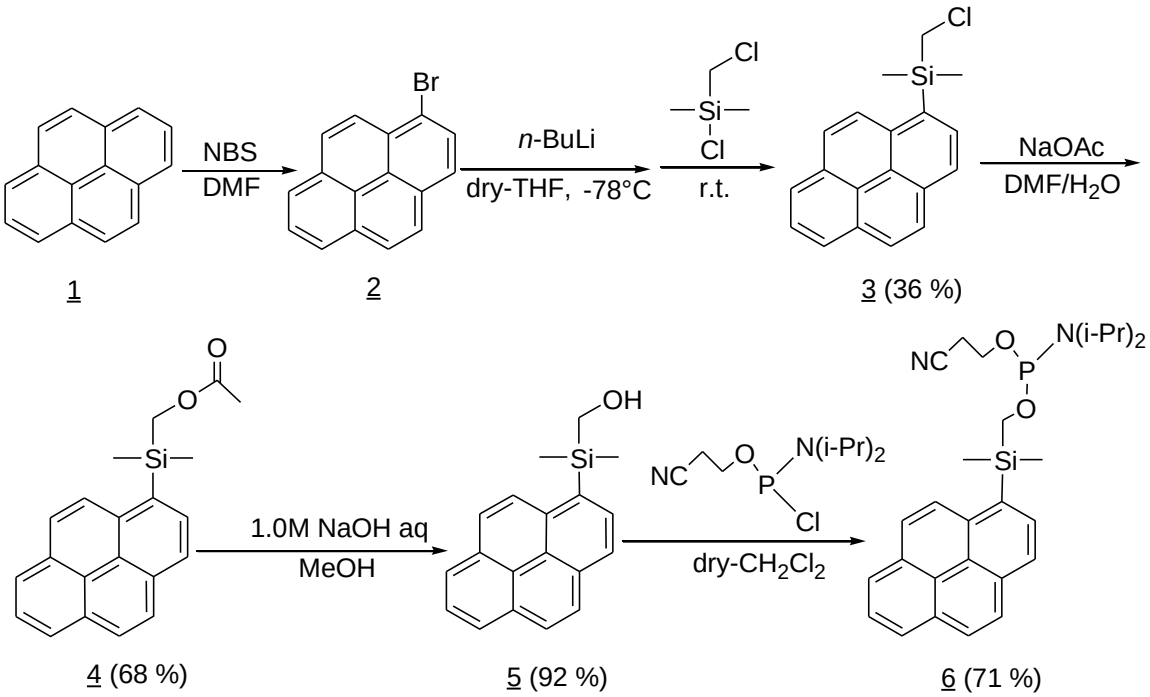


**Scheme 2.1:** Synthesis of [1-(Pyrenyl)dimethylsilylmethyl]-(2-cyanoethyl)-*N*,*N*-diiso-propylphosphoramidite (5) [ref. 48]

### 2.3.2 *Synthesis of 5´-O-(4,4´-Dimethoxytrityl)-5-[N-[2-N,N-bis(2-trifluoroacetamidethyl) amino]ethyl]carbamoylmethyl-2´-deoxyuridine-3´-O-yl(2-cyanoethyl)-N,N-diisopropyl-phosphoramidite (14).*

The synthetic pathway of compound **14** from compound **6** is depicted in the Scheme 2.2. At first, D-Arabinose (**6**) was refluxed with cyanamide and potassium carbonate in dimethylformamide (DMF) to synthesize the compound **7**. Compound **7** was then converted to compound **8** by bromomethylfumaric acid dimethyl ester in methanol under reflux. Then the 3´- and 5´- hydroxyl groups in the resulting compound 8 were protected by acetylation to prevent the formation of any unwanted by-product in the next step. The compound **9** was then refluxed in toluene with tri-*n*-butyltin hydride ($Bu_3SnH$) and alpha isobutyronitrile (AIBN) to have the de-brominated analogue of compound **10.** Then the compound **10** was mixed with tris (2-aminoethyl)amine and 4-dimethylaminopyridine in methanol to synthesize compound **11**. The reaction mixture was then evaporated and coevaporated with methanol, the residue was dissolved in a small amount of methanol and added drop wise to benzene to precipitate compound **11** as an oily residue. Then the terminal amino group of compound **11** was protected by trifluoroacetyl group without further purification and synthesized compound **12**. The incorporation of DMTr- group on compound **12** was accomplished by reacting with 4,4´-dimethoxytrityl-chloride (DMTr-Cl) in pyridine containing 4-dimethylaminopyridine at room temperature. Then the synthesized compound **13** was mixed with *N*,*N*-diisopropylethylamine in dry dichloromethane and was stirred under $N_2$ atmosphere at room temperature. Then the phosphitylating reagent, chloro-(2-cyanoethoxy) diisopropylaminophosphine was added to the previous solution to synthesize phosphoramidite derivative compound **14**. Finally, the crude product was purified by silica-gel column chromatography.

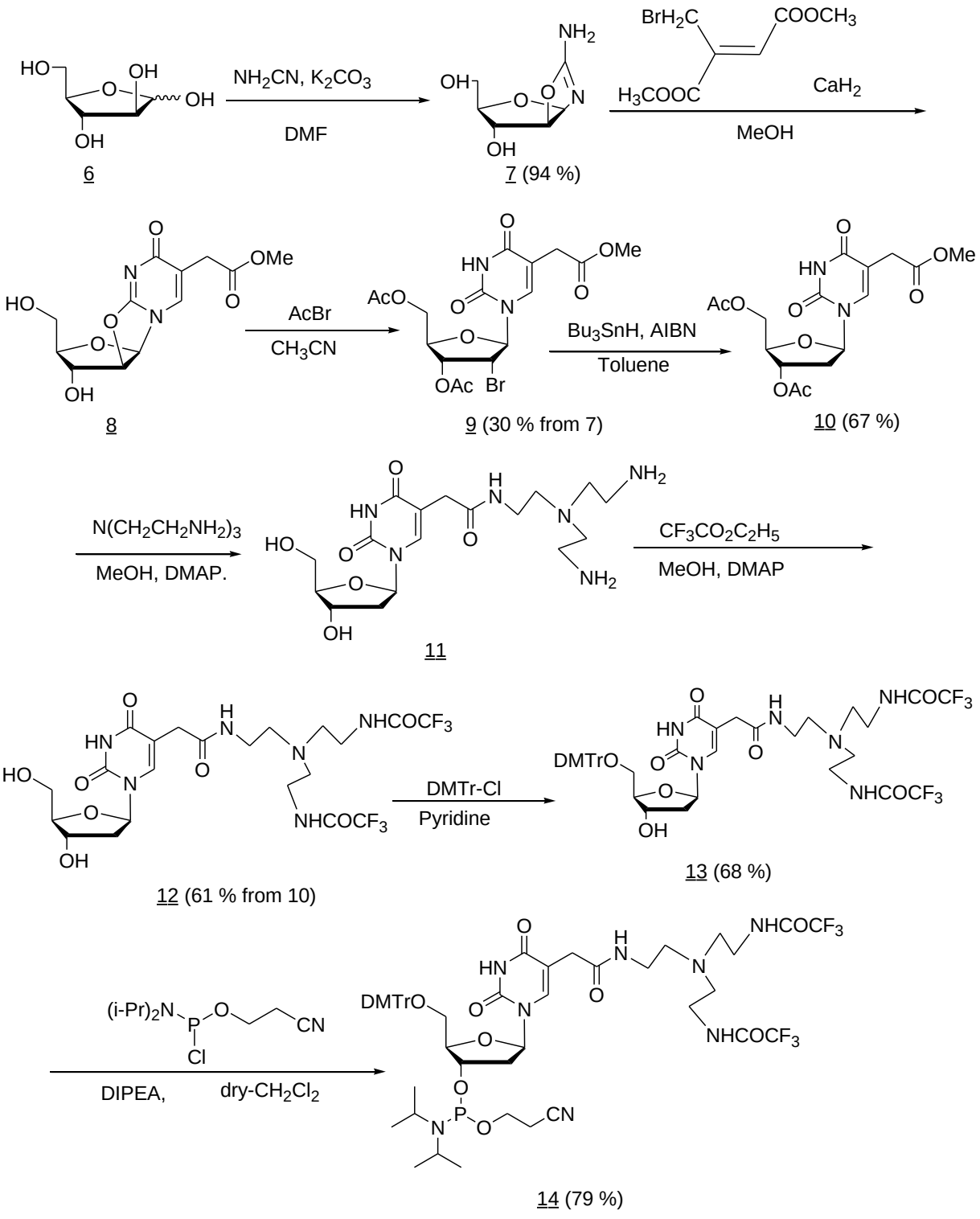


6

7 (94 %)

8

9 (30 % from 7)

10 (67 %)

11

12 (61 % from 10)

13 (68 %)

14 (79 %)

**Scheme 2.2.** Synthesis of 5´-*O*-(4,4´-dimethoxytrityl)-5-[*N*-[2-*N*,*N*-bis(2-trifluoroacetamidethyl)amino]ethyl]carbamoylmethyl-2´-deoxyuridine-3´-*O*-yl(2-cyanoethyl)-*N*,*N*-diisopropylphosphoramidite [ref. 49-50]

### 2.3.3 *Synthesis of modified oligoDNA possessing polyamine-connected deoxyuridine and silylated pyrene*

The modified oligonucleotides possessing polyamine-connected deoxyuridine and silylated pyrene (**GK-2139**) were synthesized using an automated DNA synthesizer (ABI 392). The structure and sequences of the synthesized oligonucleotides are depicted in Table 2.2. The incorporation of the C 5 polyamine-modified deoxyuridine derivative into the oligonucleotides was carried out using method described previously [49-50]. On the other hand, the incorporation of phosphoramidite derivative of dimethylsilylated pyrene was carried out in a manner similar to that described previously [48]. It should be noted that the coupling periods used in the synthesis for the phosphoramidite derivate of C 5 polyamine bearing deoxyuridine and phosphoramidite derivative of dimethyl silylated pyrene were extended to 360 s. After the assembly, the support-bound fluorescent oligoDNA was treated with concentrated ammonium hydroxide (55 ˚C, 12 h). The oligonucleotides were then purified by reversed-phase HPLC (DMTr-ON, Figure 2.5). After purified by HPLC, the oligonucleotides were subjected to ethanol precipitation and Sephadex G- 25 gel filtration. The obtained oligonucleotides were further analyzed by reverse-phase HPLC to check their purity level (DMTr-ON, Figure 2.6). The structures of the oligonucleotides were confirmed by ESI-mass Spectrophotometer (Table 3). The UV spectra analysis of these oligonucleotides also confirmed the incorporation of dimethyl silylated pyrene by showing a peak at around 350 nm (Figure 2.7). The % yield of the synthesized oligonucleotides were calculated and presented in Table 2.3.

Further, the oligonucleotides (**GK-2140**) was also synthesized by placing thymidine instead of the places of polyamine-bearing deoxyuridine to check the effect of duplex stability enhancement caused by the incorporation of polyamine-bearing deoxyuridine. At the same

time, complementary DNA (**GK-1104**) and one base mismatch complementary DNA (**GK-1105**) were also synthesize to investigate the newly designed probe **GK-2139**. The structure and sequences of the **GK-2140** and complementary DNA and non-complementary DNA are also depicted in Table 2.2. The % yield and ESI-mass data of **GK-2140**, **GK-1104** and **GK-1105** are also presented in Table 2.3.

**Table 2.2**. Sequence and structure of modified oligonucleotides

| Name | Sequence [a,b,c] |
|---|---|
| **GK-2139 (Probe 1)** | 3′-CUTTTAGUTU*AAGTACTGTTTTCGG*AAA-X-5′ |
| **GK-2140** | 3′-CTTTTAGTTT*AAGTACTGTTTTCGG*AAA-X-5′ |
| **GK-1104 (ODN-1)** | 5′-TGT*TTCATGACAAAAGCC*-3′ |
| **GK-1105 (ODN-4)** | 5′-TGT*TTCAT**C**ACAAAAGCC*-3′ |

U =

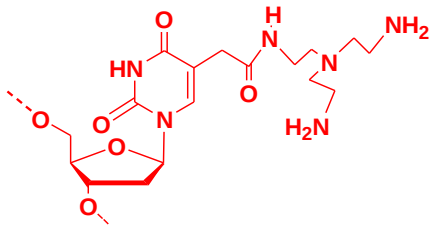


X =

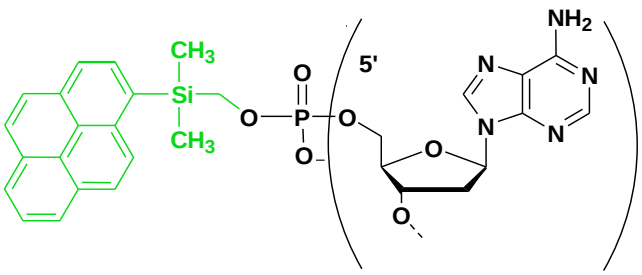


[a] U denotes the polyamine bearing deoxyuridine, X denotes the dimethyl silylated pyerene, [b] Italicized letters indicate the complementary region to ODN-Probe. [c] Bold and underlined letters in ODN 4 indicate the corresponding single-nucleotide alternations to fully matched target DNA (**ODN-1**).

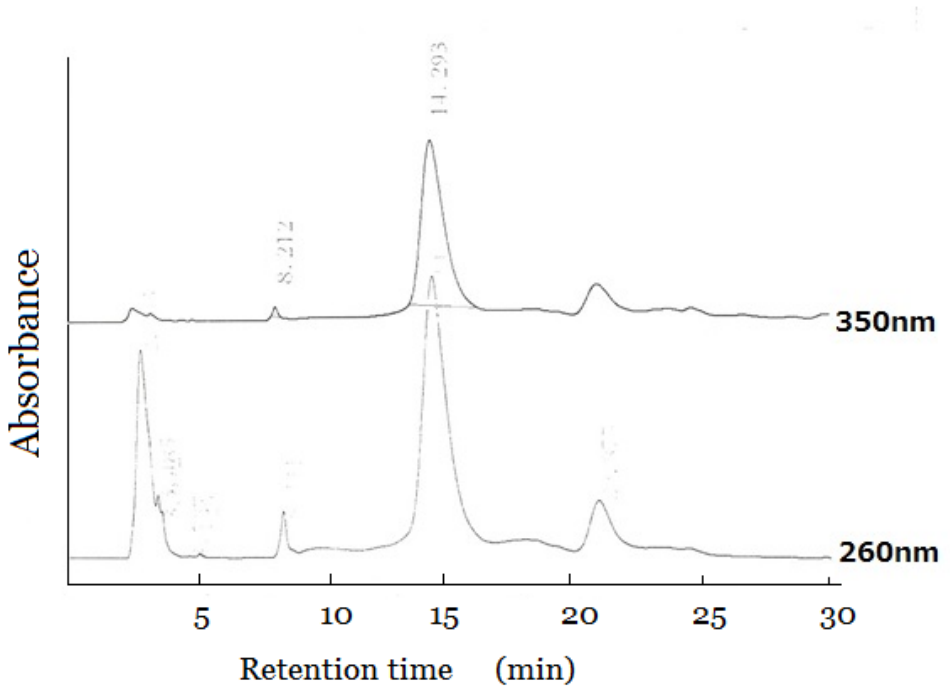


**HPLC Condition**

Column: Wakosil 5 C18 (Ø 4.6mm X 250mm)

Flow rate: 0.75 ml/min

**DMTr-ON**

Eluent: A: 100 mM TEAA

B: Acetonitrile

Gradient:

| Time (min.) | 0 | 10 | 20 | 30 |
|---|---|---|---|---|
| B (%) | 20 | 25 | 30 | 40 |

**Figure 2.5:** HPLC profile of **GK-2139** at 260 nm and 350 nm before purification.

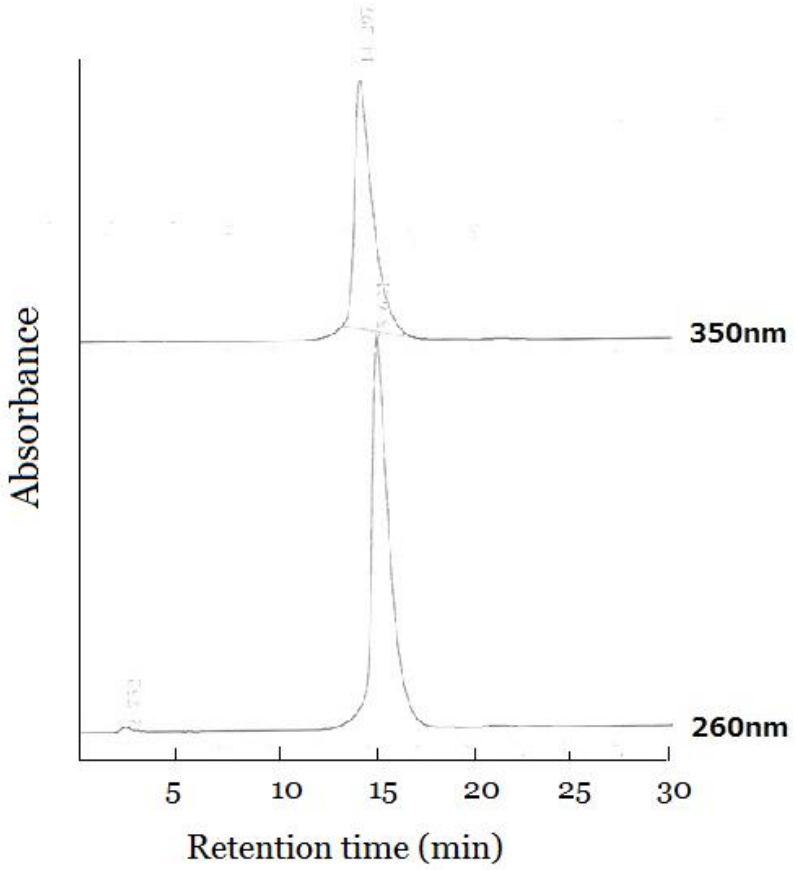


**HPLC Condition**

Column: Wakosil 5 C18 (Ø 4.6mm X 250mm)

Flow rate: 0.75 ml/min

**DMTr-ON**

Eluent: A: 100 mM TEAA

B: Acetonitrile

Gradient:

| Time (min.) | 0 | 10 | 20 | 30 |
|---|---|---|---|---|
| B (%) | 20 | 25 | 30 | 40 |

**Figure 2.6:** HPLC profile of **GK-2139** at 260 nm and 350 nm after purification.

**Table 2.3:** Optical density (OD), isolated yield and ESI-mass data of the oligonucleotides

| Oligonucleotides | ESI-mass | | OD[a] (/ml) | Isolated Yield (%) |
|---|---|---|---|---|
| | Found | Calculated | | |
| GK-2139 | 9468.79 | 9468.67 | 48.5 | 17.2 |
| GK-2140 | 8952.00 | 8951.98 | 75.7 | 27.3 |
| GK-1104 | 5562.74 | 5562.57 | 47 | 26.9 |
| GK-1105 | 5522.70 | 5522.55 | 24.5 | 14.3 |

[a]Optical density is the absorbance of the oligonucleotides at 260 nm per unit distance

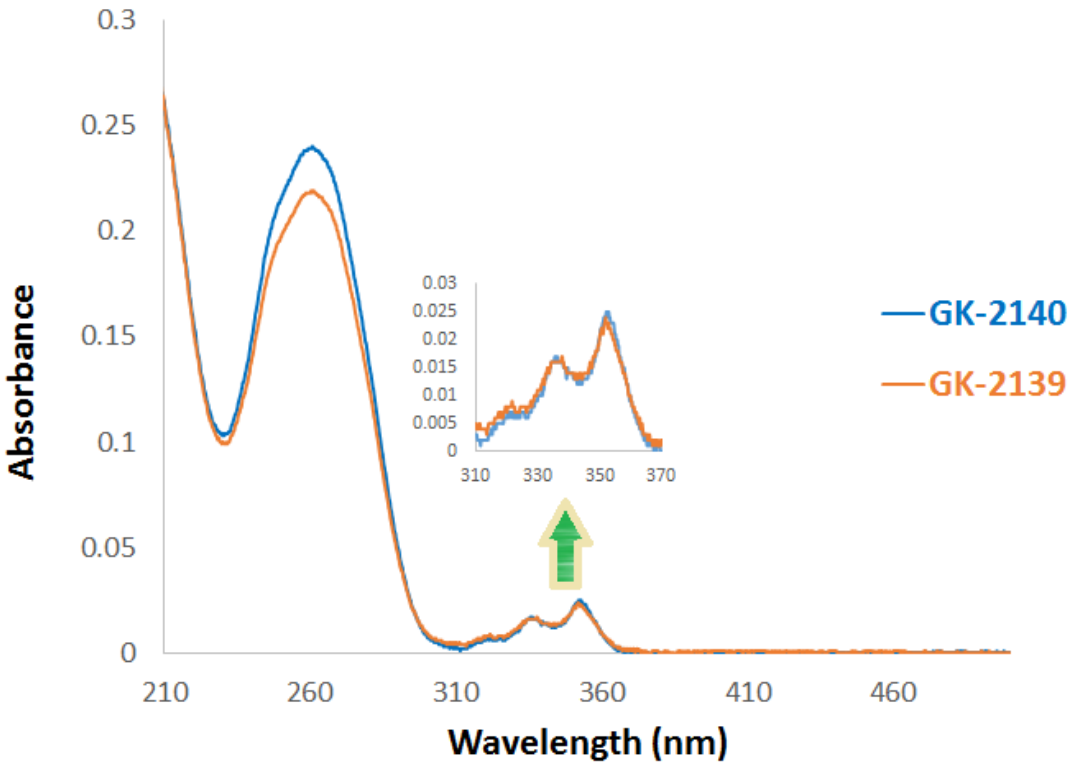


**Figure 2.7:** UV spectra of modified oligonucleotides **GK-2139** and **GK-2140**.

### 2.3.4 *Duplex forming ability of new MB probes.*

The duplex forming ability of the new molecular beacon probes possessing polyamine-connected deoxyuridine and also silylated pyrene was studied by circular dichroism (CD) spectroscopy (Figure 2.8). The CD spectra were taken for **GK-2139** and its full match duplex with complementary DNA (**GK-1104**) as well as duplex with **GK-1105** which contains one mismatch at the middle of the duplex forming region. Spectra of the corresponding duplex DNA shows clear positive and negative Cotton effect (peak and trough) within the wavelength region of 250 to 280 nm.

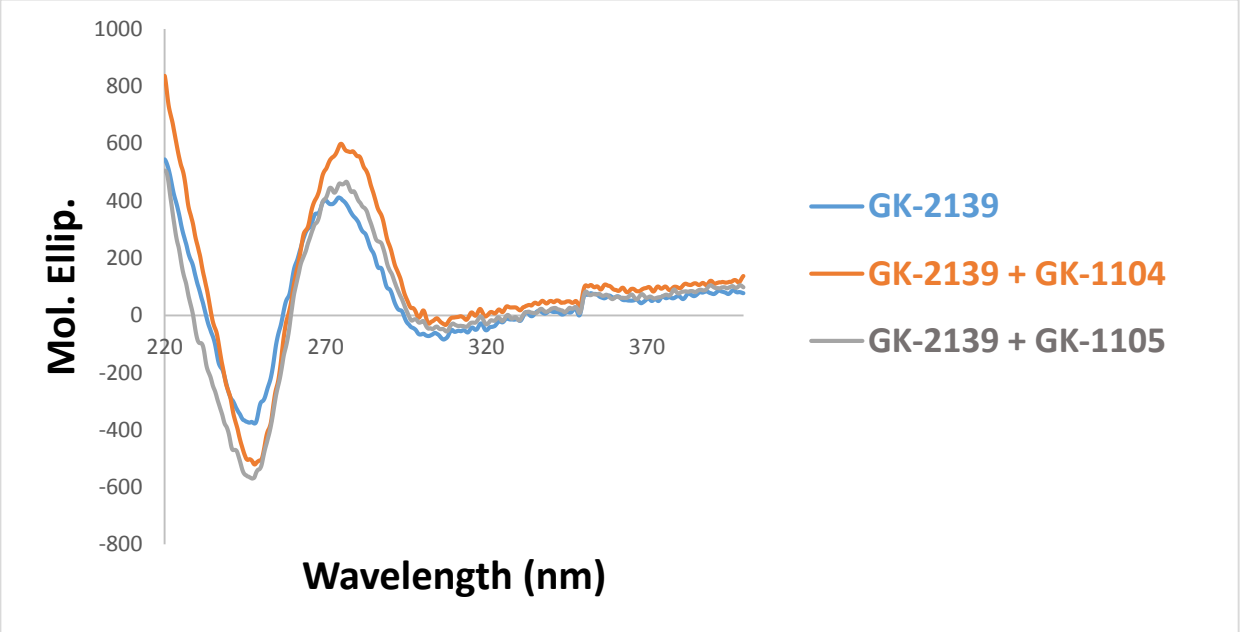


**Figure 2.8:** CD spectra of modified oligomer **GK-2139** and its duplex with full-match (**GK-1104**) and one mismatched complement (**GK-1105**). DNA concentration was 1.0 µM each, buffer: 10 mM sodium phosphate and 100 mM sodium chloride.

### 2.3.5 *Fluorescence properties of new molecular beacon probes.*

Fluorescence spectra of mononucleotides containing silylated pyrene at their 5′-terminus were measured in a buffer of 10 mM sodium phosphate and 100 mM sodium chloride at room temperature using F4500 Fluorescence Spectrophotometer with an excitation wavelength of 350 nm. The concentration of mononucleotides were used 1.5 μM in each cases. Figure 2.9 showed fluorescent spectra of 4 natural deoxynucleotide monomers bearing silylated pyrene at 5′-position along with a corresponding pseudo nucleotide having OMe group at C-1′ position instead of nucleobase [51]. As it is clear from Figure 2.9, fluorescence signal was extensively quenched on G, C and T and their $\Phi_f$ values are less than one-tenth of that of silylated pyrene. Meanwhile the quenching seems to be minimal in the case of A because its $\Phi_f$ value was close to that of the pseudo nucleotide. The observed quenching could be due to a photo-induced electron transfer (PET) mechanism between the excited pyrene moiety and the nucleobases [52].

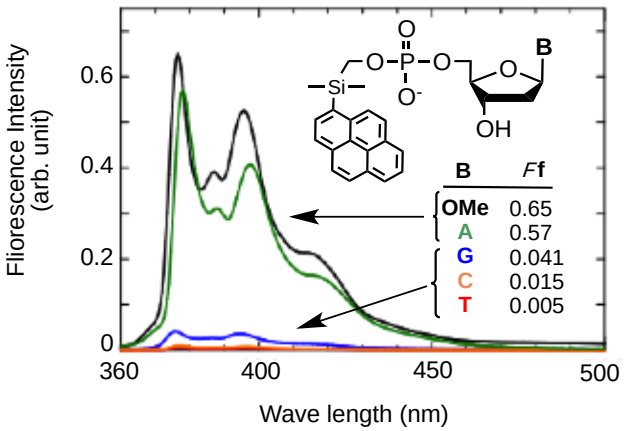


**Figure 2.9:** Fluorescence spectra and fluorescent quantum yield (Φf) of mononucleotides bearing silylated pyrene at their 5′-terminus. The spectra were measured with 1.5 μM of mononucleotide in 10 mM sodium phosphate buffer (pH 7.2) containing 100 mM NaCl. (Reproduced with the permission from ref. 53. Copyright 2015, Chemical Society of Japan)

Based on these findings, I prepared a novel stem-loop type molecular beacon probe without end labeled-quencher molecule. Figure 2.10 showed the sequence and tentative structures of the probe (**GK-2139**). The large loop-portion of **GK-2139** consisting of 15 nucleotide units was expected to act as the binding portion to an oligonucleotide having complementary sequence. The small loop-portion and the stem-portion were expected to put the silylated pyrene of the 5 ′-terminus to the proximal position of the quencher nucleotide (C) 3′-terminus. In the stem-portion, natural T residues were substituted with C-5 polyamine-bearing deoxyuridine residues (U) as it is indicated in the Figure 2.10. The polyamine-bearing deoxyuridine was effective to increase thermal stability of duplex involved.

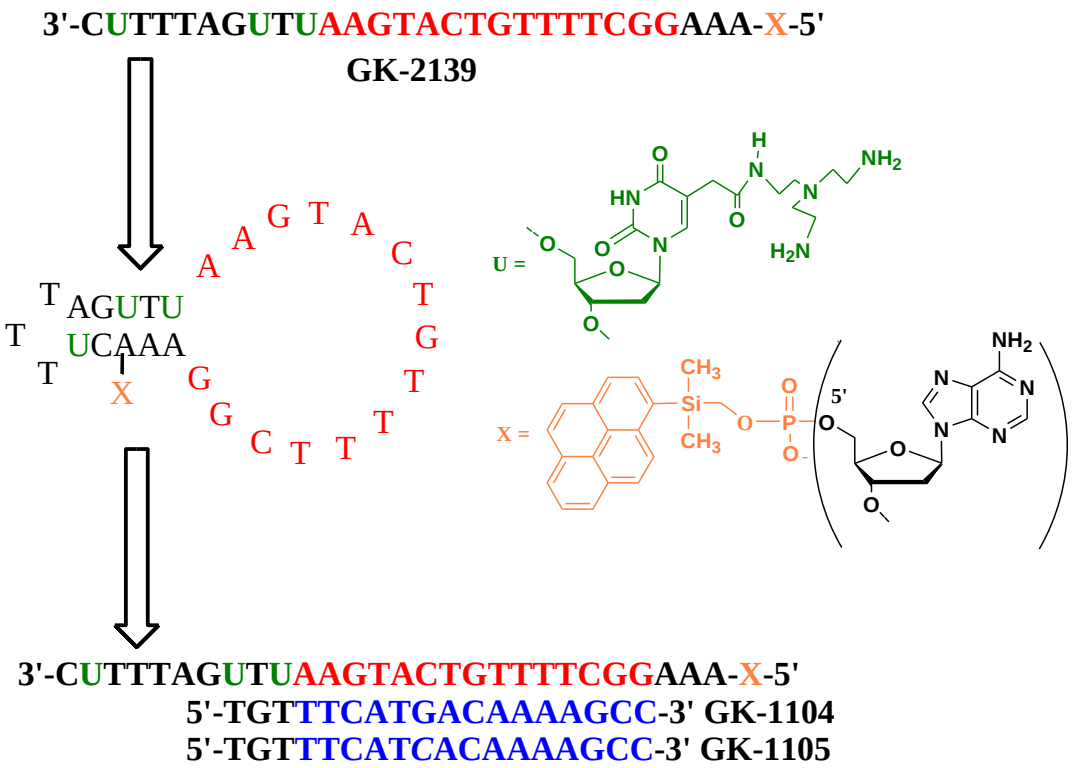


**Figure 2.10:** Sequence and tentative structure of **GK-2139** bearing silylated pyrene moiety at its 5′-terminus through phosphodiester linkage. The red colored part in **GK-2139** is complementary to the blue colored part in **GK-1104**. In **GK-1105**, the ninth nucleotide of **GK-1104** is substituted with C (italicized). (Reproduced with the permission from ref. 53. Copyright 2015, Chemical Society of Japan)

Next, fluorescence spectra of the probes in the absence and presence of the complementary oligoDNA were measured to find out whether the fluorescence signal of the probes responds to the presence of the target oligoDNA. The spectra were measured in 10 mM sodium phosphate and 100 mM sodium chloride at room temperature using F4500 Fluorescence Spectrophotometer with an excitation wavelength of 350 nm. The results are depicted in Figure 2.11. As it is shown in Figure, **GK-2139** exhibited very faint signal under the absence of GK-1104. $\Phi_f$ value for **GK-2139** in the condition was 0.008 (Table 2.4). This could be

**Table 2.4**. Quantum yield value of **GK-2139** and **GK-2140** and their duplexes with full match targets and mismatch targets

| Oligonucleotides | Quantum Yield |
|---|---|
| GK-2139 | 0.008 |
| GK-2140 | 0.015 |
| GK-2139+GK-1104 | 0.160 |
| GK-2140+GK-1104 | 0.162 |
| GK-2139+GK-1105 | 0.050 |

attributed by the fluorescence-quenching effect of C as described above since **GK-2139** is expected to form secondary structure in which the silylated pyrene at the 5′-terminus is in the proximal position of the quencher nucleotide (C) at 3'-terminus. Fluorescence signal of **GK-2140** was also quenched ($\Phi_f$ = 0.015) under the absence of **GK-1104**, however, the extent of the quenching is not as extensive as the case of **GK-2139**. Because the thermal stability of the secondary structure of **GK-2140** is lower than that of **GK-2139**, the

probability for the silylated pyrene to be in the proximal position to the quencher nucleotide in **GK-2140** would also be lower than that of **GK-2139**.

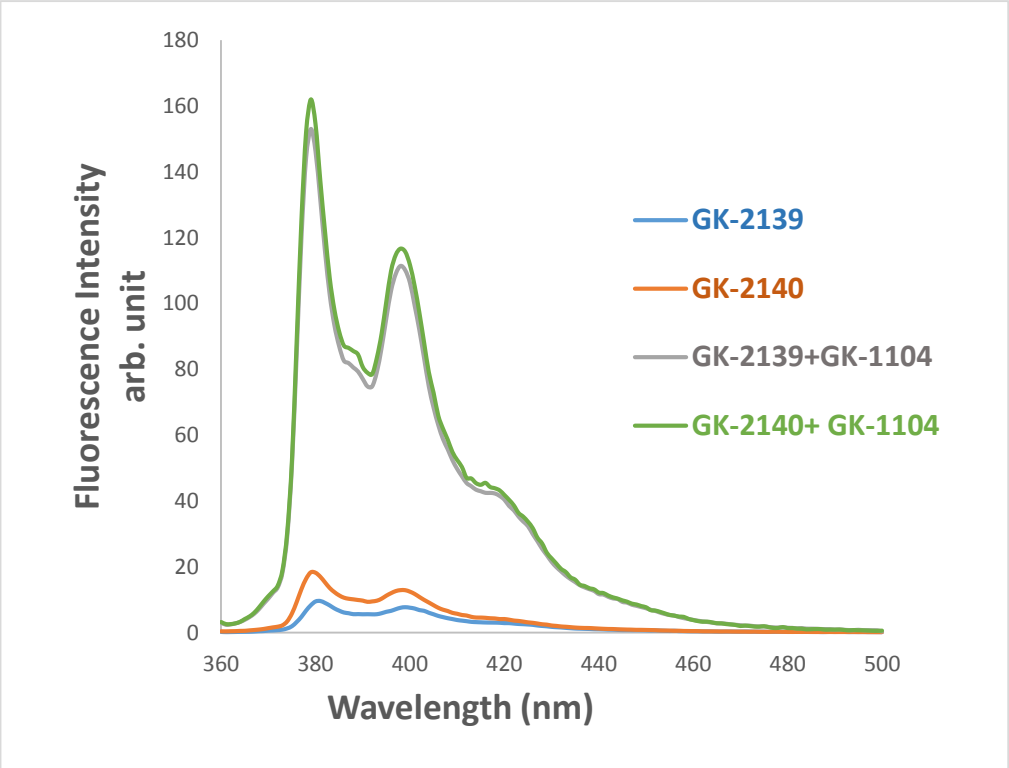


**Figure 2.11**: Fluorescence spectra of **GK-2139** and **GK-2140** under the absence and presence of the complements with 1 μM of DNA in 10 mM sodium phosphate buffer (pH 7.2) containing 100 mM NaCl under the irradiation of uv-light (350 nm) at room temperature. (Reproduced with the permission from ref. 53. Copyright 2015, Chemical Society of Japan)

On the other hand, fluorescence signals of the probes were markedly increased under the presence of **GK-1104** as those are shown in Figure 2.11. The intensity of the signal for **GK-2139** and **GK-2140** under the condition are almost same magnitude and observed $\Phi_f$ values were about 0.16. The change of the fluorescence signal of **GK-2139** under the absence and

presence of **GK-1104** can be clearly recognized by naked eyes as it is depicted in Figure 2.12.

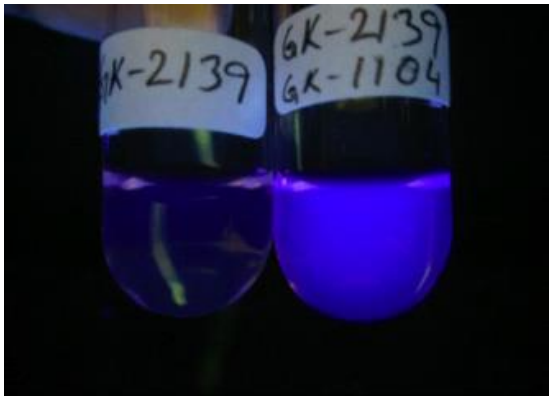


**Figure 2.12:** Fluorescence signal of **GK-2139** alone (left), **GK-2139**+**GK-1104** (right) with concentration of 3 μM of DNA in the same buffer system as above under the irradiation of uv-light (350 nm) at room temperature. (Reproduced with the permission from ref. 53. Copyright 2015, Chemical Society of Japan)

The observed increment of the signal can be attributed to the resolution of the secondary structure of the probes along with the formation of double helical complex with the complement. Φf values of **GK-2139** and **GK-2140** under the presence of **GK-1104** was, however, rather lower than that of silylated pyrene attached to 5′-terminus of deoxyadenosine mononucleotide described above ($\Phi_f$ = 0.57). This could be partially reasoned by long-range fluorescence quenching effect of deoxyguanosine residues near 5′-terminus [54-55].

### 2.3.6 *The effect of mismatch in the target DNA to the fluorescence signal of the probes*

I further examined the effect of the one-base substitution in the complementary DNA to the fluorescence signal of the complex using **GK-1105** in which the ninth deoxyguanosine residue from 5′-terminus of **GK-1104** is substituted with cytidine residue. The fluorescence spectrum of the complex consisting of **GK-2139** and **GK-1105** is also depicted in Figure 2.13.

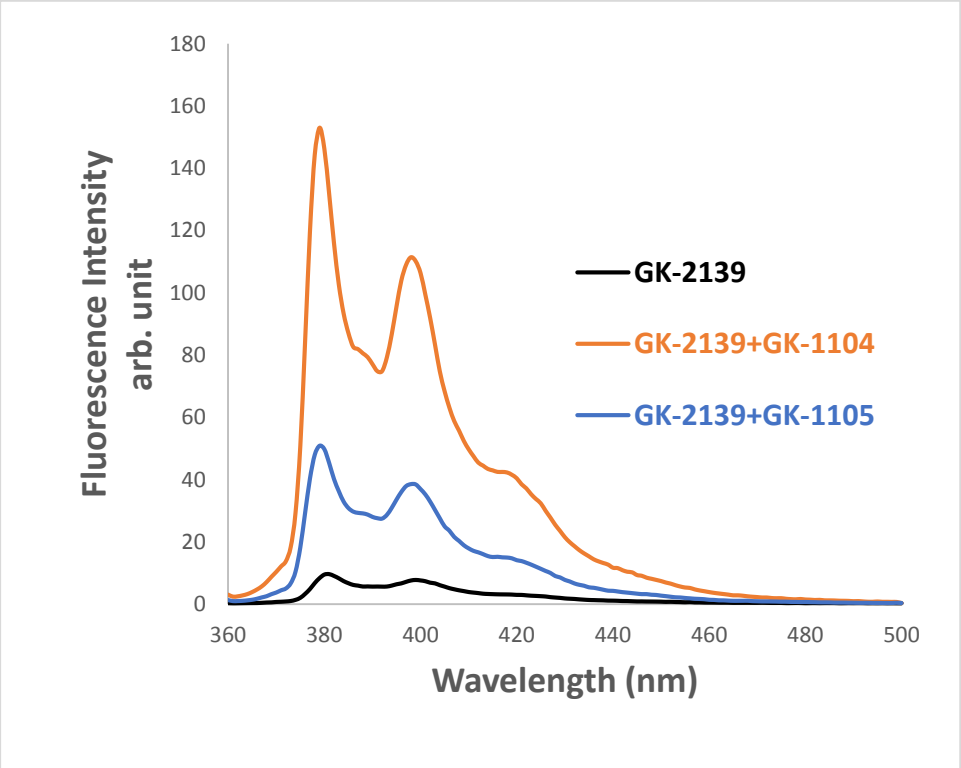


**Figure 2.13:** Fluorescence spectra of **GK-2139** under the absence and presence of the complements with 1 μM of DNA in 10 mM sodium phosphate buffer (pH 7.2) containing 100 mM NaCl under the irradiation of uv-light (350 nm) at room temperature.

As it is shown in Figure 2.13, fluorescence signal of the complex was significantly lower than that of the complex consisting of **GK-2139** and **GK-1104**. Thus, the current stem-loop type of probe may have some sequence discrimination ability in term of its fluorescence signal strength and would be useful new probe to detect gene fragments in solution.

### 2.3.7 *Thermal stability of new molecular beacon probes.*

The thermal stability of the secondary structure of **GK-2139** along with the corresponding oligoDNA, **GK-2140**, which has natural T residues instead of polyamine-bearing deoxyuridine residues was carried out by uv-melting experiments and the results are summarized in Table 2.5. As it is clear from Table 2.5, secondary structure of **GK-2139** bearing 3 residues of C-5 polyamine-bearing deoxyuridine in the stem-portion exhibited much higher stability compared to the corresponding **GK-2140** since observed melting temperature of **GK-2139** is more than 10°C higher than that of **GK-2140**. This could be attributed by the duplex-stabilizing effect of the modified deoxyuridine residues in **GK-2139** [47]. **GK-2139** and **GK-2140** were annealed with complementary oligoDNA, **GK-1104**, and the melting points of the resulting complexes were also measured. Obtained data indicates that the thermal stability of the complex consisting of **GK-2139** and **GK-1104** is nearly same as that of the complex consisting of **GK-2140** and **GK-1104** since their melting points are almost same value. This would be reasonable because the sequence-recognizing portion (a large loop-portion) in **GK-2139** and **GK-2140** is identical. Further, the effect of the one-base substitution in the complementary DNA to the thermal stability of the complex using **GK-1105** was investigated. The melting temperature ($T_m$) of the **GK-2139** and **GK-1105** duplex was 36.9°C and it was significantly lower (-14.5°C) than that of the **GK-2139** and **GK-1104** duplex.

**Table 2.5**. Melting temperatures (*Tm*) of the probes and their duplexes. ((Reproduced with the permission from ref. 53. Copyright 2015, Chemical Society of Japan)

| **Oligonucleotides** | $T_m$ (°C) | $\Delta T_m$ (°C) |
|---|---|---|
| GK-2139 | 37.3 | +10.4[a] |
| GK-2140 | 26.9 | - |
| GK-2139+GK-1104 | 51.4 | +1.6[b] |
| GK-2140+GK-1104 | 49.8 | - |
| GK-2139+GK-1105 | 36.9 | -14.5[c] |

Melting Temperatures were measured with 3 μM of DNA in 10 mM sodium phosphate buffer (pH 7.2) containing 100 mM NaCl.

$\Delta T_m$[a] indicates deviation from $T_m$ of **GK-2140,**

$\Delta T_m$[b] indicates deviation from $T_m$ of **GK-2140**+**GK-1104** and

$\Delta T_m$[c] indicates deviation from $T_m$ of **GK-2139**+**GK-1104**.

## 2.4 Conclusion

In conclusion, the new molecular beacon probe (**GK-2139**) possessing polyamine-connected deoxyuridine and silylated pyrene at their 5´-terminus was successfully prepared using phosphoramidite chemistry. The probe was effectively quenched in the buffer solution while they stayed alone by forming a pseudo dumbbell shaped structure. Moreover, it showed strong fluorescence signal only upon binding to the perfectly matched complementary DNA (**GK-1104**). However, in the case of duplexes with single base alteration in the middle of complementary sequences namely, **GK-1105**, only a weak fluorescence emission was observed compared with the fluorescence emission of the duplex

with perfectly matched complementary DNA. Thus, the current probe can nicely discriminate a single-nucleotide substitution in the complementary DNA strand via its fluorescent signal and would be a practically feasible probe to detect certain gene fragments in solution by simple mixing.

## 2.5 Experimental

### 2.5.1 *General Information*

Reactions under anhydrous conditions were carried out under an atmosphere of nitrogen. Reaction progress was observed by thin layer column chromatography on Merck silica gel 60 F254-precoated plate under UV lamp. Column Chromatography was performed with silica gel 60N (neutral, spherical, 63-210µm). $^{1}$HNMR and $^{31}$PNMR spectra were recorded on JOEL (JNM-ECA 400) FT NMR SYSTEM at 400 MHz and 161.8 MHz, respectively, using tetramethylsilane as internal standard. ESI-MS spectra were recorded on Perkin Elmer API-100 ESI-MS Spectrophotometer. UV-VIS spectra were taken on UV-2450 Spectrophotometer (Shimadzu). Fluorescence spectra were recorded on F-4500 Fluorescence Spectrophotometer (HITACHI). Oligonucleotides were purified by reversed-phase HPLC (PU-2089 plus, JASCO) attached with UV-VIS detector (SPD-10A, Shimadzu) and Chromatopac (C-R8A, Shimadzu) using Wakosil 5 C18 column (Ø 4.6 mm X 250 mm).

### 2.5.2 *Synthesis of 1-(Chloromethyldimethylsilyl) pyrene (2).*

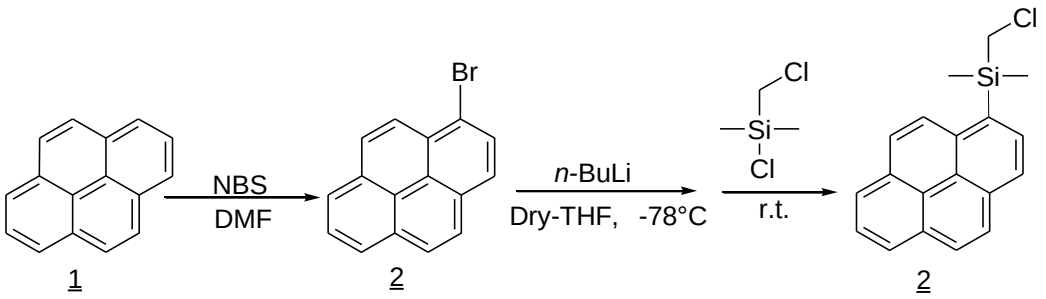


1-Bromopyrene (3.10 g, 11.0 mmol) was vacuum dried for 30 min in two-open eggplant flask. 50 ml of dry THF was added into it and placed the flask on ethanol dry ice bath (-78 °C). The solution was stirred for ten minutes. Then *n*-butyllithium (10.2 ml, 16.5 mmol) was added into the reaction mixture slowly and maintained the ethanol bath temperature between -74 °C to -78 °C for 1 hour. Chloromethyldimethylchlorosilane (3.0 ml, 22.0 mmol) was added dropwise to the reaction mixture and stirred for another 1 hour at the same temperature. The mixture was then stirred at room temperature for 4 hours. At a suitable time, an aliquot was taken from the mixture and monitored by TLC using a solvent system of 10 % $CH_2Cl_2$ in hexane. The mixture was evaporated under reduced pressure and portioned between $CH_2Cl_2$ and saturated solution of sodium bicarbonate. The organic layer was collected, washed 3 times with saturated solution of sodium bicarbonate, dried over sodium sulfate, filtered, and finally evaporated under reduced pressure. The crude product was purified by silica-gel column chromatography using 10 % $CH_2Cl_2$ in hexane as an eluent and obtained compound **2** (1.21 g, 36 %). $^1$H NMR (400 MHz, $CDCl_3$) δ (ppm) = 0.73 (s, 6H, dimethyl), 3.29 (s, 2H, Si-2H), 8.01-8.27 (m, 9H, pyrene).

### 2.5.3 *Synthesis of 1-(Acetoxymethyldimethylsilyl) pyrene (3).*

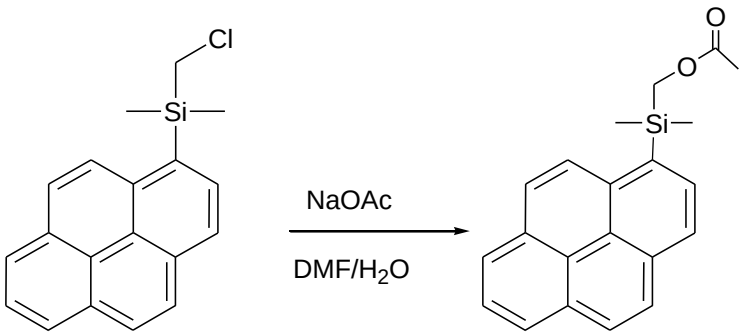


2 3

Compound **2** (1.2 g, 3.88 mmol) was dissolved into 25 ml DMF and stirred for few minutes. Then 3.19 g NaOAc and 14 ml of water were added into the reaction mixture. The reaction mixture was stirred at 100°C for 24 hours and progress of the reaction was monitored by TLC at the ending of stirring using a solvent system of 50 % $CH_2Cl_2$ in hexane. The mixture was then evaporated under reduced pressure and dissolved in 100 ml ethyl acetate washed 3 times by deionized water. The organic layer was dried with $Na_2SO_4$, filtered, and concentrated to dryness under reduced pressure to give a crude compound **3** as brown oil. The resultant brown oil was purified by silica gel column chromatography with 50 % $CH_2Cl_2$ in hexane and obtained compound **3** (0.89 g, 68 %). $^1$H NMR (400 MHz, $CDCl_3$) δ (ppm) = 0.66 (s, 6H, dimethyl), 2.04 (s, 3H, $COOCH_3$), 4.27 (s, 2H, Si-2H) 8.01-8.33 (m, 9H, pyrene).

**2.5.4** ***Synthesis of 1-(Hydroxymethyldimethylsilyl) pyrene (4).***

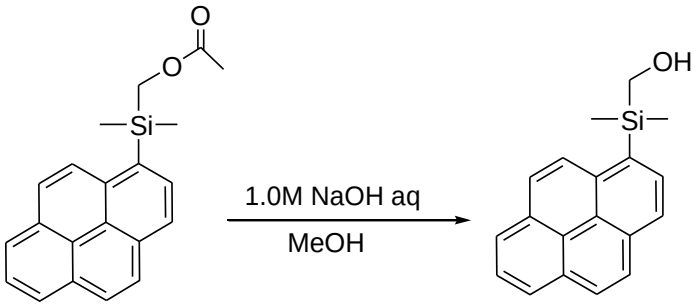


3 4

Compound **4** was obtained from compound **3** (0.883 g, 2.66 mmol) by the reaction 1 M NaOH (4 ml) in the presence of MeOH (65 ml). The reaction mixture was stirred at room temperature for 17 hours. The reaction mixture was then concentrated to a small volume under reduced pressure. The resulting residue was portioned between ethyl acetate and saturated solution of sodium chloride. The organic layer collected, washed with saturated solution of sodium chloride three times, dried over $Na_2SO_4$, filtered, and concentrated to dryness under reduced pressure. The crude product was then purified by column chromatography using 40 % ethyl acetate in hexane and obtained compound **4** (0.71 g, 92 %). $^1$H NMR (400 MHz, $CDCl_3$) δ (ppm) = 0.65-0.66 (t, 6H, dimethyl), 1.56 (s, 1H, OH), 3.91 (s, 2H, Si-2H), 8.00-8.36 (m, 9H, pyrene).

### 2.5.5 *Synthesis of [1-(Pyrenyl)dimethylsilylmethyl]-(2-cyanoethyl)-N,N-diisopropyl-phosphoramidite (5).*

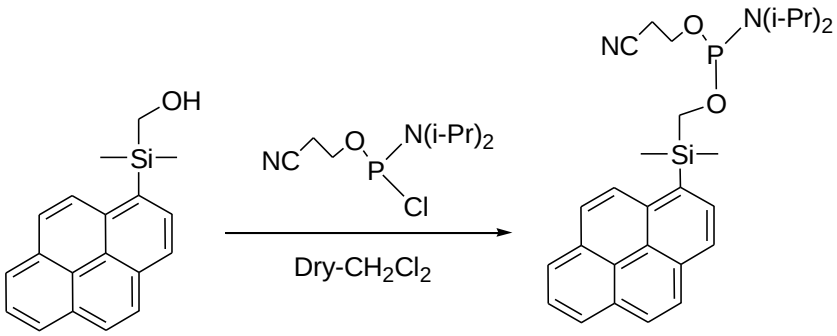


4 5

Compound **4** (0.13 g, 4.48 mmol) was vacuum dried for 30 minutes in two necked round bottom flask and 10 ml of dry $CH_2Cl_2$ was added into it and stirred on ice bath for 10 minutes. 0.5 ml *N*,*N*-diisopropylethylamine was added to the reaction mixture and once again stirred for another 10 minutes. To the reaction mixture, 2-cyanoethyl-*N*,*N*-diisopropylchloro phosphoramidite (0.3 ml) was added drop wise and stirred under cooling in ice bath for 40 minutes. The resultant product was then dissolved in 100 ml $CH_2Cl_2$ and washed three times with saturated solution of sodium bicarbonate. The organic layer was dried with $Na_2SO_4$, filtered, and concentrated under reduced pressure. The residue was then purified by silica gel column chromatography with hexane-ethyl acetate-triethylamine (7:3:0.2, v/v/v) and obtained compound **5** (0.155 g, 71 %). $^{1}$H NMR (400 MHz, $CDCl_3$) δ (ppm) = 0.69-0.70 (d, 6H, dimethyl), 1.15-1.27 (m, 12H, iPr), 2.44-2.48 (m, 2H, $CH_2$) 3.58-3.83 (m, 2H, Si-2H), 8.01-8.39 (m, 9H, pyrene). $^{31}$P NMR (400 MHz, $CDCl_3$) δ (ppm) = 151.58.

**2.5.6** ***Synthesis of 3´, 5´-O-Diacetyl-5-methoxycarbonylmethyl-2´-bromo-2´-deoxyuridine (9).***

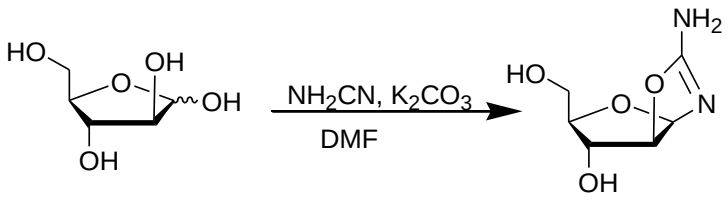


6 7

At first, D-Arabinose (4.0 g, 26.6 mmol) was dissolved into 50 ml DMF and stirred for few minutes. 1.344 g cyanamide and 0.184 g potassium carbonate were added into it and refluxed overnight at 50 °C. The reaction mixture was then cooled to room temperature. 40 ml ethyl acetate was added to the reaction mixture and stirred once again in an ice bath for 30 minutes. After ice bathing the reaction mixture was filtered and vacuum dried and obtained compound **7** as crude residue (4.7 g.).

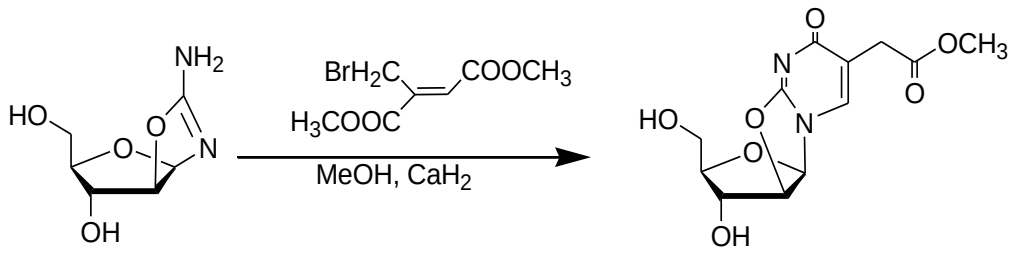


7 8

4.67 g of compound **7** (26.8 mmol) was dissolved in methanol and added 9.5 g bromomethyl fumaric acid dimethyl ester and 1.35 g calcium hydride to the reaction mixture. The reaction mixture was then refluxed at 80 °C for 3 hours. The reaction progress was checked by TLC using 10 % MeOH in $CH_2Cl_2$. The resulting residue was dried under reduced pressure and dissolved into 13 ml methanol then added sufficient amount of $CH_2Cl_2$ (290 ml) to it to

make precipitate. The mixture was then centrifuged and collected the supernatant. The supernatant was then transferred into a separating funnel and added water and washed three times with $CH_2Cl_2$ and then with ethyl acetate. The aqueous layer was collected, filtered, and dried under reduced pressure and obtained the compound **8** as crude residue (12.9 g).

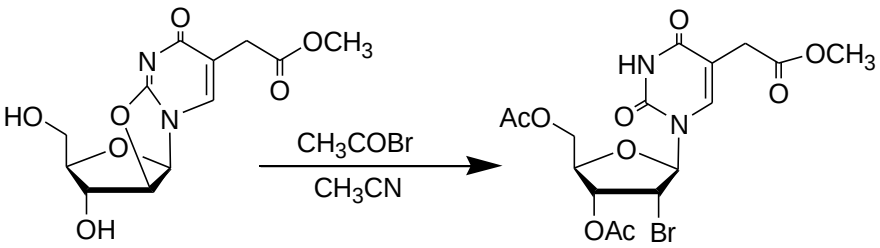


8 9

The obtained crude of compound **8** (12.94 g, 43.3 mmol) was dried under reduced pressure and was then dissolved into dry $CH_3CN$ (60 ml). Thereafter 10 ml AcBr was added to it and stirred at 102 °C for 4 hours and confirmed the end point of reaction by TLC using 10 % MeOH in $CH_2Cl_2$. The reaction output was dissolved into saturated solution of sodium bicarbonate, filtered, and then washed three times by $CH_2Cl_2$. The organic layer was collected and dried with $Na_2SO_4$, filtered, and concentrated under reduced pressure. The resulting residue was then purified by silica gel column chromatography using a solvent system of 10 % MeOH in $CH_2Cl_2$ and obtained compound **9** (3.65 g, 30 % from 7). $^1$H NMR (400 MHz, $CDCl_3$) δ (ppm) = 2.11-2.17 (m, 6H, 3´-methyl, 5´-methyl), 3.35-3.37 (d, 2H, 5-$CH_2$), 3.70 (s, 3H, 5-OMe) 4.36-4.39 (m, 2H, 5´-$CH_2$), 4.55 (t, 1H, 3´-H), 5.15-5.17(m, 1H, 4´-H), 6.19-6.21(d, 1H, 1´-H), 7.49 (s, 1H, 6-H), 8.32 (s, 1H, 3-NH).

### 2.5.7 *Synthesis of 3´, 5´-O-Diacetyl-5-methoxycarbonylmethyl-2´-deoxyuridine (10).*

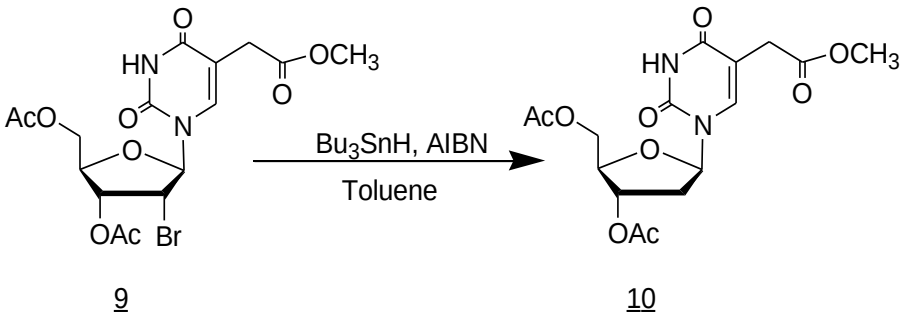


9 10

The compound **9** (3.65 g, 7.9 mmol) was refluxed in toluene with 4.25 g (15.8 mmol) tri-*n*-butyltin hydride ($Bu_3SnH$) and 135 mg (0.8 mmol) α-bisisobutyronitrile (AIBN) for 4 hours. The end point of the reaction was confirmed by doing TLC test using 20 % hexane in ethyl acetate and concentrated under reduced pressure. The resulting oily residue was then purified by silica gel column chromatography with the same solvent system and the amount of pure compound **10** is 2.02 g (67 %). $^1$H NMR (400 MHz, $CDCl_3$) δ (ppm) = 2.03-2.10 (m, 6H, 3´-methyl, 5´-methyl), 2.48-2.50 (m, 1H, 2´-H), 3.30-3.39 (d, 2H, 5-$CH_2$), 3.70 (s, 3H, 5-OMe) 4.09 (m, 2H, 5´-CH2), 4.25-4.36 (m, 1H, 3´-H), 5.19-5.21 (m, 1H, 4´-H), 6.26-6.29 (m, 1H, 1´-H), 7.53 (s, 1H, 6-H), 8.30 (s, 1H, 3-NH).

### 2.5.8 *Synthesis of 5-[N-[N,N-Bis(2-trifluoroacetamidethyl)amino]ethyl]carbamoyl-methyl-2´-deoxyuridine (12).*

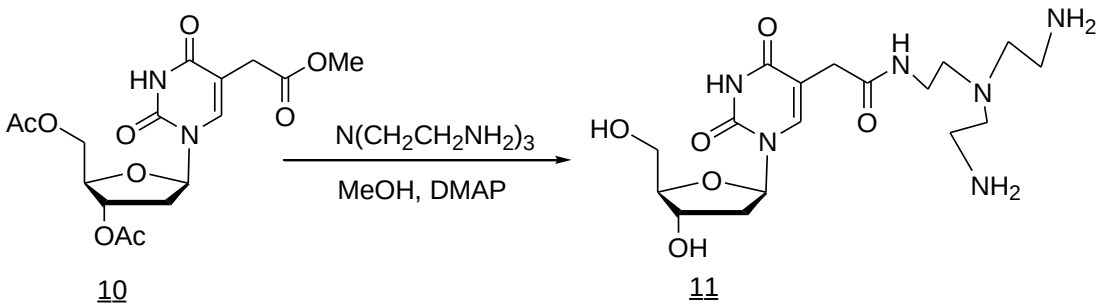


10 11

The compound **10** (0.986 g, 2.56 mmol) was reacted with tris(2-aminoethyl)amine (3.75 g, 25.6 mmol) and 4-dimethylaminopyridine (0.01 g, 0.077 mmol) in methanol and stirred at room temperature for 17 hours. The reaction progress was monitored by doing TLC test using 15 % MeOH in $CH_2Cl_2$. After reaction, the solution was evaporated and the residue was dissolved in a small amount of methanol and added drop wise to benzene (200 ml) to precipitate 5´-[*N*-[*N*,*N*-bis(2-aminoethyl)-amino]ethyl]carbamoylmethyl-2´-deoxyuridine (compound **11**) as an oily residue. Then the terminal amino groups were protected without further purification.

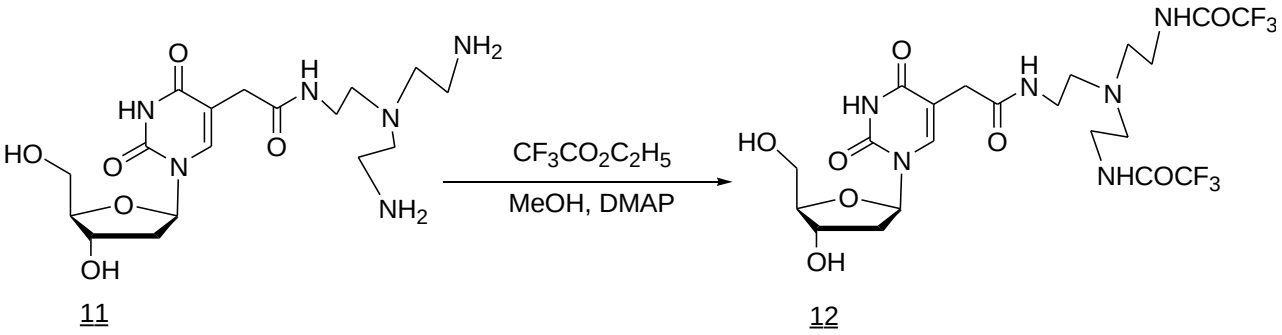


11 12

Ethyl trifluoroacetate (3.94 ml, 33.1 mmol) was added drop wise to a solution of compound **11** in methanol (100 ml) containing 4-dimethylaminopyridine (0.01 g, 0.077 mmol). The reaction mixture was stirred at room temperature for 20 hours and progress of reaction was checked by TLC using a solvent system of 15 % MeOH in $CH_2Cl_2$. The resulting reaction residue was then concentrated under reduced pressure and was purified by silica gel column chromatography with the same solvent system. The amount of obtained pure compound **12** is 0.942 g (61 % from 10). $^1$H NMR (400 MHz, $D_2O$) δ (ppm) = 2.26-2.31 (m, 2H, 2´-H), 2.60-2.66 (m, 6H, $N(CH_2\text{-})_3$), 3.19-3.31 (m, 8H, C5-$CH_2$- and $NHCH_2$- X3), 3.66-3.72 (m, 2H, 5´-$CH_2$), 3.92 (m, 1H, 3´-H), 4.35-4.36 (m, 1H, 4´-H), 6.16-6.20 (t, 1H, 1´-H), 7.69 (s, 1H, 6-H).

### 2.5.9 *Synthesis of 5´-O-(4,4´-Dimethoxytrityl)-5-[N-[2-N,N-bis(2-trifluoroacetamid-ethyl)amino]ethyl]carbamoylmethyl-2´-deoxyuridine (13).*

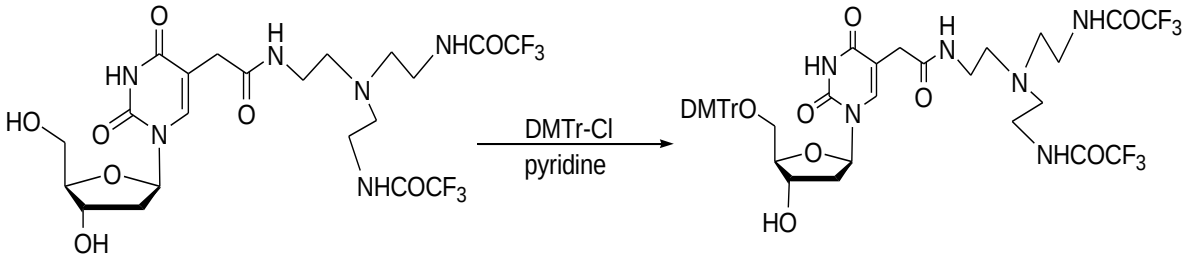


12 13

The compound **12** (0.812 g, 1.34 mmol) was reacted with 4,4´-dimethoxytrityl chloride (DMTr-Cl, 0.59 g, 1.74 mmol) in dry pyridine(15 ml) containing 4-dimethylaminopyridine (10 mg, 0.082 mmol) at room temperature for 2 hours. The reaction progress was monitored with TLC using 10 % MeOH in $CH_2Cl_2$ with 1 % TEA. After reaction, a small amount of methanol (5 ml) was added to the reaction mixture and then dissolved this reaction mixture into $CH_2Cl_2$ (100 ml) and washed three times with saturated solution of sodium bicarbonate. The organic layer was then collected, dried with $Na_2SO_4$, filtered, and solvent was evaporated under reduced pressure. The product was purified by silica-gel column chromatography using 10 % MeOH in $CH_2Cl_2$ with 1% TEA as an eluent. Yield of compound **13** is 68%. $^1$H NMR (400 MHz, $CDCl_3$) δ (ppm) = 2.46-2.56 (m, 6H, $N(CH_2-)_3$), 2.60-2.64 (m, 8H, C5-$CH_2$), 3.30-3.36 (m, 6H, $NHCH_2$- X3), 3.47 (s, 2H, 5´-$CH_2$), 3.76 (s, 6H, $OCH_3$ of DMTr), 4.03-4.04 (d, 1H, 3´-H), 4.55-4.56 (t, 1H, 4´-H), 6.21-6.25 (t, 1H, 1´-H), 6.81-6.83 (m, 4H, H-Ar of DMTr), 7.24-7.27 (m, 9H, H-Ar of DMTr), 7.76 (s, 1H, 6-H).

**2.5.10** ***Synthesis of 5´-O-(4,4´-Dimethoxytrityl)-5-[N-[2-N,N-bis(2-trifluoroacetamid-ethyl)amino]ethyl]carbamoylmethyl-2´-deoxyuridine-3´-O-yl(2-cyanoethyl)-N,N-diiso-propylphosphoramidite (14).***

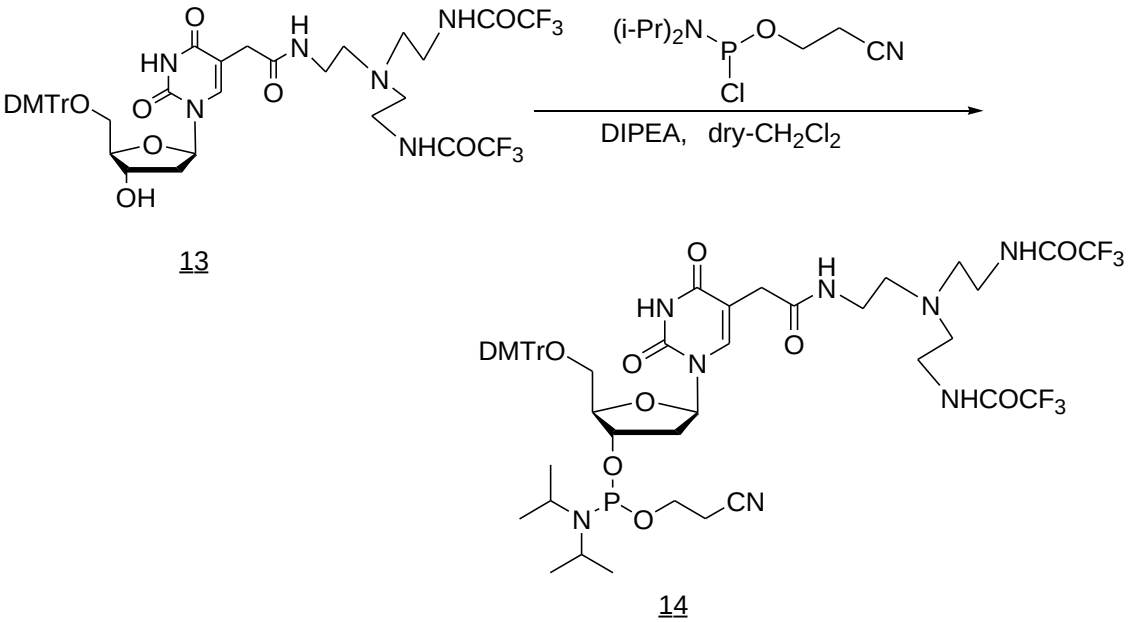


13




14

5´-DMTr-Nucleoside derivative (Compound **13**, 0.804 g, 0.88 mmol) was dissolved into dry dichloromethane and added *N*,*N*-diisopropylethylamine (1.0 ml) to the mixture and stirred few minutes under $N_2$ atmosphere at room temperature. Thereafter, 0.6 ml 2-cyanoethyl-*N*,*N*-diisopropylchloro phosphoramidite solution was added drop wise to the reaction mixture and continued stirring for another 2 hours. The reaction progress was monitored by TLC using ethyl acetate-methanol-triethylamine (16/1/2, v/v/v). After reaction, 6 ml methanol was added to the reaction mixture and dissolved it into ethyl acetate (100 ml) and washed three times by saturated solution of sodium bicarbonate, collected the organic layer, dried with $Na_2SO_4$, filtered, and solvent was evaporated under reduced pressure. Finally, the product was purified by silica gel column chromatography using the same solvent system used for TLC test. The appropriate fractions were collected, evaporated under reduced

pressure and the obtained compound **14** is 0.774 g (79 %). $^{1}$H NMR (400 MHz, $CDCl_3$) δ (ppm) = 1.04-1.24 (m, 12H, iPr), 2.03 (s, 2H, 2´-H), 2.48-2.62 (m, 16H, $N(CH_2\text{-})_3$, C5-CH2, $N(CH=)_2$), 3.17-3.19 (m, 6H, $NHCH_2$- X3), 3.31-3.33 (m, 2H, 5´-$CH_2$) , 3.77 (s, 6H, $OCH_3$ of DMTr), 4.66-4.67 (m, 1H, 4´-H), 6.30-6.33 (t, 1H, 1´-H), 6.82-6.84 (m, 4H, H-Ar of DMTr), 7.24-7.28 (m, 9H, H-Ar of DMTr), 7.78 (s, 1H, 6-H), 7.87-7.88 (d, 6H, $NHCH_2$-X3) . $^{31}$P NMR (400 MHz, $CDCl_3$) δ (ppm) = 149.51-149.59.

### 2.5.11 *Oligonucleotides Synthesis.*

The oligonucleotides containing C-5 modified 2´-deoxyuridine and a dimethylsilylated pyrene at the 5´-terminus were synthesized on an automated DNA synthesizer (Applied Biosystems ABI-392) using standard protocol. The C-5 polyamine bearing modified 2´-deoxyuridine analogs were incorporated into the oligonucleotides in a manner similar to that reported previously [48-49]. The phosphoramidite derivative of dimethylsilylated pyrene was incorporated at the oligomers' 5´-termini using higher concentration of the amidite, as described previously [50]. After the assembly, the support bound modified oligoDNA was treated with concentrated ammonium hydroxide at 55 $^{0}$C for 12 hours. Thereafter the oligomer was purified by reversed-phase HPLC, ethanol precipitation and Sephadex G-25 gel filtration.

### 2.5.12 *Melting Temperature Analysis.*

A solution of either 3 µM oligonucleotide or its complex of 3 µM of each strand in a buffer of 10 mM sodium phosphate containing 100 mM NaCl was heated 90 ˚C for 3 minutes, cooled gradually to room temperature, and then used for the melting temperature study. UV absorbance was measured at 260 nm on a Shimadzu UV-2450 Spectrophotometer equipped

with a temperature controller. The rate of heating was 0.1°C/min. $T_m$ values were determined from the first differentials of the absorbance versus temperature plot using Igor graphing and data analysis program (Wave Matrices, Inc.).

### 2.5.13 *Fluorescence Measurements.*

Fluorescence measurements were carried out in F-4500 Fluorescence Spectrophotometer in a 3 ml cuvette with excitation at 350 nm and detection at 360-500 nm. All measurements were conducted in 10 mM sodium phosphate containing 100 mM sodium chloride with a concentration of 1.0 µM each strand.

## References


1. Maxam, A. M.; Gilbert, W. *Proc. Natl. Acad. Sci., USA* 1977, **74**, 560.
2. Sanger, F.; Coulson, A. R. *J. Mol. Biol.*, 1975, **94**, 444.
3. Fodor, S. P. A. *Science*, 1997, **277**, 393.
4. Eng, C.; Vijg, J. *Nat. Biotechnol.*, 1997, **15**, 422.
5. Rees, J. *Science*, 2002, **296**, 698.
6. Hood, L.; Galas, D. *Nature*, 2003, **421**, 444.
7. Marti, A. A.; Jockusch, S.; Stevens, N.; Ju, J.; Turro, N. J. *Acc. Chem. Res.*, 2007, **40**, 402.
8. Moriguchi, T.; Hattori, M.; Sekiguchi, T.; Ichimura, M.; Kato, T.; Shinozuka, K. *Nucleic Acids Symposium*, 2008, **52**, 255.
9. Shinozuka, K.; Sekiguchi T.; Ebara Y.; Moriguchi T. *Nucleic Acids Symposium*, 2007, **51**, 7.

10. Sekiguchi, T.; Ebara, Y.; Moriguchi, T.; Shinozuka, K. *Bioorg. Med. Chem. Lett*., 2007, **17**, 6883.

11. Tyagi, S.; Kramer, F. R. *Nat. Biotechnol*., 1996, **14**, 303.

12. Tan, W.; Fang, X.; Liu, X. *Chem. Eur. J*., 2000, **6**, 1107.

13. Zhang, P.; Beck, T.; Tan, W. *Angew. Chem. Int. Ed. Engl.*, 2001, **40**, 402.

14. Hwang, G. T.; Seo, Y. J.; Kim, B. H. *J. Am. Chem. Soc.*, 2004, **126**, 6528.

15. Seo, Y. J.; Ryu, J. H.; Kim, B. H. *Organic Lett.*, 2005, **7**, 493.

16. Okamoto, A.; Tainaka, K.; Saito, I. *J. Am. Chem. Soc*., 2003, **125**, 4972.

17. Okamoto, A.; Kanatani, K.; Saito, I. *J. Am. Chem. Soc.*, 2004, **126**, 4820.

18. Hrdlicka, P. J.; Babu, B. R.; Sorensen, M. D.; Harrit, N.; Wengel, J. *J. Am. Chem. Soc.*, 2005, **127**, 13293.

19. Tyagi, S.; Bratu, D. P.; Kramer, F. R. *Nat. Biotechnol*., 1998, **16**, 49.

20. Chen, W.; Martinez, G.; Mulchandani, A, *Anal. Biochem.*, 2000, **280**,166.

21. Liu, X.; Farmerie, W.; Schuster, S.; Tan, W. *Anal. Biochem.*, 2000, **283**, 56.

22. Perlette, J.; Tan, W. *Anal. Chem.*, 2001, **73**, 5544.

23. Fang, X. H.; Mi, Y. M.; Li, J. W. J.; Tan, W., *Cell Biochem. Biophys*., 2002, **37**, 71.

24. Tan, W.; Wang, K.; Drake, T. J. *Curr. Opin. Chem. Biol.*, 2004, **8**, 547.

25. Peng, X. H.; Cao, Z. H.; Xia, J. T.; Carlson, G. W.; Lewis, M. M.; Wood, W. C.; Yang, L., *Cancer Res.*, 2005, **65**, 1909.

26. Yang C. J.; Medley, C. D.; Tan, W., *Curr. Pharm. Biotechnol.*, 2005, **6**, 445.

27. Noya, O.; Patarroyo, M. E.; Guzman, F.; De Noya, B. A. *Curr. Protein Peptide Sci.*, 2003, **4**, 299.

28. Solomon, B. *Immunization Against Alzheimer's Disease and Other Neurodegenerative Disorders*, 2003, 11.

29. Perlette, J.; Li, J.; Fang, X.; Schuster, S.; Lou, J.; Tan, W. *Rev. Anal. Chem.*, 2002, **21**, 1.

30. 7. Tsourkas, A.; Bao, G., *Briefings in Functional Genomics and Proteomics*, 2003, **1**, 372.

31. Wang, K. ; Li, J.; Fang, X.; Schuster, S.; Vicens, M.; Kelley, S.; Lou, H. ; Li, J. J.; Beck, T.; Hogrefe, R.; Tan, W. *Biomed. Photonics Handbook*, 2003, **57**, 1.

32. Maeda, H.; Inoue, Y.; Ishida, H.; Mizuno, K., *Chem. Lett.*, 2001, 1224.

33. Moriguchi T.; Hattori M.; Sekiguchi T.; Shinozuka, K. *Nucleic Acids Symposium* 2009, **53**, 31.

34. Du, H.; Disney, M. D.; Miller, B. L.; Krauss, T. D. *J. Am. Chem. Soc.*, 2003, **125**, 4012.

35. Yang, C. J.; Lin, H.; Tan, W. *J. Am. Chem. Soc.*, 2005, **127**, 12772.

36. Stoermer, R. L.; Cederquist, K. B.; McFarland, S. K.; Sha, M. Y.; Penn, S. G.; Keating, C. D. *J. Am. Chem. Soc.*, 2006, **128**, 16892.

37. Cazzato, A.; Capobianco, M. L.; Zambianchi, M.; Favaretto, L.; Bettini, C.; Barbarella, G. *Bioconjug. Chem.*, 2007, **18**, 318.

38. Grossmann, T. N.; Roglin, L.; Seitz, O. *Angew. Chem., Int. Ed.*, 2007, **46**, 5223.

39. Conlon, P.; Yang, C. J.; Wu, Y.; Chen, Y.; Martinez, K.; Kim, Y.; Stevens, N.; Marti, A. A.; Jockusch, S.; Turro, N. J.; Tan, W. *J. Am. Chem. Soc.*, 2008, **130**, 336.

40. Seo, Y. J.; Ryu, J. H.; Kim, B. H. *Org. Lett.*, 2005, **7**, 4931.

41. Saito, Y.; Mizuno, E.; Bag, S. S.; Suzuka, I.; Saito, I. *Chem. Commun.*, 2007, 4492.

42. Hwang, G. T.; Seo, Y. J.; Kim, B. H. *J. Am. Chem. Soc.*, 2004, **126**, 6528.

43. Venkatesan, N. Y.; Seo, J.; Kim, B. H. *Chem. Soc. Rev.*, 2008, **37**, 648.

44. Heinlein, T.; Knemeyer, J. P.; Piestert, O.; Markus Sauer, M. *J. Phys. Chem. B*, 2003, **107**, 7957.

45. Saito, Y.; Shinohara, Y.; Bag, S. S.; Takeuchi, Y.; Matsumoto, K.; Saito, I., *Tetrahedron*, 2009, **65**, 934.

46. Mogi, M.; Uddin, M. G.; Ichimura, M.; Moriguchi, T. and Shinozuka, K. *Chem. Lett.* 2010, **39**, 1254.

47. Matsukura, M.; Okamoto, T.; Miike, T.; Sawai, H.; Shinozuka, K. *Biochem. Biophys. Res. Commun.*, 2002, **293**, 1341.

48. Shinozuka, K.; Sekiguchi, T.; Ebara, Y.; Moriguchi, T. *Nucleic Acids Symp. Ser.*, 2007, **51**, 7.

49. Ozaki, H.; Nakamura, A.; Arai, M.; Endo, M.; Sawai, H. *Bull. Chem. Soc. Jpn.*, 1995, **68**, 1981.

50. Sawai, H.; Nakamura, A.; Sekiguchi, S.; Yumoto, K.; Endo, M.; Ozaki, H. *J. Am. Chem. Soc. Chem. Commun.*,1994, **1**, 1997.

51. Leonard, N. J.; Sciavolino, F. C.; Nair, V. *J. Org. Chem.*, 1968, **33**, 3169.

52. Netzel, T. L.; Nafisi, K.; Headrick, J.; Eaton, B. E. *J. Phys. Chem.*, 1995, **99**, 17948.

53. Chowdhury, J. A., Moriguchi, T.; Shinozuka, K. *Chem. Lett.*, 2014, **43**, 1915.

54. Hall, D. R.; Holmlin, R. E.; Barton, J. K. *Nature*, 1996, **382**, 731.

55. Lewis, F. D.; Letsinger, R. L. *J. Biol. Inorg. Chem.*, 1998, **3**, 215.

# Chapter 3

# Synthesis and Fluorescence Properties of Pseudo-Dumbbell Type of Molecular Beacon Probes bearing Modified Deoxyuridine and a Silylated Pyrene as a Fluorophore

## 3.1 Abstract

A novel pseudo-dumbbell type molecular beacon probe (**Probe 1,** formerly designated as **GK-2139**) possessing polyamine-connected deoxyuridine (U) and silylated pyrene has discussed in the previous chapter. The probe showed weak fluorescence signal while it stayed alone. Fluorescence signal of the probe was increased in the presence of the complementary DNA. In this study, I prepared new molecular beacon probes. **Probe 2** and **Probe 3** possess elongated stem portion of **Probe 1**. In addition, one U in **Probe 2** is substituted by anthraquinone-bearing deoxyuridine residue (Y) in **Probe 3**. **Probe 4** is essentially same as **Probe 1** but one deoxyguanosine in the loop portion of **Probe 1** is substituted by a deoxyinosine in **Probe 4**. In **Probe 5**, 3′-terminal deoxycytidine of **Probe 3** is substituted by deoxyadenosine. Fluorescence signal of these probes is effectively quenched in the absence of target DNA. Among all, **Probe 3** shows the most effective quenching. On the other hand, the signal of all probes is substantially increased in the presence of complementary DNA. The ratio of signal to background in case of **Probe 3** is the highest. All these probes can also recognize single nucleotide alternation in the target DNA in different extent. The sequence recognition ability of **Probe 3** is also the highest among all the probes.

## 3.2 Introduction

Fluorescently labeled oligonucleotide probe is remarkably important as a tool in modern life science for medical diagnostics and genetic studies [1-3]. One of the most useful probe for the detection of nucleic acid is a so-called molecular beacon probe (MB) [4-10]. Molecular beacon probe undergoes a close to open conformational change in the absence and presence of target DNA with simultaneous characteristics changes in their fluorescent intensities [11-15]. Traditional molecular beacon probe is doubly end-labeled with a fluorophore

(fluorescence donor) and a fluorescence quencher (acceptor) that is usually formed a stem-loop structure of oligonucleotides (Figure 3.1) [16-17]. The stem structure brings the

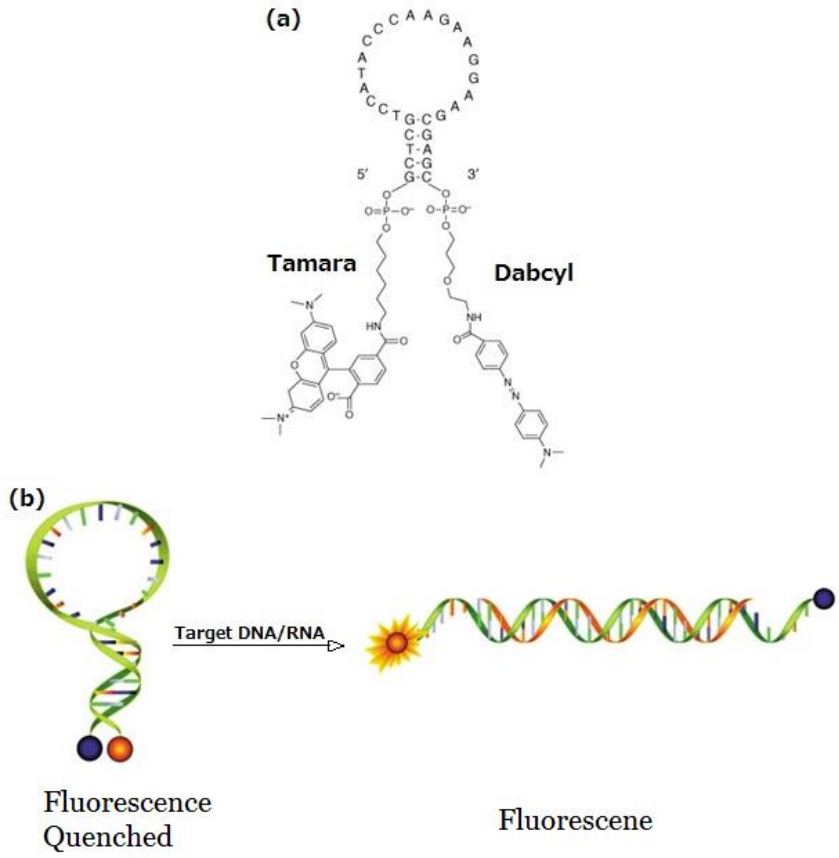


**Figure 3.1:** Structural characteristics of molecular beacon probes. **(a)** A typical molecular beacon DNA probe. **(b)** Molecular beacon working principle. (cited from ref. 16)

fluorophore and quencher in close proximity allowing energy to be transferred directly from the fluorophore to the quencher. When the probe meets a target DNA or RNA molecule, the stem-loop structure is resolved into a linear probe-target hybrid that is longer and more stable than the stem hybrid. As a result of this conformational rearrangement, the fluorophore and the quencher move apart from each other, restoring fluorescence emission. Since the first invention of molecular beacon by Tyagi *et al.* [18], many approaches have been developed by many researchers [19-24]. A recent most attractive of such development

is the inclusion of quencher free molecular beacon probes [25-28]. The quencher free molecular beacons are the oligonucleotides which are mono-labelled in the loop [25], or in the stem [26] and also multi-labelled in the loop [27], or in the stem [28] (Figure 3.2 and 3.3). In those quencher free molecular beacon probes, natural nucleobase, guanine and thymine, are used as an internal quencher [26-27] and graphene oxide [25] is used as an external quencher. The monomer-excimer emission is also used to develop this kind of quencher free molecular beacon [28].

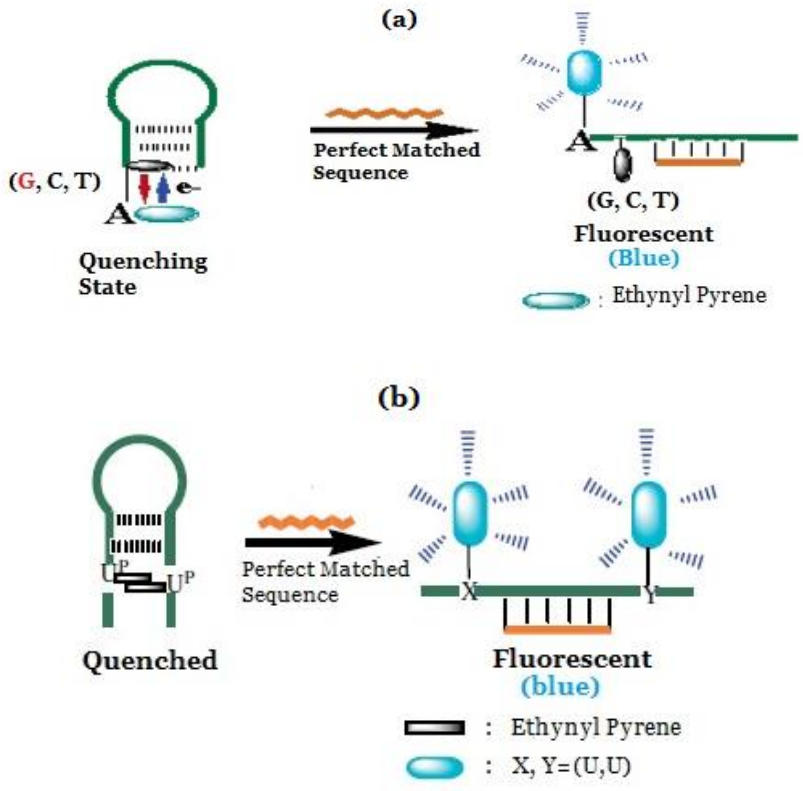


**Figure 3.2:** Quencher free molecular beacon **(a)** mono-labelled and **(b)** multi-labelled in the stem portion. [cited from ref. **(a)** 29, **(b)** 30 ]

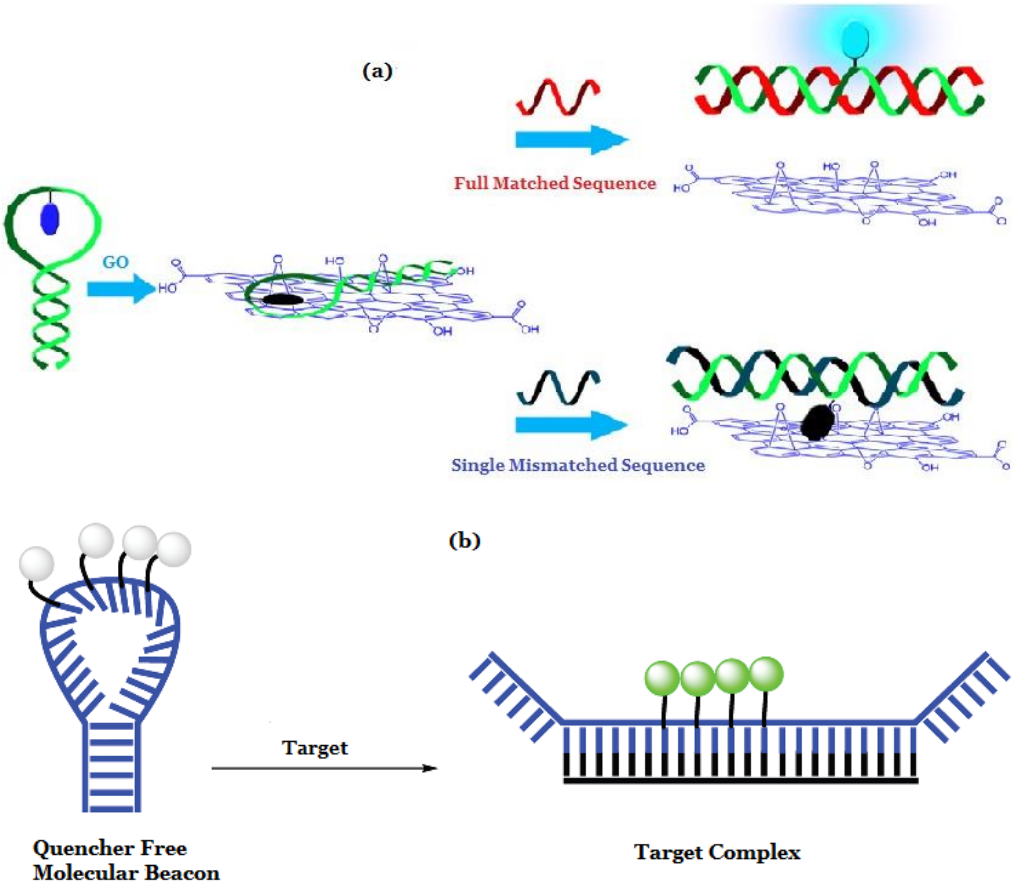


**Figure 3.3:** Quencher free molecular beacon **(a)** mono-labelled and **(b)** multi-labelled in the loop portion. [cited from ref. **(a)** 25, **(b)** 27 ]

Meanwhile, our group has developed a novel silylated pyrene derivative possessing dimethylsilyl function with modifiable terminal group as a new labeling agent of biological substances such as oligoDNA [31-33] and lipids [34]. The compound is more advantageous as a fluorescent labeling agent compared to original pyrene since it exhibits enhanced (more than 2 times) fluorescent quantum yield along with the bathochromic shift in absorption and emission, due to the Si-associated $\sigma^*-\pi^*$ interaction [35-36]. Once the derivative is incorporated into 5′-terminus of DNA molecule, however, the fluorescence signal of the

derivative is severely quenched by neighboring nucleobase including thymine, cytosine and guanine because of the photoinduced electron transfer [37]. Utilizing these unique features of silylated pyrene molecule, I have developed a novel quencher-free MB system (**Probe 1**, Figure 3.4) and recently reported [38]. The probe has partial self-complementary sequence and, therefore, it forms pseudo-dumbbell type of secondary structure. In that form, silylated pyrene molecule introduced at 5′-terminus of the probe is presumed to be in the proximal

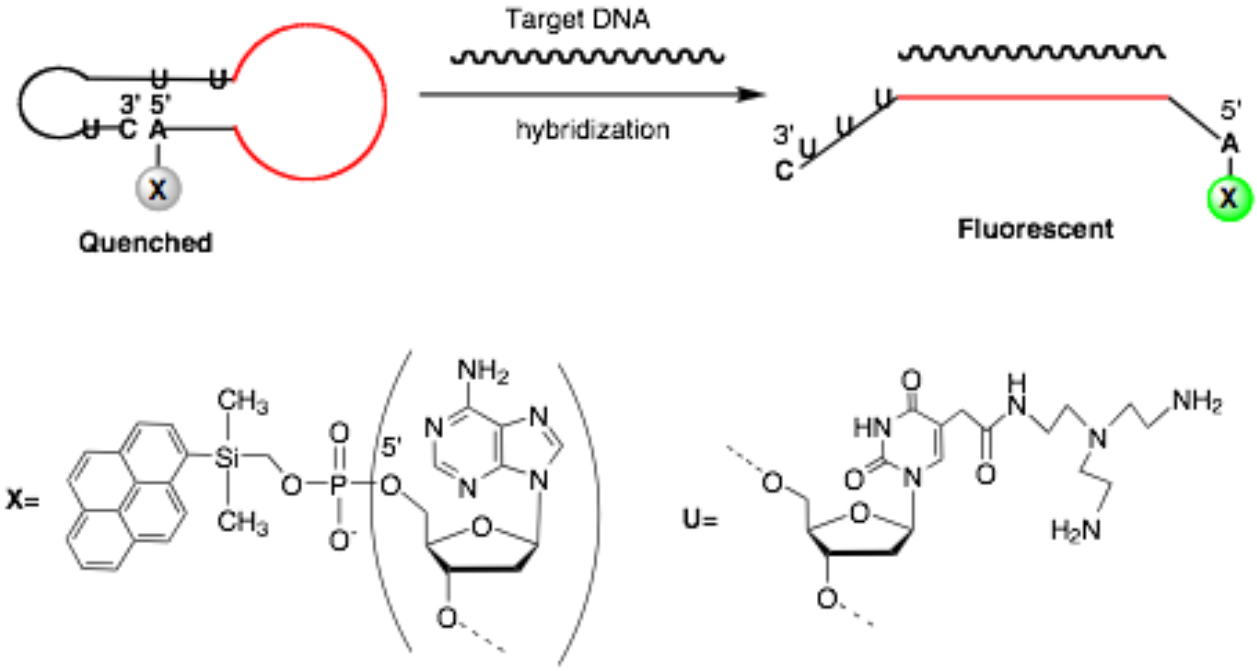


**Figure 3.4:** Basic structure and working principle of newly developed quencher free molecular beacon **Probe-1** bearing silylated pyrene at 5′-terminus.

position to deoxycytidine residue at 3′-terminus. In the study, I have found that the probe gives only a weak fluorescence signal while it stays alone in near physiological conditions. Whereas, the signal substantially increases upon binding to the complementary DNA with the loop portion. Thus, the probe possesses target-detecting ability in terms of its

characteristic change on fluorescence signal. The probe also exhibits certain sequence discriminating ability.

For further exploration to develop a new fluorescent probe for the detection of specific gene fragments, I have synthesized several new molecular beacon probes (**Probes 2 to 5**) by modifying their stem portion or substituting certain deoxyguanosine residue to deoxyinosine residue. Here, I would like to present the results of the studies about the fluorescence properties as well as the thermal stabilities of both the secondary structures of the new probes and the duplexes containing the probes to find out the influence of those modifications to the fluorescence properties of the probes.

## 3.3 Results and Discussion

### 3.3.1 *Synthesis of [1-(Pyrenyl)dimethylsilylmethyl]-(2-cyanoethyl-N,N-diisopropyl-phosphoramidite (5)*

The phosphoramidite derivative of dimethylsilylated pyrene was prepared from a starting material of pyrene using the same procedure as described in the previous chapter 2, Section 2.3.1.

### 3.3.2 *Synthesis of 3´, 5´-O-Diacetyl-5-methoxycarbonylmethyl-2´-deoxyuridine (10).*

The synthesis of compound **10** from D-Arabinose using the same procedure described in Chapter 2, Section 2.3.2.

### 3.3.3 *Synthesis of 1-(2-Aminoethylamino) anthraquinone (16)*

The anthraquinolyldiamine derivative (compound **16**) was prepared from 1-chloroanthraquinine (compound **15**) and ethylenediamine is shown in Scheme 3.1. The starting material (**15**) was reacted with ethylenediamine in toluene under reflux at 120 °C for 24 hours. The appropriate fractions were collected, evaporated under reduced pressure and the obtained compound **16**.

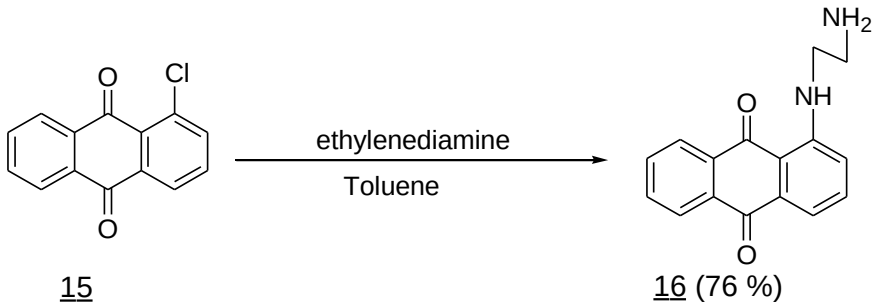


15 16 (76 %)

**Scheme 3.1:** Synthesis of 1-(2-Aminoethylamino) anthraquinone

### 3.3.4 *Synthesis of 5-Carboxy methyl-5′-O-DMTr-2′-deoxyuridine (19)*

The synthesis of 5-Carboxy methyl-*5′-O*-DMTr-2′-deoxyuridine (compound **19**) from compound **10** is shown in Scheme 3.1. At first, the compound **17** was synthesized from compound **10** by reacting with triethlyamine using MeOH as a solvent at room temperature. The incorporation of DMTr- group into compound **17** was then by dissolving it into dry-pyridine and reacting with DMTr-Cl at room temperature. The compound **18** was then hydrolyzed by 1 M LiOH.$H_2O$ at room temperature and prepared compound **19**.

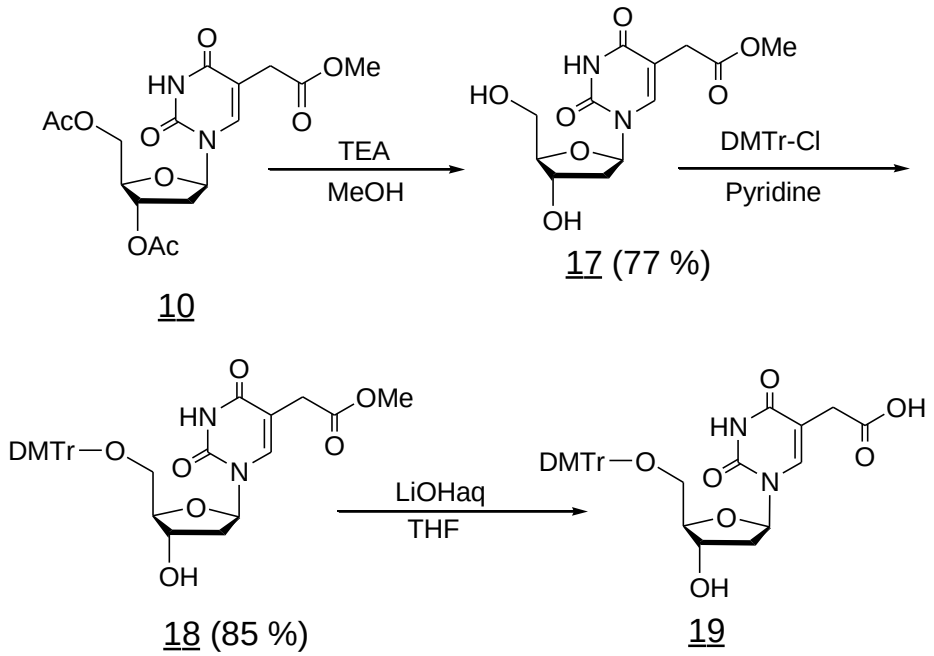


10

17 (77 %)

18 (85 %)

19

**Scheme 3.2:** Synthesis of 5-Carboxy methyl-5′-*O*-DMTr-2′-deoxyuridine [ref. 39-41]

### 3.3.5 *Introduction of anthraquinone moiety to the C-5 position of deoxyuridine*

5-Carboxy methyl-5′-*O*-DMTr-2′-deoxyuridine (compound **19**) was condensed with 1-(2-Aminoethylamino) anthraquinone (compound **16**) with dimethoxytriazinyl *N*-methymorpholinium chloride (DMT-MM) in DMF at room temperature and the desired compound (20) was obtained which was subsequently converted to corresponding phosphoramidite (21). The phosphoramidite derivative was synthesized by mixing with N-ethyl-*N,N′*-diisopropylamine in dry dichloromethane and was stirred under $N_2$ atomosphere at room temperature for 10 min. Thereafter, the phosphitylating reagent, chhloro-(2-cyanoethoxy) diisopropylaminophosphine was added drop wise to the previous mixture under $N_2$ atmosphere at room temperature. After this mixture was stirred for another 1 hour and extracted with dichloromethane. The organic layer was then dried with anhydrous

sodium sulfate and evaporated to dryness. The crude product was purified by silica-gel column chromatography using Ethyl acetate with 2% triethylamine as an eluent. The compound was further purified by treating into a cold solution of 20% diethyl ether in hexane to get a more pure compound. The synthesis steps are shown in Scheme 3.3.

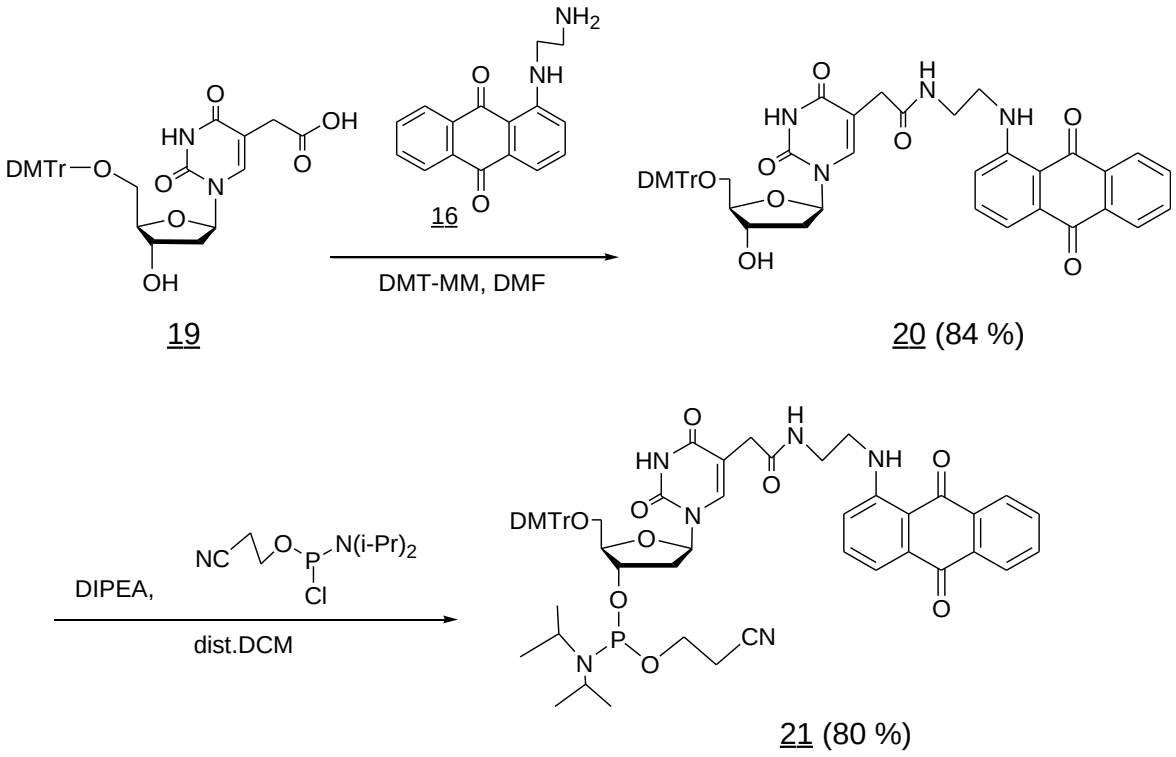


**Scheme 3.3:** Synthesis of 5´-*O*-(4,4´-dimethoxytrityl)-5-[*N*-[2-[*N*-(anthraquinon-1-yl)amino]ethyl]carbamoylmethyl]-2´-deoxyuridine-3´-*O*-yl (2-cyanoethyl)-*N*,*N*-diiso-propylphosphoramidite (21) [ref. 39-41]

### 3.3.6 *Synthesis of modified oligoDNA possessing C-5 modified deoxyuridine and silylated pyrene*

All the modified oligomers were synthesized using an automated DNA synthesizer (ABI 392). Incorporation of the C-5 modified 2´-deoxyuridine derivative into the oligomers was carried out using previously reported methods [39-41]. Incorporation of phosphoramidite derivative of dimethylsilylated pyrene was carried out in a manner similar to that described previously [31]. After the assembly, the support-bound fluorescent oligoDNA was treated with concentrated ammonium hydroxide (55 ˚C, 12 h) followed by reversed-phase HPLC and gel-filtration as usual. The structure and sequences of all modified oligonucleotides and complementary DNA as well as complementary DNA with one base mismatches are shown in Table 3.1. In the molecular beacon probes, the silylated pyrene molecule (X) was placed at the 5´-terminus neighboring consecutive deoxyadenosine residues through phosphodiester linkage. In addition, modified deoxyuridine residues bearing either polyamine molecule (U) or anthraquinone molecule (Y) at their C-5 position are placed instead of natural thymidine residues in the stem-forming region. In all cases, oligoDNA probes were designed by comprising a self-complementary sequence stem portion and a 15 nt long loop portion which is complementary to HIV-1 *tat*/*rev* sequence. In this structure, silylated pyrene connected next to consecutive dA residues will be in a closed proximately position of dC residue at 3´-terminus (Figure 3.5). After synthesis, the oligonucleotides were then purified by reversed phase HPLC, ethanol precipitation and Sephadex G-25 gel filtration. HPLC spectrum of **Probe 1** formerly designated as **GK-2139** are shown in Chapter 2, Figure 2.6 and 2.7. The HPLC spectrum of other oligomers before purification and after purifications are shown in Figure 3.6 to 3.13. On the other hand, the ESI-mass data with optical density and yield of **Probe 1**, **ODN-1** (**GK-1104**), **ODN-4** (**GK-1105**) are also shown in Chapter 2, Table 2.3. However, the structures of the other oligomers which were

also confirmed by ESI-mass spectrophotometer and their optical density, % yield and calculated and found ESI-mass data are shown in Table 3.2.

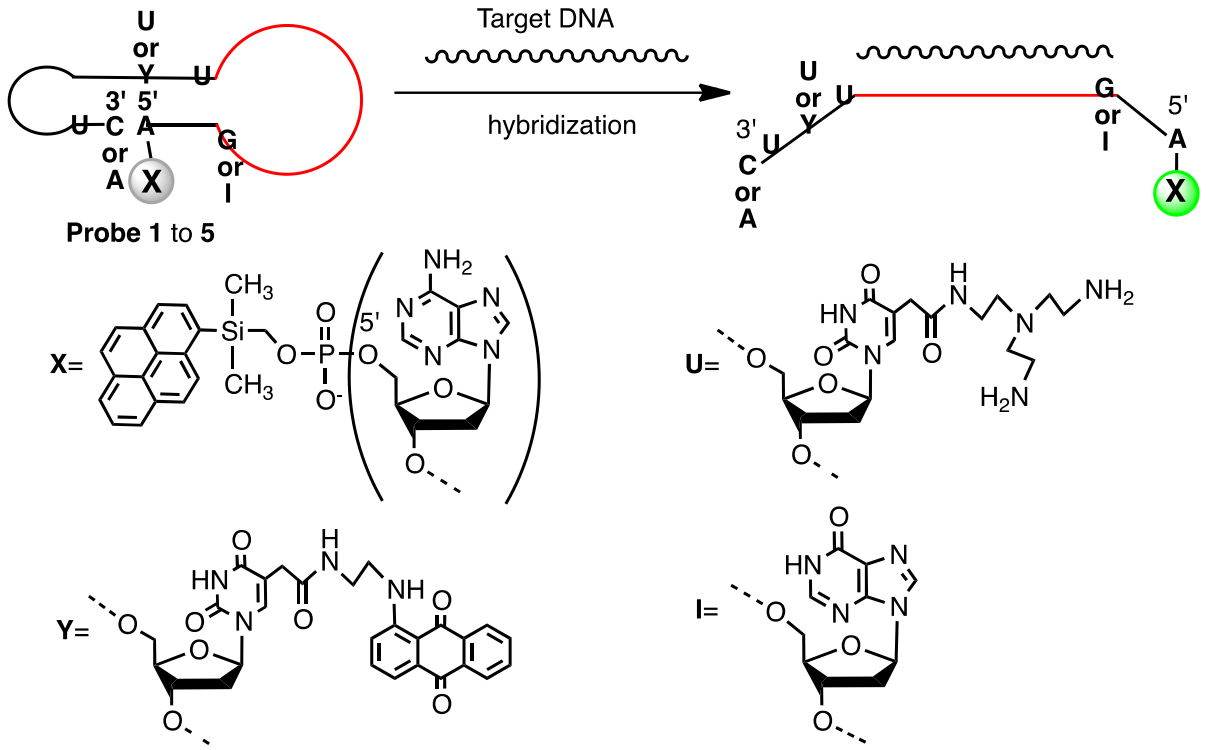


**Figure 3.5:** Basic structure and principle of molecular beacon probe bearing silylated pyrene at 5′-terminus. (Reproduced with permission from ref. 42. Copyright 2015, Chemical Society of Japan)

**Table 3.1:** Sequence and structure of modified oligonucleotides. (Reproduced with permission from ref. 42. Copyright 2015, Chemical Society of Japan)

| Name | Sequence [a,b,c] |
|---|---|
| **Probe 1** | 3′-CUTTTAGUTU*AAGTACTGTTTTCGG*AAA-X-5′ |
| **Probe 2** | 3′-CCUTTTAGGUTU*AAGTACTGTTTTCGG*AAA-X-5′ |
| **Probe 3** | 3′-CCUTTTAGGYTU*AAGTACTGTTTTCGG*AAA-X-5′ |
| **Probe 4** | 3′-CUTTTAGUTU*AAGTACTGTTTTCGI*AAA-X-5′ |
| **Probe 5** | 3′-ACUTTTAGTYTU*AAGTACTGTTTTCGG*AAA-X-5′ |
| **ODN-1** | 5′-TGT*TTCATGACAAAAGCC*-3′ |
| **ODN-2** | 5′-TGT*TTCATGA**G**AAAAGCC*-3′ |
| **ODN-3** | 5′-TGT*TTCATG**T**CAAAAGCC*-3′ |
| **ODN-4** | 5′-TGT*TTCAT**C**ACAAAAGCC*-3′ |

[a] U denotes the polyamine bearing deoxyuridine, X denotes the dimethyl silylated pyerene, Y denotes the anthraquinone bearing deoxyuridine and I denotes deoxyinosine. [b] Italicized letters indicate the complementary region to ODN-Probe. [c] Bold and underlined letters in **ODN 2-4** indicate the corresponding single-nucleotide alternations to fully matched target DNA (**ODN-1**).

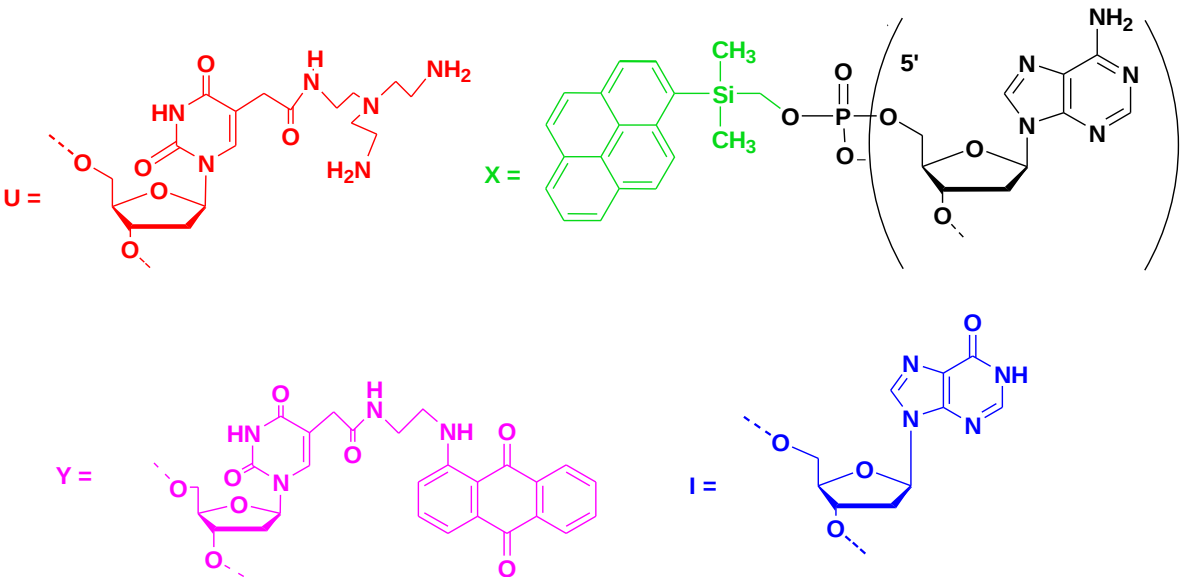

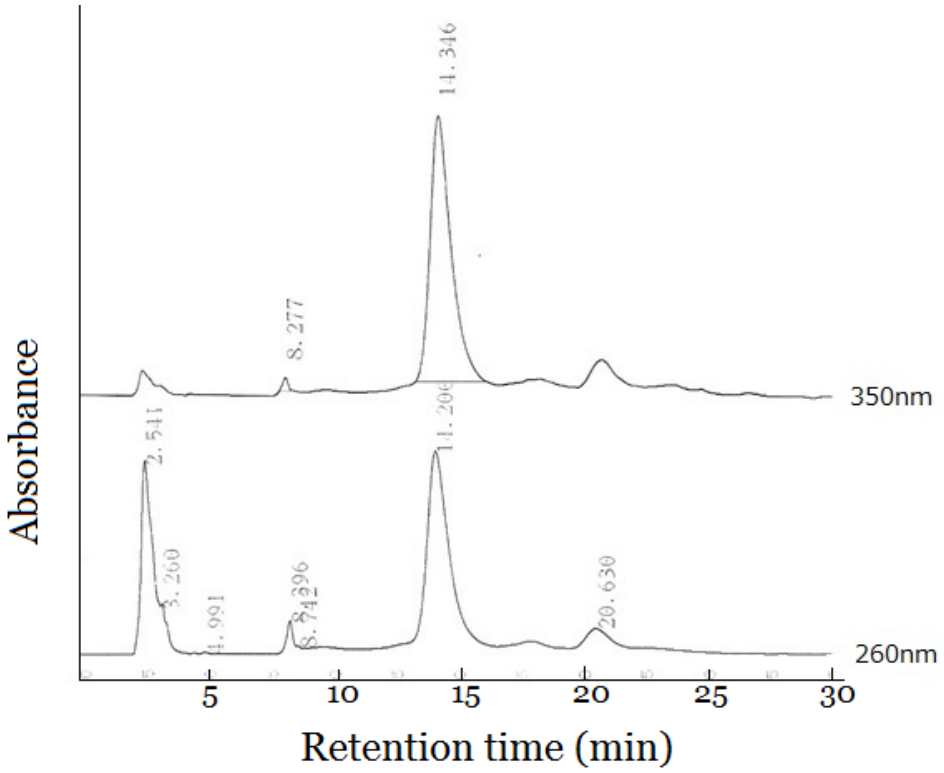


**HPLC Condition**

Column: Wakosil 5 C18 (Ø 4.6 mm X 250 mm)

Flow rate: 0.75 ml/min

**DMTr-ON**

Eluent: A: 100 mM TEAA

B: Acetonitrile

Gradient:

| Time (min.) | 0 | 10 | 20 | 30 |
|---|---|---|---|---|
| B (%) | 20 | 25 | 30 | 40 |

**Figure 3.6:** HPLC profile of **Probe 2** at 260 nm and 350 nm before purification.

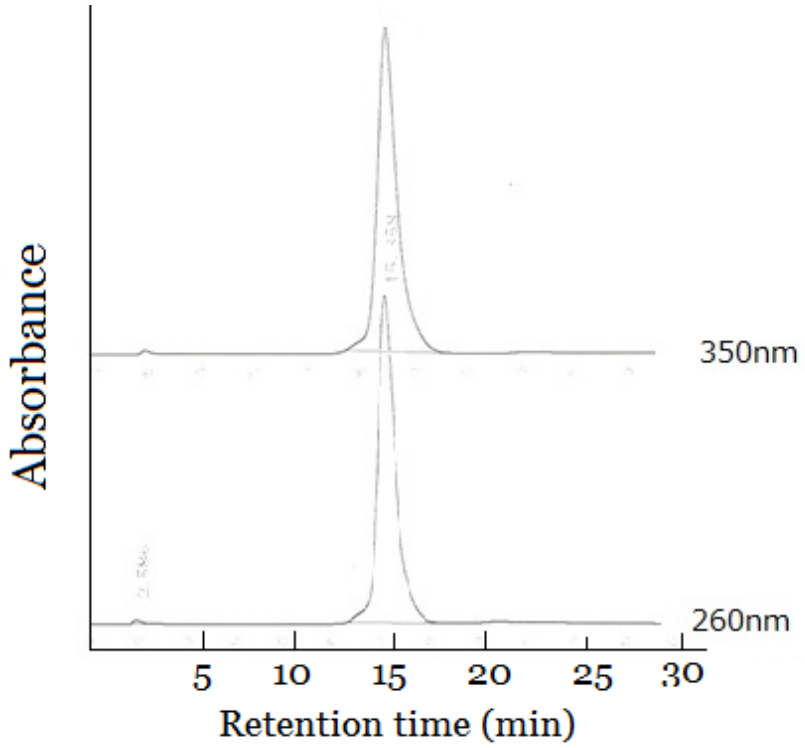


**HPLC Condition**

Column: Wakosil 5 C18 (Ø 4.6mm X 250mm)

Flow rate: 0.75 ml/min

**DMTr-ON**

Eluent: A: 100 mM TEAA

B: Acetonitrile

Gradient:

| Time (min.) | 0 | 10 | 20 | 30 |
|---|---|---|---|---|
| B (%) | 20 | 25 | 30 | 40 |

**Figure 3.7:** HPLC profile of **Probe 2** at 260 nm and 350 nm after purification.

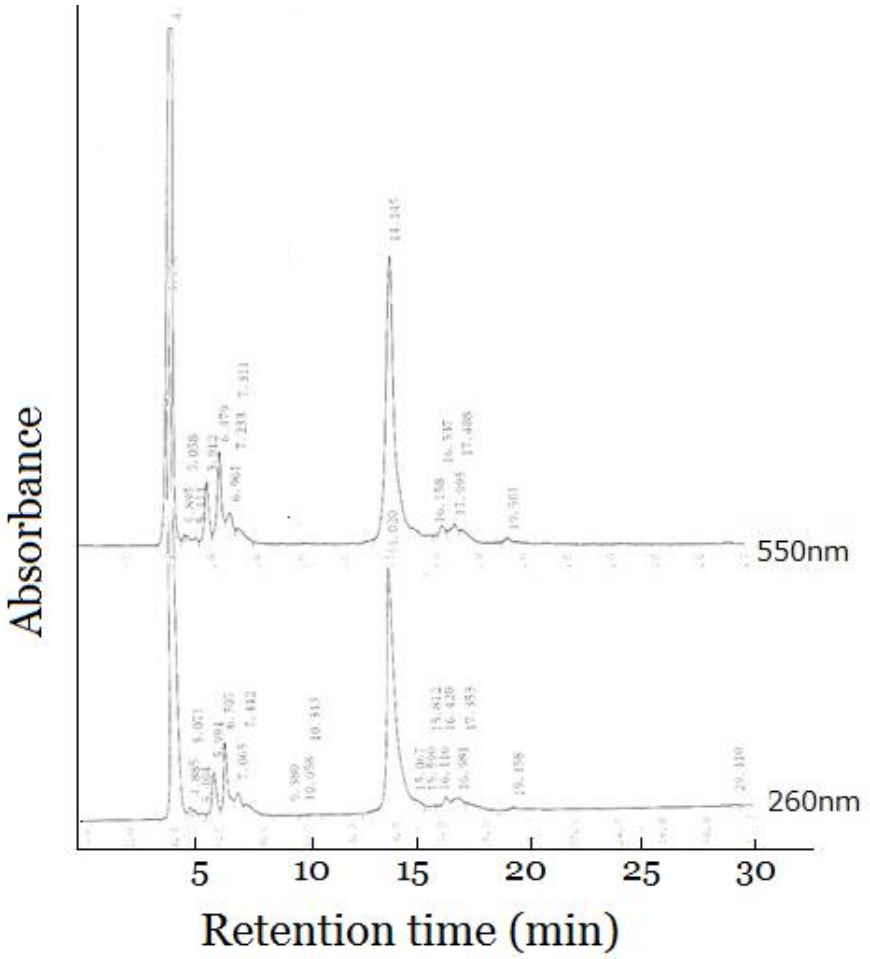


**HPLC Condition**

Column: Wakosil 5 C18 (Ø 4.6mm X 250mm)

Flow rate: 0.75 ml/min

**DMTr-ON**

Eluent: A: 100 mM TEAA

B: Acetonitrile

Gradient:

| Time (min.) | 0 | 10 | 20 | 30 |
|---|---|---|---|---|
| B (%) | 20 | 30 | 30 | 40 |

**Figure 3.8:** HPLC profile of **Probe 3** at 260 nm and 550 nm before purification.

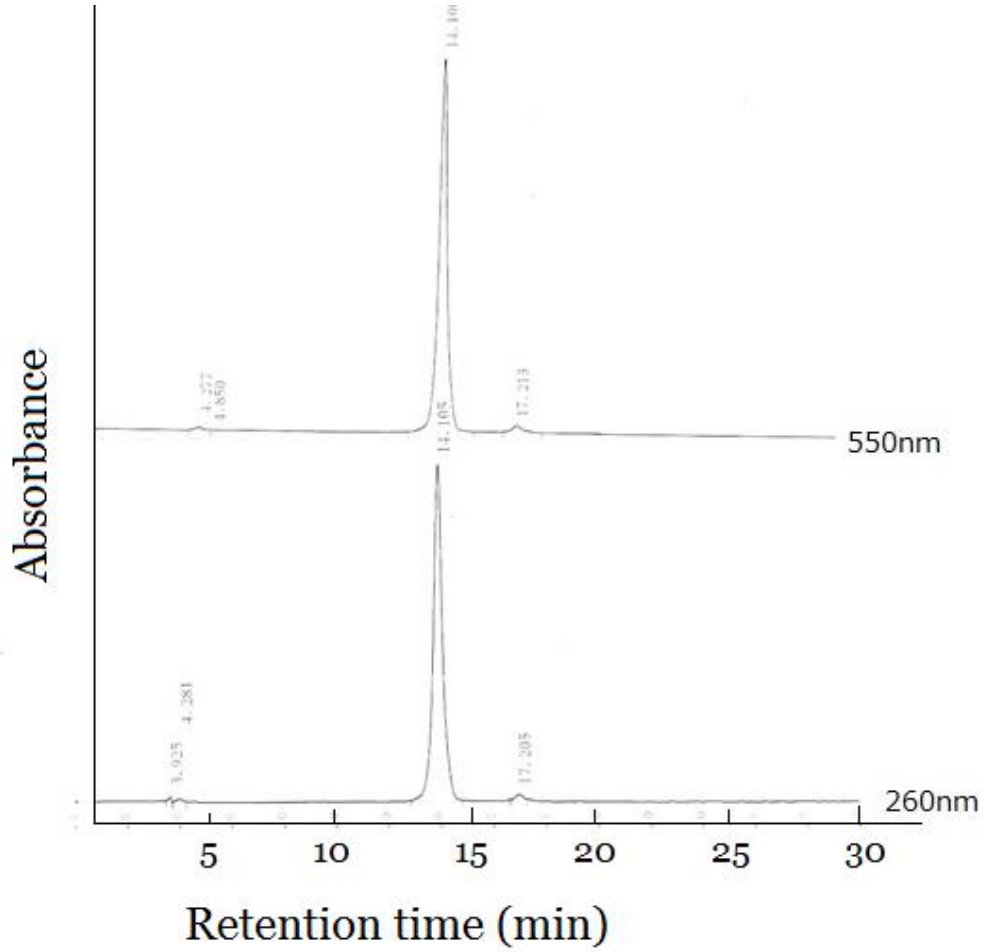


**HPLC Condition**

Column: Wakosil 5 C18 (Ø 4.6mm X 250mm)

Flow rate: 0.75 ml/min

**DMTr-ON**

Eluent: A: 100 mM TEAA

B: Acetonitrile

| Time (min.) | 0 | 10 | 20 | 30 |
|---|---|---|---|---|
| B (%) | 20 | 30 | 30 | 40 |

**Figure 3.9:** HPLC profile of **Probe 3** at 260nm and 550nm after purification.

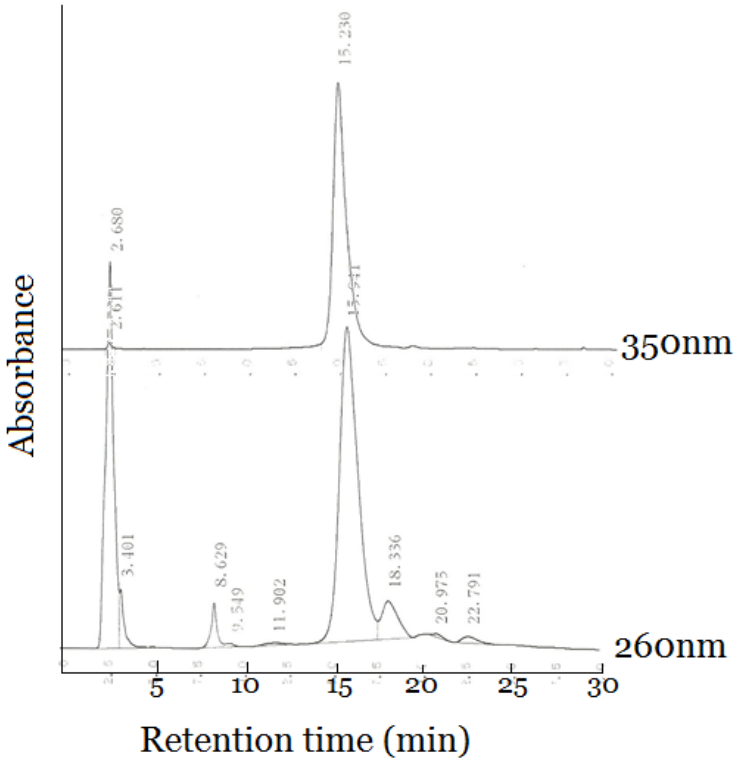


**HPLC Condition**

Column: Wakosil 5 C18 (Ø 4.6mm X 250mm)

Flow rate: 0.75 ml/min

**DMTr-ON**

Eluent: A: 100 mM TEAA

B: Acetonitrile

| Time (min.) | 0 | 10 | 20 | 30 |
|---|---|---|---|---|
| B (%) | 20 | 25 | 30 | 40 |

**Figure 3.10:** HPLC profile of **Probe 4** at 260 nm and 350 nm before purification

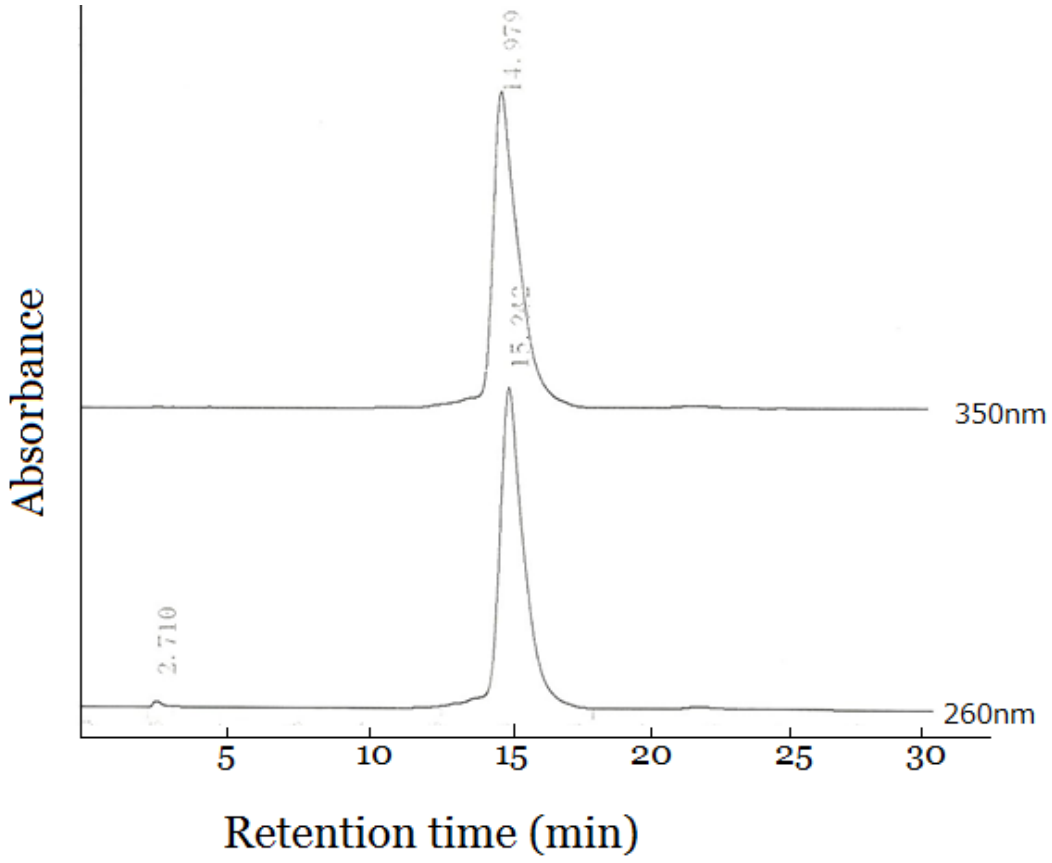


**HPLC Condition**

Column: Wakosil 5 C18 (Ø 4.6mm X 250mm)

Flow rate: 0.75 ml/min

**DMTr-ON**

Eluent: A: 100 mM TEAA

B: Acetonitrile

Gradient:

| Time (min.) | 0 | 10 | 20 | 30 |
|---|---|---|---|---|
| B (%) | 20 | 25 | 30 | 40 |

**Figure 3.11:** HPLC profile of **Probe 4** at 260 nm and 350 nm after purification.

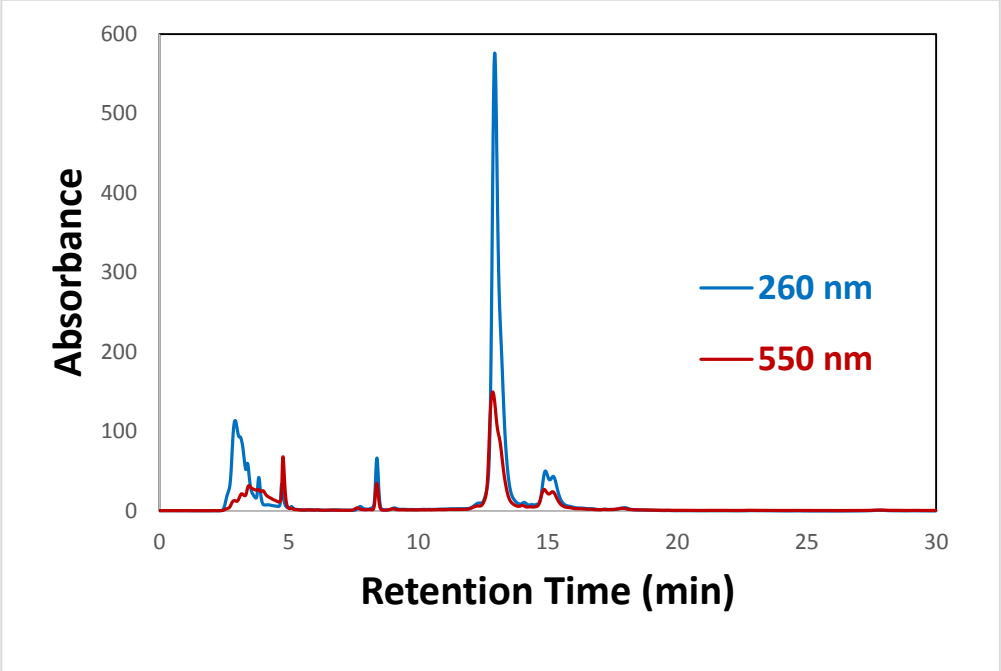


**HPLC Condition**

Column: Wakosil 5 C18 (Ø 4.6mm X 250mm)

Flow rate: 0.75 ml/min

**DMTr-ON**

Eluent: A: 100 mM TEAA

B: Acetonitrile

Gradient:

| Time (min.) | 0 | 10 | 20 | 30 |
|---|---|---|---|---|
| B (%) | 20 | 30 | 30 | 40 |

**Figure 3.12:** HPLC profile of **Probe 5** at 260 nm and 550 nm before purification.

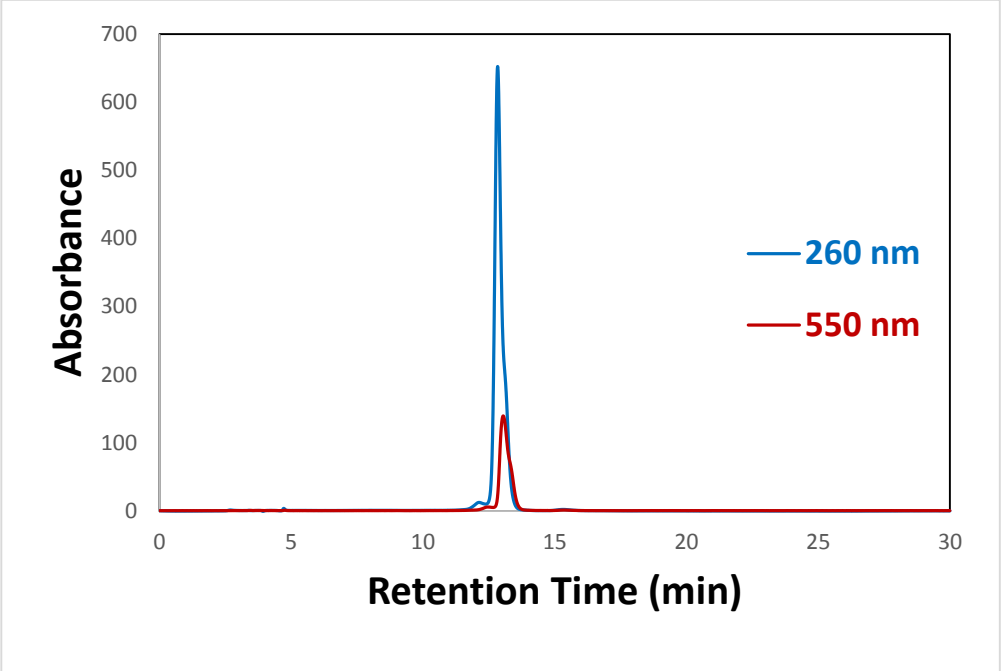


**HPLC Condition**

Column: Wakosil 5 C18 (Ø 4.6mm X 250mm)

Flow rate: 0.75 ml/min

**DMTr-ON**

Eluent: A: 100 mM TEAA

B: Acetonitrile

| Time (min.) | 0 | 10 | 20 | 30 |
|---|---|---|---|---|
| B (%) | 20 | 30 | 30 | 40 |

**Figure 3.13:** HPLC profile of **Probe 5** at 260 nm and 550 nm after purification.

**Table 3.2:** ESI-mass data of oligonucleotides

| Oligonucleotides | ESI-mass | | OD[a] (/ml) | Isolated Yield (%) |
|---|---|---|---|---|
| | Found | Calculated | | |
| Probe 2 | 10087.14 | 10087.05 | 41.2 | 13.7 |
| Probe 3 | 10209.15 | 10209.13 | 9.6 | 3.2 |
| Probe 4 | 9453.86 | 9453.65 | 70.0 | 31.7 |
| Probe 5 | 10208.07 | 10208.14 | 51.4 | 16.8 |
| ODN-2 | 5602.66 | 5602.60 | 52.6 | 29.5 |
| ODN-3 | 5553.57 | 5553.56 | 70.0 | 40.9 |

[a]Optical density is the absorbance of the oligonucleotides at 260nm per unit distance

### 3.3.7 *Duplex forming ability of new MB probes.*

The duplex forming ability of all new molecular beacon probes possessing polyamine-connected deoxyuridine, anthraquinine-connected deoxyuridine and also silylated pyrene was studied by Circular Dichroism (CD) Spectroscopy (Figure 3.14). The CD spectra were measured by taking the probe alone and duplex with their complementary DNA. In all cases, the spectra of the corresponding duplex DNA showed clear positive and negative Cotton effect (peak and trough) within the wavelength region of 250 to 280nm.

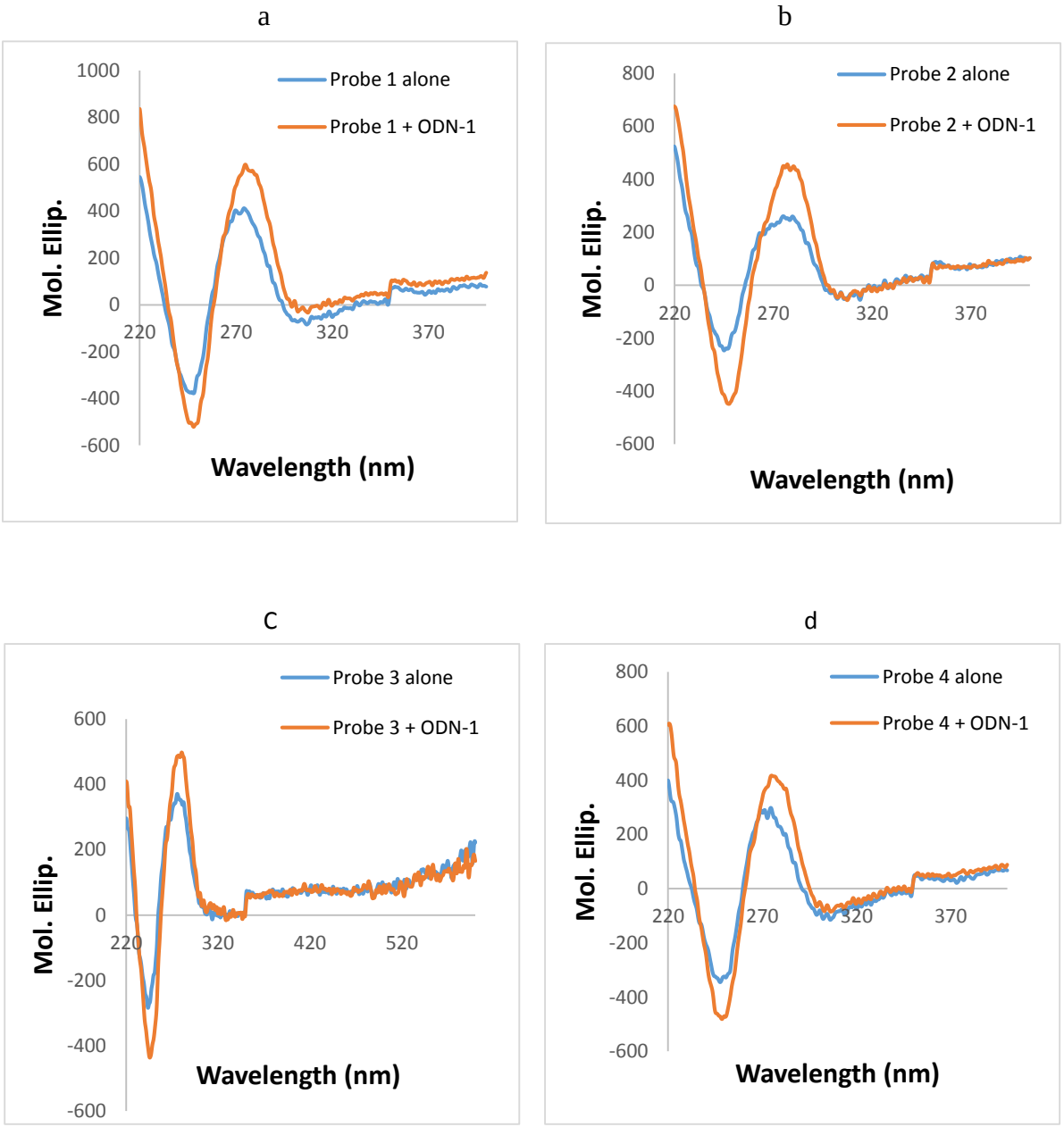


**Figure 3.14:** CD spectra of MB probes alone and its duplex with full-match (ODN-1). **(a) Probe 1** and its duplex with ODN-1 **(b) Probe 2** and its duplex with ODN-1 **(c) Probe 3** and its duplex with ODN-1 DNA **(d) Probe 4** and its duplex with **ODN-1**. 1.0 µM concentration of each oligonucleotides was used in this study and the buffer system used was 10 mM sodium phosphate and 100 mM sodium chloride.

### 3.3.8 *Fluorescence properties of the probes*

The fluorescence properties of the novel stem-loop type MB (**Probe 1**) possessing polyamine-connected deoxyuridine and silylated pyrene has discussed in chapter. The probe gives only a weak fluorescence signal while it stays alone in near physiological conditions. Under the conditions, the probe forms a pseudo-dumbbell shaped structure (Figure 3.5) and observed fluorescence quenching is presumably due to the photoinduced electron transfer involving the adjacent deoxycytidine (dC) residue in the structure. Whereas, the signal substantially increased upon binding to form a complex with the complementary DNA to the loop portion.

At first, I investigated the time dependency of the observed fluorescence increment of **Probe 1** in the same conditions mentioned above (10 mM sodium phosphate buffer containing 100 mM sodium chloride). Thus, the fluorescence signal of **Probe 1** under the presence of **ODN-1** was measured in different time periods and the results are depicted in Figure 3.15-a. As shown in the figure, the probe exhibited marked fluorescence signal at 380 nm upon excitation at 350 nm within few minutes after the addition of **ODN-1** in the solution. Figure 3.15-b summarizes the time-dependent increment of the fluorescence signal at 380 nm. As it is clear from Figure 3.15-b, the fluorescence signal increased rapidly and almost reached a plateau within 10 min. In the following experiments, therefore, fluorescence signal was measured at about 30 min after the mixing of the probes and the complements.

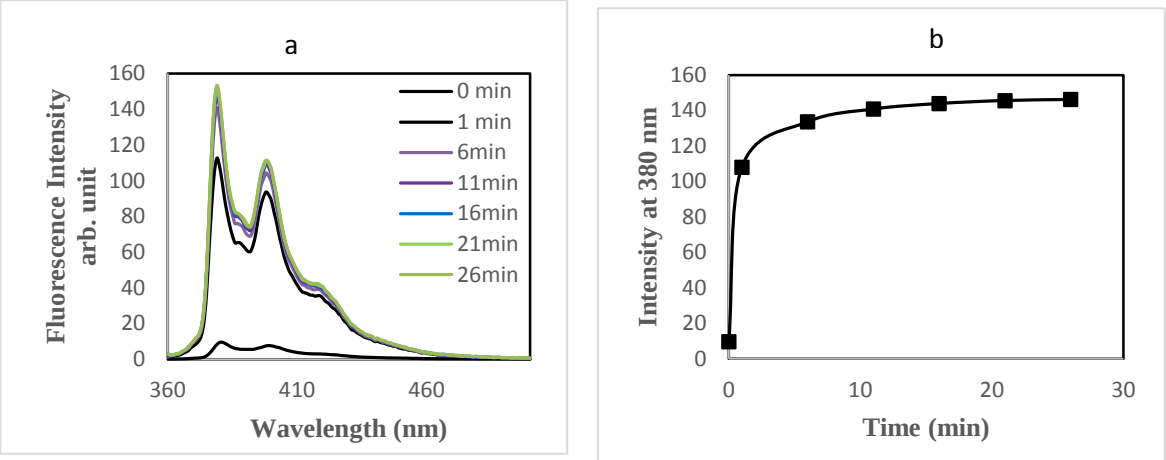


**Figure 3.15: (a)** Fluorescent spectra of **Probe-1** (1.0 μM) changes upon addition of **ODN-1** in 10 mM sodium phosphate buffer (pH 7.2) containing 100 mM NaCl at room temperature. The spectra were collected at 5 minutes intervals after addition of **ODN-1** to the solution of **Probe 1**. **(b)** Kinetic curve of fluorescence signal of **Probe 1** (1.0 μM) at 380 nm with **ODN-1** (1.0 μM). Excitation wavelength is 350 nm. (Reproduced with permission from ref. 42. Copyright 2015, Chemical Society of Japan)

The fluorescence spectra of **Probe 1** were also investigated by changing the concentration of **ODN-1** (complementary DNA) concentration at room temperature using the same buffer system (Figure 3.16). Two different concentration of **ODN-1** were used in this study (1 μM and 5 μM). However, the concentration of **Probe 1** in both cases of **ODN-1** was used 1.0 μM solution. Thus it makes the solutions of two different ratio of **Probe 1** and **ODN-1** (1:1 and 1:5). The fluorescence intensity of **Probe 1** significantly increased with the increase of the **ODN-1** concentration. The quantum yield of **Probe 1** with **ODN-1** at a 1:1 ratio was 0.16. However, the quantum yield at a 1: 5 ratio showed around 0.27.

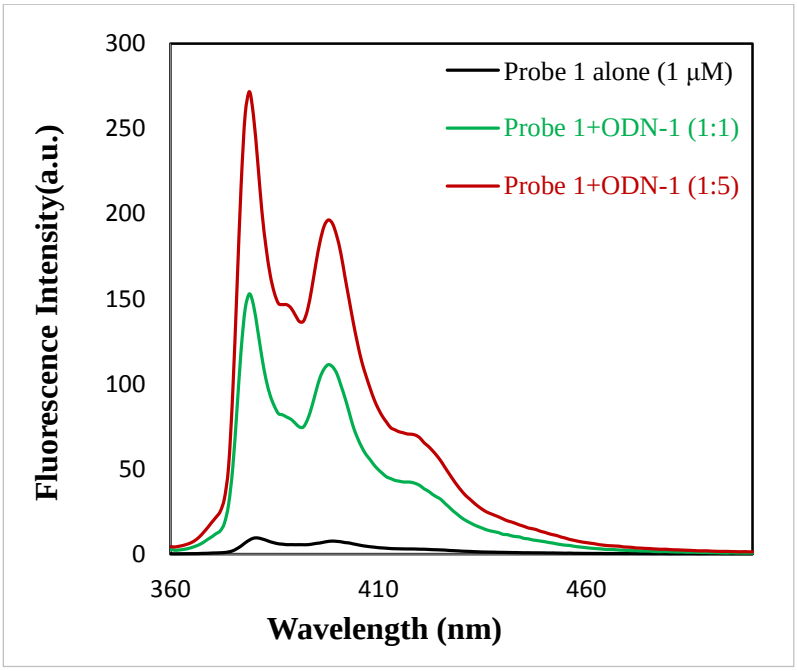


**Figure 3.16:** Fluorescent spectra of Probe 1 alone and duplex with ODN-1 in 10 mM sodium phosphate buffer (pH 7.2) containing 100 mM NaCl at room temperature. The concentration of probe 1 used in all cases is 1.0 μM and concentration of ODN-1 used 0, 1 and 5 μM. Excitation wavelength is 350nm.

The florescence spectra of other molecular beacon probes as well as the complexes with their complement are shown in Figure 3.17. In all cases, fluorescence signal of the probes were effectively quenched while they stayed alone in the solution. As shown in Figure 3.17, however, the extent of the quenching is varied among the probes. The quenching in **Probe 2** and **Probe 4** seems to be slightly less effective compared to that of the original **Probe 1**.

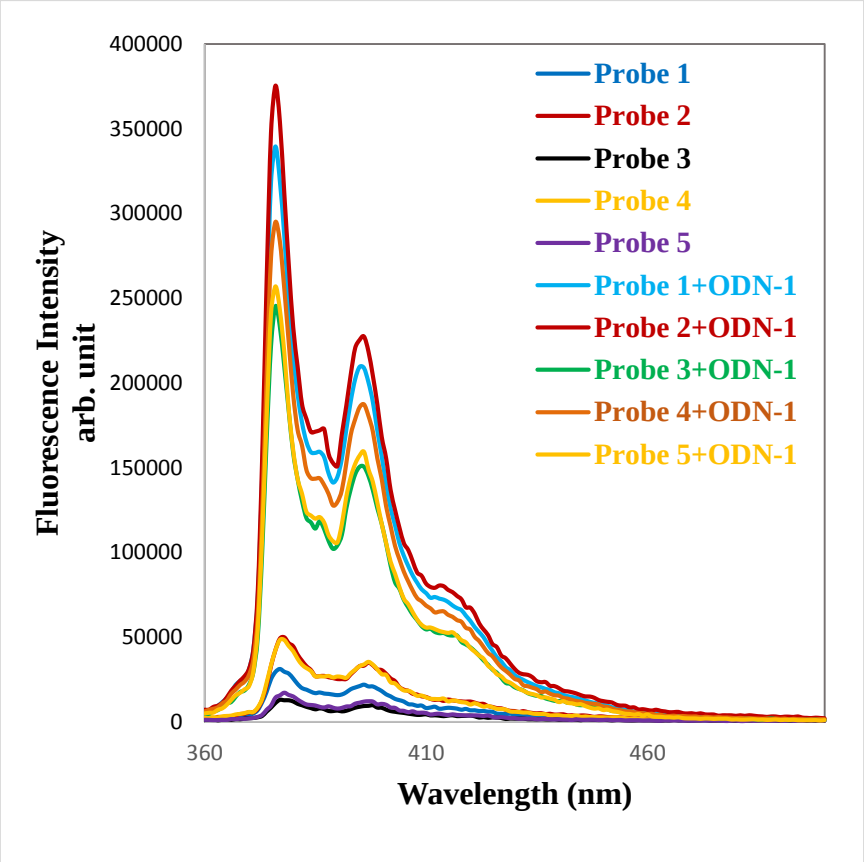


**Figure 3.17:** Fluorescent spectra of MB probes and complexes with **ODN-1** in 10 mM sodium phosphate buffer (pH 7.2) containing 100 mM NaCl at room temperature. The concentration of each oligonucleotide is 1.0 μM. Excitation wavelength is 350 nm. (Reproduced with permission from ref. 42. Copyright 2015, Chemical Society of Japan)

The quenching of fluorescence signal in **Probe 3** is found to be the most effective among the probes. The observed quantum yield ($\Phi_f$) of **Probe 3** is 0.002 and the value is significantly lower than that of **Probe 1** ($\Phi_f$ = 0.008), **Probe 2** ($\Phi_f$ = 0.017) and **Probe 4** ($\Phi_f$ = 0.015). Since **Probe 3** possesses modified deoxyuridine residue bearing anthraquinone moiety, a well known fluorescence quencher, at its C-5 position, the observed effective quenching in **Probe 3** could be attributed due to the additional quenching effect brought by the anthraquinone moiety in the stem portion. Using **Probe 5** which does not have

deoxycytidine at 3'-terminas, we tried to estimate the quenching effect of anthraquinone in **Probe 3**. As it is listed in Table 1, the observed quantum yield of **Probe 5** is 0.003 and the value is nearly same as that of **Probe 3**. The result strongly suggests that the effective quenching in **Probe 3** is mainly brought by the anthraquinone moiety and the effect is greater than that of deoxycytidine, at least, in the current probes.

The presence of complementary DNA (**ODN-1**) brought about the distinct increase on the fluorescence signal of all probes as those are depicted in Figure 3.17. The observed increment of the signal can be attributed to the loss of the secondary structure of the probes along with the formation of a double helical complex with **ODN-1**. Although the sequence recognition portion in all the probes are identical, there were slight differences in the magnitude of their fluorescence signal. The $\Phi_f$ values of the complexes of **Probe 2**, **Probe 3, Probe 4** and **Probe 5** with **ODN-1** were 0.165, 0.120 0.153 and 0.124 respectively ($\Phi_f$ for the complex of **Probe 1** + **ODN-1** is 0.160). Among the complexes, the complex of **Probe 2** + **ODN-1** exhibited highest $\Phi_f$ value and that is slightly larger than that of **Probe 1**. The quantum yield of probe-target complex of **Probe 3** was the lowest among all. On the other hand, the ratio between the quantum yield of probe itself versus probe-target complex (background to signal) in **Probe 3** was 1:60 and it was the highest ratio since the ratio for **Probe 1**, **Probe 2, Probe 4** and **Probe 5** are 1:20, 1:9.7, 1:10.2 and 1:41.3, respectively (Table 3.3). The data indicate that **Probe 3** is a quite sensitive probe reporting the existence of certain gene fragment in solution through the change of its fluorescence signal.

**Table 3.3:** Sequence discrimination ability of different MB probes. (Reproduced with permission from ref. 42. Copyright 2015, Chemical Society of Japan)

| Oligonucleotides | Quantum Yield | $Q_{complex}/Q_{probe}$[a] | $Q_{mis}/Q_{full}$[b] |
|---|---|---|---|
| Probe 1 | 0.008 | -- | -- |
| Probe 1+ODN-1 | **0.160** | 20.00 | 1.00 |
| Probe 1+ODN-2 | 0.102 | 12.75 | 0.64 |
| Probe 1+ODN-3 | 0.104 | 13.00 | 0.65 |
| Probe 1+ODN-4 | 0.050 | 6.25 | 0.31 |
| Probe 2 | 0.017 | -- | -- |
| Probe 2+ODN-1 | **0.165** | 9.71 | 1.00 |
| Probe 2+ODN-2 | 0.122 | 7.18 | 0.74 |
| Probe 2+ODN-3 | 0.125 | 7.35 | 0.76 |
| Probe 2+ODN-4 | 0.089 | 5.24 | 0.54 |
| Probe 3 | 0.002 | -- | -- |
| Probe 3+ODN-1 | **0.120** | 60.00 | 1.00 |
| Probe 3+ODN-2 | 0.062 | 31.00 | 0.52 |
| Probe 3+ODN-3 | 0.071 | 35.50 | 0.59 |
| Probe 3+ODN-4 | 0.049 | 24.50 | 0.41 |
| Probe 4 | 0.015 | -- | -- |
| Probe 4+ODN-1 | **0.153** | 10.20 | 1.00 |
| Probe 4+ODN-2 | 0.115 | 7.67 | 0.75 |
| Probe 4+ODN-3 | 0.119 | 7.93 | 0.78 |
| Probe 4+ODN-4 | 0.087 | 5.80 | 0.57 |
| Probe 5 | 0.003 | -- | -- |
| Probe 5+ODN-1 | **0.124** | 41.33 | 1.00 |
| Probe 5+ODN-2 | 0.101 | 33.66 | 0.81 |
| Probe 5+ODN-3 | 0.088 | 29.33 | 0.71 |
| Probe 5+ODN-4 | 0.079 | 26.33 | 0.64 |

[a] Ratio of quantum yield of complexes ($Q_{complex}$) with that of probes alone ($Q_{probe}$). [b] Ratio of quantum yield of mismatched complexes ($Q_{mis}$) with that of matched strand ($Q_{full}$)

### 3.3.9 *The effect of mismatch in the target DNA to the fluorescence signal of the probes*

The effect of single nucleotide alteration in the complementary DNA to the fluorescent signal was also investigated using single mismatched targets, namely **ODN-2** to **ODN-4**. In the targets, one nucleotide unit near middle of the complementary sequence to the probes is altered from the full-matched target (**ODN-1**) as those are indicated in Table 3.1. The combination of the mismatch includes G/G, T/T and C/C. The obtained fluorescence signal of the complexes consisting of the probes and mismatched targets decreased in all cases compared to those of the corresponding complexes consisting of the probes and fully matched target (**ODN-1**) as those are shown in Figure 3.18 to 3.22. Thus, all probes recognized single nucleotide alternation in the target in terms of the fluorescence signal. However, recognition of **ODN-4** by the probes seems to be accomplished most effectively since the decrement of the fluorescence signal on **ODN-4** was more prominent compare to those on other combination of mismatch in all tested cases. Recognition of **ODN-2** seems to be almost same or a little bit worth than the recognition of T/T mismatch using **ODN-3**.

According to the results, **Probe 3** recognizes nicely all the three mismatches since the ratio between the quantum yields of probe-fully matched target versus probe-mismatched targets in **Probe 3** exhibited smaller values than other cases.

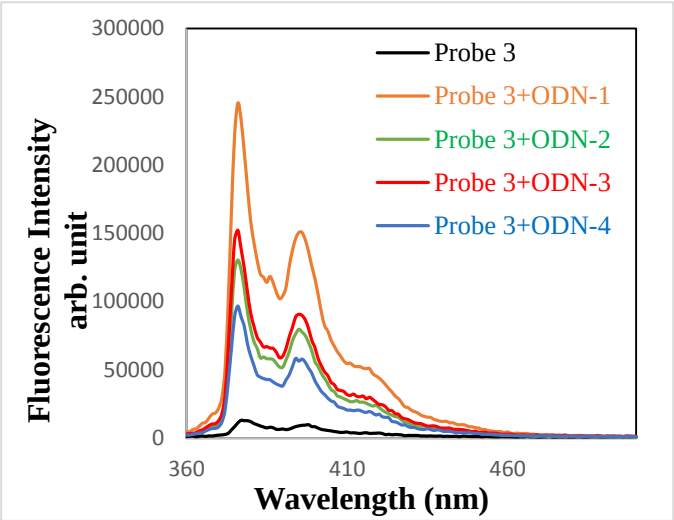


**Figure 3.18:** Fluorescent spectra of **Probe 3** and complexes with **ODN-1** to **4** in 10 mM sodium phosphate buffer (pH 7.2) containing 100 mM NaCl at room temperature. The concentration of each oligonucleotide is 1.0 μM. Excitation wavelength is 350 nm. (Reproduced with permission from ref. 42. Copyright 2015, Chemical Society of Japan)

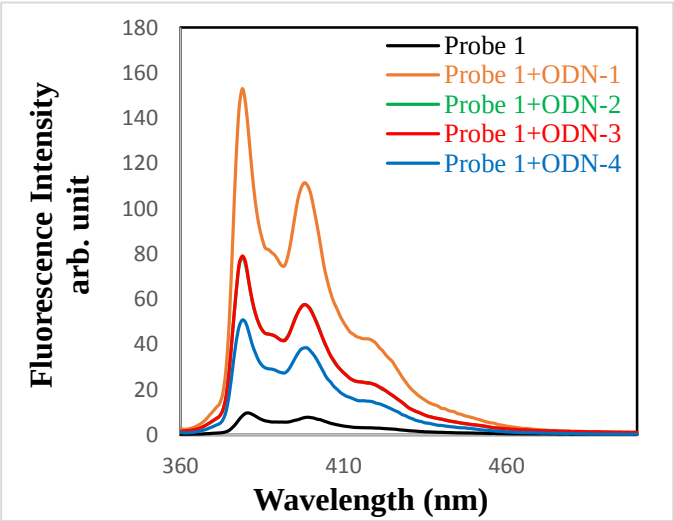


**Figure 3.19:** Fluorescent spectra of **Probe 1** and complexes with **ODN-1** to **4** in 10 mM sodium phosphate buffer (pH 7.2) containing 100 mM NaCl at room temperature. The concentration of each oligonucleotide is 1.0 μM. Excitation wavelength is 350 nm.

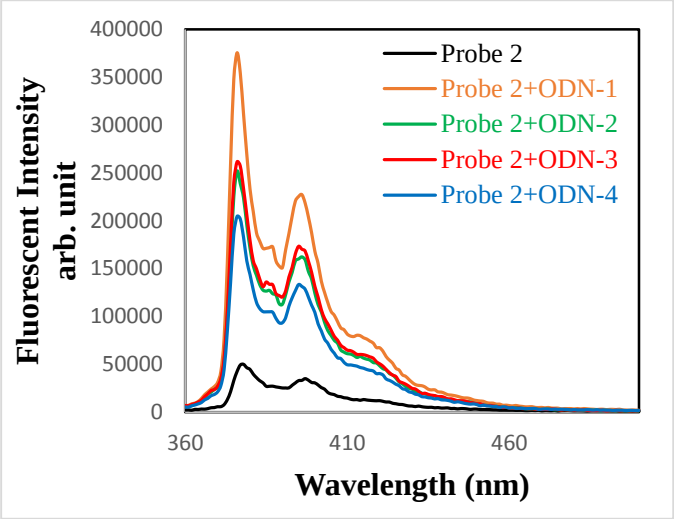


**Figure 3.20:** Fluorescent spectra of **Probe 2** and complexes with **ODN-1** to **4** in 10 mM sodium phosphate buffer (pH 7.2) containing 100 mM NaCl at room temperature. The concentration of each oligonucleotide is 1.0 μM. Excitation wavelength is 350 nm.

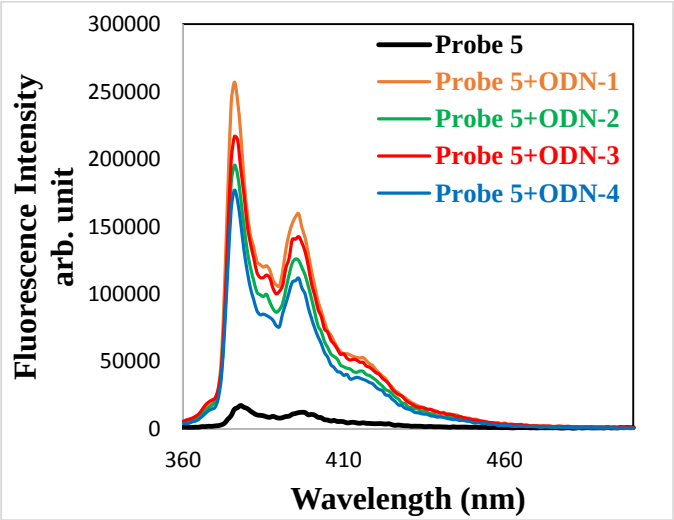


**Figure 3.21:** Fluorescent spectra of **Probe 5** and complexes with **ODN-1** to **4** in 10 mM sodium phosphate buffer (pH 7.2) containing 100 mM NaCl at room temperature. The concentration of each oligonucleotide is 1.0 μM. Excitation wavelength is 350 nm. (Reproduced with permission from ref. 42. Copyright 2015, Chemical Society of Japan)

### 3.3.10 *The effect of deoxyinosine to the fluorescence signal of Probe 4*

As the $\Phi_f$ value of the complex consisting of **Probe 1** and **ODN-1** was much smaller than that of silylated pyrene, it was speculated that this could be partially reasoned by long-range fluorescence quenching effect of deoxyguanosine residues near 5′-teminus. Therefore, I have substituted the 4th deoxyguanosine residue in **Probe 1** to deoxyinosine in **Probe 4** expecting to have larger $\Phi_f$ value for **Probe 4** after the formation of complex with **ODA-1**. However, it could not see any such effect since fluorescent quantum yield of the complex consisting of **Probe 4** and **ODN-1** was almost same as that of the complex consisting of **Probe 1** and **ODN-1** as it is shown in Table 3.3.

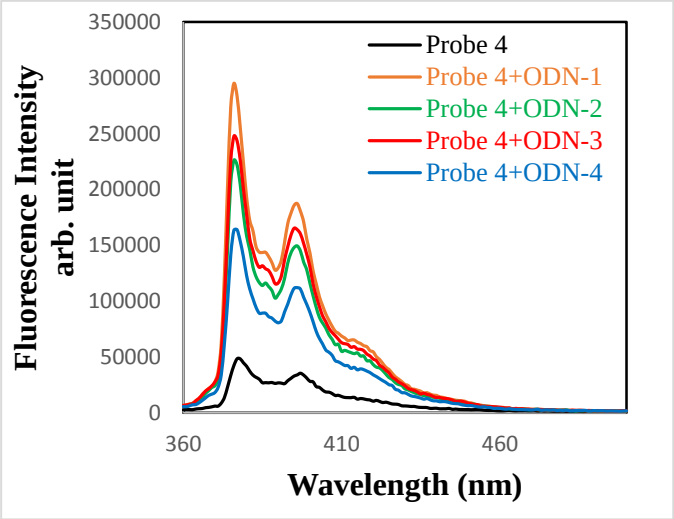


**Figure 3.22:** Fluorescent spectra of **Probe 4** and complexes with **ODN-1** to **4** in 10 mM sodium phosphate buffer (pH 7.2) containing 100 mM NaCl at room temperature. The concentration of each oligonucleotide is 1.0 μM. Excitation wavelength is 350 nm.

### 3.3.11 *Hybridization abilities of molecular beacon type probe.*

The UV melting studies were performed to identify the duplex forming ability as well as the sequence discriminating ability of the molecular beacon type probes. The melting temperatures (*Tm*) of the molecular beacon probes as well as the complexes with their full-matched and single mismatched targets obtained from the studies are listed in Table 3.4. As it mentioned earlier [38], *Tm* value of **Probe 1** possessing three polyamine bearing

**Table 3.4:** UV melting temperatures of MB probes. (Reproduced with permission from ref. 42. Copyright 2015, Chemical Society of Japan)

| OligoDNA | Alone | ODN-1 | ODN-2 | | ODN-3 | | ODN-4 | |
|---|---|---|---|---|---|---|---|---|
| | | $T_m(^0C)$ | $T_m(^0C)$ | $\Delta T_m(^0C)$ | $T_m(^0C)$ | $\Delta T_m(^0C)$ | $T_m(^0C)$ | $\Delta T_m(^0C)$ |
| Probe 1 | 37.3 | 51.4 | 40.8 | 10.6 | 43.0 | 8.4 | 36.9 | 14.5 |
| Probe 2 | 41.2 | 51.3 | 42.6 | 8.7 | 45.7 | 5.6 | 36.0 | 15.3 |
| Probe 3 | 45.2 | 53.7 | 40.6 | 13.1 | 41.7 | 12.0 | 36.6 | 17.1 |
| Probe 4 | 35.8 | 49.5 | 39.0 | 10.5 | 40.0 | 9.5 | 32.8 | 16.7 |
| Probe 5 | 45.1 | 52.9 | 43.7 | 9.2 | 44.7 | 8.2 | 35.8 | 17.1 |

Conditions: UV melting temperature profile was measured in 10mM sodium phosphate buffer containing 100 mM NaCl and 3 µM of each oligonucleotide.
$\Delta T_m$= ($T_m$ value with full matched complement - $T_m$ value with mismatched complement).

deoxyuridine within the 5-bp stem portion was 37.3 °C and it is about 10 °C higher than that of the corresponding oligoDNA possessing natural thymidine residues instead of the modified deoxyuridine residues. This could be attributed to the duplex-stabilizing effect of the modified deoxyuridine residues in **Probe 1** [43]. *Tm* value of **Probe 2** possessing three

polyamine bearing deoxyuridine within the longer (6-bp) stem portion was around 41 °C. Meanwhile, *Tm* value of **Probe 3** was around 45 °C and it is about 4 °C higher than that of **Probe 2**. In Probe 3, one polyamine bearing deoxyuridine in Probe 2 is substituted with anthraquinone bearing deoxyuridine. Thus, the result can be explained that anthraquinone molecule attached at C-5 position of deoxyuridine through an alkyl linker intercalates into double helical portion of Probe 3 to increase the thermal stability [44]. In addition, the data indicates that the duplex-stabilizing effect of anthraquinone is stronger than that of the polyamine, at least in this case. *Tm* value of **Probe 4** was slightly smaller than that of **Probe 1**. The sequence of **Probe 4** is almost identical to that of **Probe 1** except one deoxyguanosine residue in the loop portion of **Probe 1** is substituted to deoxyinosine residue (Figure 3.5). Probe 5 possessing the same numbers of polyamine bearing deoxyuridine and anthraquinone bearing deoxyuridine as Probe 3 exhibited almost same *Tm* value as Probe 3.

The $T_m$ values of the complexes containing mismatched targets decreased compared to those of the complexes containing full matched target (ODN-1) in all cases, however, with different extent. Based on the data in Table 3.4, all probes seem to recognize the existence of mismatch in **ODN-4** most nicely among the tested mismatched targets because the $\Delta T_m$ values for **ODN-4** exhibited the largest values. On the other hand, recognition of **ODN-3** was the lowest. In addition, such sequence recognition ability seems to be highest in **Probe 3** because the obtained $\Delta T_m$ values for **Probe 3** exhibited the largest values to all mismatched targets. Figure 3.23 shows a comparison of $T_m$ values of different probes and their complexes with full matched target and mismatched targets.

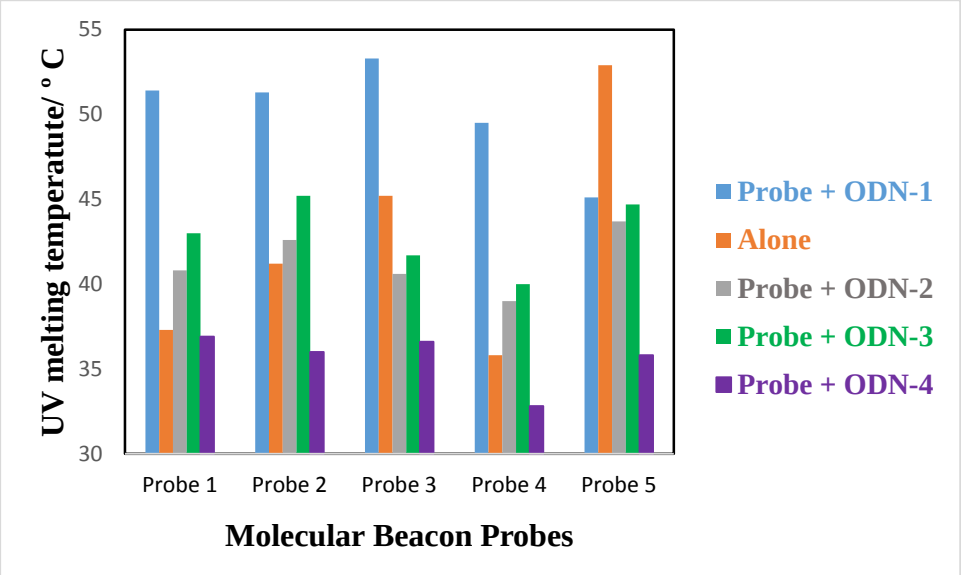


**Figure 3.23:** UV melting temperature of MB probes (alone) and complexes with full matched target **ODN-1** and single mismatched targets **ODN-2 to 4**.

As discussed earlier, quenching of fluorescence signal in **Probe 3** is most effective among the probes while they are staying alone. Also, recognition of the mismatched target by the probes in term of fluorescence signal was most effective on **ODN-4** since the decrement of the fluorescence signal on **ODN-4** compared to **ODN-1** was the most prominent among all the mismatched targets. Thus, there are some correlations between the fluorescence signal and thermal stability of the complex formed by the probe and the target. In the cases described in this study, we found overall trend that fluorescence signal of the probe was effectively quenched as the melting temperature of the probe is increased when the probe stays alone. However, in the cases of **Probe 3** and **Probe 5**, anthraquinone moiety affects both the increment of thermal stability of the probe and the quenching of the fluorescence signal. In the complex, the complex having larger $\Delta T_m$ value gives smaller fluorescence signal.

## 3.4 Conclusion

New molecular beacon type of probes bearing modified deoxyuridine derivatives and a silylated pyrene as a fluorophore were synthesized. The probes have a part of self-complementary sequence and forms pseudo-dumbbell secondary structure while they stay alone. The modified deoxyuridine derivatives are located in the stem portion of the structure and 3'-terminal deoxycytidine is presumed to be in the proximal position to silylated pyrene at 5'-terminus in the structure. Under the condition, fluorescence signal of the probes are efficiently quenched. The terminal deoxycytidine is responsible to the quenching, however, anthraquinone moiety located in the opposite position of silylated pyrene seems to have greater quenching effect. Also the thermal stability of the secondary structure depends on the kind of modification on the modified deoxyuridine residues. On the other hand, the signal of the probes markedly recovered while they formed complexes with oligoDNA having fully complementary sequence to their large loop portion. The signal, however, significantly decreased while they formed complexes with oligoDNA having mismatched sequence, in different extent. Thus, the all probes tested in the study possess, more or less, an ability to recognize one base alternation in the complementary region of the target in term of fluorescence signal. The complex with mismatched target exhibiting larger decrement of *Tm* compared to the complex with full-matched target gives smaller fluorescence signal. Thus the thermal stabilities of the secondary structure of the probe and the complex with the targets are the part of factors to influence the fluorescence signal of the probe in addition to the effective fluorescence quenching brought by anthraquinone.

## 3.5 Experimental

### 3.5.1 *General Information*

Reactions under anhydrous conditions were carried out under an atmosphere of nitrogen. Reaction progress was observed by thin layer column chromatography on Merck silica gel 60 F254-precoated plate under UV lamp. Column Chromatography was performed with silica gel 60N (neutral, spherical, 63-210µm). $^{1}$HNMR and $^{31}$PNMR spectra were recorded on JOEL (JNM-ECA 400) FT NMR SYSTEM at 400 MHz and 161.8 MHz, respectively, using tetramethylsilane as internal standard. ESI-MS spectra were recorded on Perkin Elmer API-100 ESI-MS Spectrophotometer. UV-vis spectra were taken on UV-2450 Spectrophotometer (Shimadzu). Fluorescence spectra were recorded on F-4500 Fluorescence Spectrophotometer (HITACHI) and Fluoromax-4 Spectrofluorometer (HORIBA). Oligonucleotides were purified by reversed-phase HPLC (PU-2089 plus, JASCO) attached with UV-vis detector (SPD-10A, Shimadzu) and Chromatopac (C-R8A, Shimadzu) using Wakosil 5 C18 column (Ø 4.6 mm X 250 mm).

### 3.5.2 *Synthesis of 1-(2-Aminoethylamino)anthraquinone (16).*

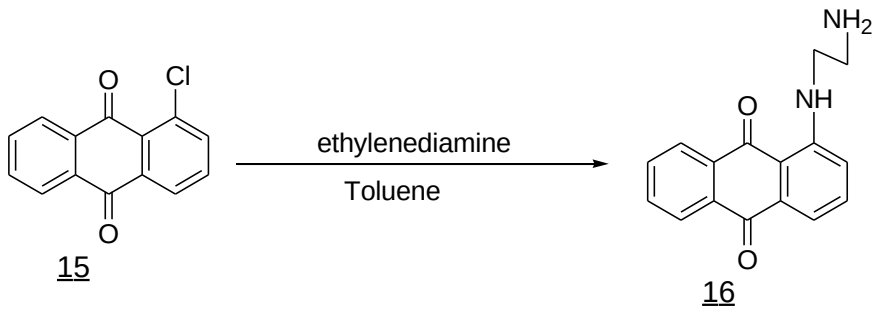


15 16

The mixture of ethylenediamine (3 ml, 82 mmol) and 1-chloroanthraquinone (**15**, 2.0 g, 8.24 mmol) was stirred at 120 °C for 24 hours. The reaction progress was monitored by TLC using 15 % MeOH in $CH_2Cl_2$ with 1 % TEA. After reaction, the reaction mixture was cooled then concentrated by evaporation. The residue was then chromatographed on a column of silica gel with 15 % MeOH in $CH_2Cl_2$ with 1 % TEA. The appropriate fractions were collected, evaporated under reduced pressure to give an obtained compound **16** (1.66 g, 76 %). $^1$H NMR (400 MHz, $CDCl_3$) δ (ppm) = 3.06-3.09 (m, 2H, - $CH_2$-), 3.39-3.46 (m, 2H, - $CH_2$), 7.05-7.07 (m, 2H, H-Ar of Aq), 7.52-7.57 (m, 2H, H-Ar of Aq), 8.20-8.27 (m, 2H, H-Ar of Aq), 9.90 (br. 1H, -NH)

### 3.5.3 *Synthesis of 5-Methoxycarbonyl methyl-2′-deoxyuridine (17)*

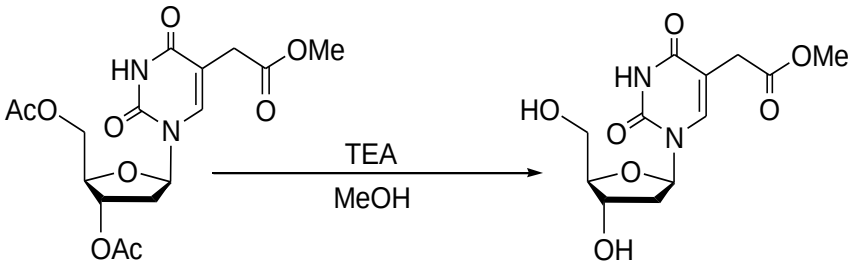


10 17

Compound **10** (0.817 g, 2.1 mmol) was dissolved in dry MeOH (20 ml) and 6 ml of triethylamine (TEA) was added into it and stirred for 24 hours at room temperature. After reaction, TLC test was done to check the end point of reaction using solvent system of 10 % MeOH in $CH_2Cl_2$. Compound **17** (0.502 g, 77 %) was then purified by silica-gel column chromatography using 15 % MeOH in $CH_2Cl_2$. $^1$H NMR (400 MHz, $CDCl_3$) δ (ppm) = 1.85-1.86 (m, 2H, 3′- OH, 5′- OH), 2.23-2.28 (m, 2H, 5-$CH_2$-), 3.58-3.63 (m, 3H, 5-OMe), 3.9 (s, 1H, 3′- H), 4.32-4.33 (m, 2H, 5′- $CH_2$), 6.13-6.17 (m, 1H, 4′-H), 7.7 (s, 1H, 6-H).

### 3.5.4 *Synthesis of 5-Methoxycarbonyl methyl-5´-O-DMTr-2´-deoxyuridine (18)*

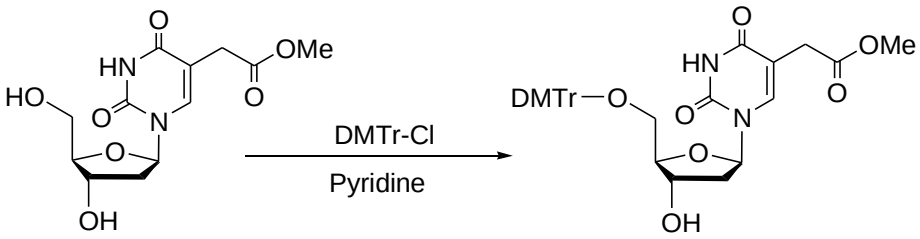


17 18

Compound 17 (0.465 g, 1.55 mmol) was dissolved into dry-pyridine (20 ml) and DMTr-Cl (0.787 g, 2.32 mmol) was added into the reaction vessel and stirred the mixture at room temperature and TLC checked at 1.5 hr (50 % EtOAc in $CH_2Cl_2$ + 1% TEA). The mixture was evaporated under reduced pressure by a prior addition of 5 ml methanol to the mixture. The residue is then partitioned between dichloromethane and saturated $NaHCO_3$ solution. The organic layer was collected, washed with saturated $NaHCO_3$ solution, dried over $Na_2SO_4$, and evaporated under reduced pressure and subsequently purified the desired compound **18** by silica-gel column chromatography (50 % EtOAc in $CH_2Cl_2$ + 1 % TEA). The yield of compound **18** was 85 % (0.796 g). $^1$H NMR (400 MHz, $CDCl_3$) δ (ppm) = 2.32-2.44 (m, 2H, 2´-H), 3.32-3.35 (m, 2H, C5-$CH_2$-), 3.52 (s, 3H, -$OCH_3$), 3.72 (s, 6H, $OCH_3$ of DMTr), 4.04-4.08 (m, 1H, 4´-H ), 4.57-4.58 (t, 1H, 3´-H ), 6.41-6.44 (t, 1H, 1´-H ), 6.77-6.79 (m, 4H, H-Ar of DMTr), 7.20-7.23 (m, 9H, H-Ar of DMTr), 7.76 (s, 1H, 6-H),

### 3.5.5 *Synthesis of 5-Carboxy methyl-5´-O-DMTr-2´-deoxyuridine (19)*

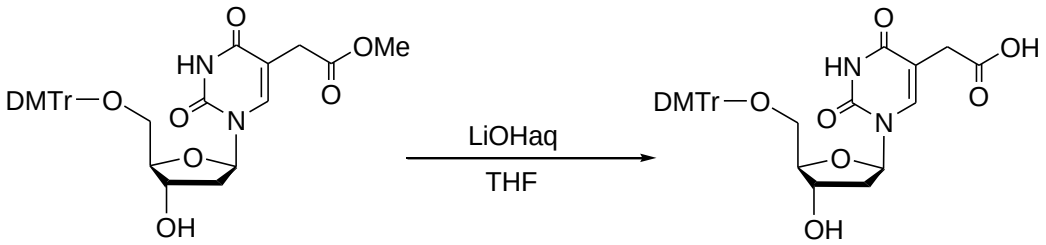


18 19

Compound **18** (0.766 g, 1.27 mmol) was dissolved in THF and 14 ml 1M $LiOH.H_2O$ was added and stirred at room temperature for 2 hours. Reaction progress was checked by TLC (10% MeOH in $CH_2Cl_2$). The mixture was then treated in ice bath for 15 minutes. After cooling, 15 ml dichloromethane was added to the mixture. To make the pH of the solution between 5 and 6, sufficient amount of 5% citric acid was added dropwisely to the reaction mixture. The mixture was then partitioned between dichloromethane and saturated $NaHCO_3$ solution. The organic layer was collected, washed with saturated NaCl solution. Thereafter, 1 ml TEA was added and evaporated under reduced pressure. The yield of crude compound **19** was 107 % (0.830 g). 1H NMR (400 MHz, $CDCl_3$): δ (ppm) = 2.25-2.28 (m, 2H, 2´-H), 2.84-2.89 (m, 2H, C5-$CH_2$-), 3.28-3.30 (m, 2H, C5´-$CH_2$), 3.72 (s, 6H, $OCH_3$ of DMTr), 3.94-3.95 (m, 1H, 4´-H), 4.40-4.41 (d, 1H, 3´-H ), 6.26-3.29 (t, 1H, 1´-H ), 6.77-6.80 (m, 4H, H-Ar of DMTr), 7.21-7.43 (m, 9H, H-Ar of DMTr).

### 3.5.6 *Synthesis of 5´-O-(4,4´-dimethoxytrityl)-5-[N-[2-[N-(anthraquinon-1-yl)amino]-ethyl]carbamoyl-methyl]-2´-deoxyuridine (20)*

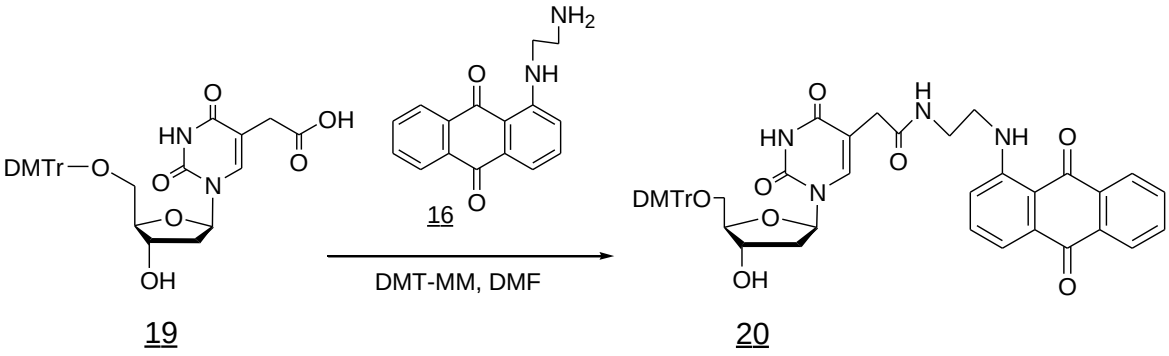


Compound **16** (0.376 g, 1.41 mmol) and compound **19** (0.830 g, 1.41 mmol) were condensed in dimethyl formamide with condensation reagent DMT-MM (1.28 g, 4.65 mmol). The reaction mixture was then stirred at room temperature for 3 hours. The reaction output was monitored by TLC using a solvent system of 10 % MeOH in $CH_2Cl_2$ +1 % TEA. After stopping reaction, the mixture was poured dropwise in a saturated solution of NaCl. The mixture was then filtered and washed several times with water during the filtration process. The solid residue was vacuum dried and the dried outcome was dissolved into $CH_2Cl_2$ and evaporated under reduced pressure. Subsequently isolated the desired compound **20** by silica-gel column chromatography (10 % MeOH in $CH_2Cl_2$ + 1 % TEA). The yield of compound **20** was 84 % (0.995 g). $^1$H NMR (400 MHz, $CDCl_3$) δ (ppm) = 1.01-1.05 (m, 2H, -$CH_2$-NH-), 2.54-2.57 (m, 2H, -NH-$CH_2$), 3.75 (s, 6H, $OCH_3$ of DMTr), 3.96-3.97 (d, 1H, 4´-H ), 4.51-4.53 (t, 1H, 3´-H), 6.20-6.23 (t, 1H, 1´-H ), 6.82-6.84 (m, 4H, H-Ar of DMTr), 7.24-7.29 (m, 2H, H-Ar of Aq), 7.36-7.38 (m, 9H, H-Ar of DMTr), 7.52-7.67 (m, 3H, H-Ar of Aq), 8.15-8.19 (m, 1H, H-Ar of Aq), 9.71 (s, 1H, base NH).

### 3.5.7 *Synthesis of 5´-O-(4,4´-dimethoxytrityl)-5-[N-[2-[N-(anthraquinon-1-yl)amino]-ethyl]carbamoyl-methyl]-2´-deoxyuridine-3´-O-yl(2-cyanoethyl)-N,N-diisopropyl-phosphoramidite (21).*

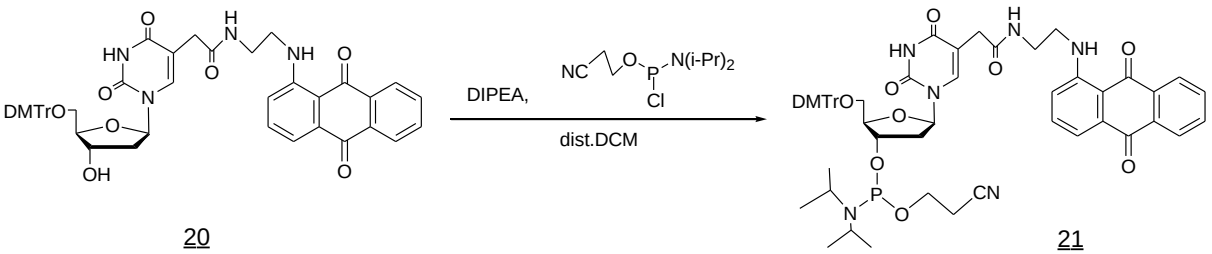


20 21

To the solution of **20** (0.493 g, 0.589 mmol) in dry $CH_2Cl_2$ (20 ml), DIPEA (0.513 ml, 2.9 mmol) and 2-cyanoethyl-*N*,*N*-diisopropylchlorophosphoramidite (0.387 ml, 1.76 mmol) were added drop wise under cooling with ice then stirred at room temperature for 45 minutes. The reaction end point was determined by TLC using a solvent system of 100 % ethyl acetate with 2 % TEA. The excess phosphoramidite reagent was decomposed by the addition of MeOH (5 ml). To the mixture, $CH_2Cl_2$ was added and the solution was washed with saturated solution of $NaHCO_3$. The organic layer was collected, dried over $Na_2SO_4$, and evaporated under reduced pressure. The residue was chromatographed on a column of silica gel with 100 % ethyl acetate with 2 % TEA. The compound was once again purified by treating the output into a cold solution of 20 % diethyl ether in hexane to get a more pure compound. The yield of isolated compound **21** was 80% (0.491 g). $^1$H NMR (400 MHz, $CDCl_3$) δ (ppm) = 1.03-1.24 (m, 12H, iPr), 2.30-2.69(m,6H, -$CH_2$-CO, -$CH_2$-CN, $CH_2$-NH-), 3.75 (s, 6H, $OCH_3$ of DMTr), 4.12-4.13 (d, 1H, 4´-H), 4.61-4.64 (m, 1H, 3´-H), 6.26-6.29 (t, 1H, 1´-H), 6.69 (m, 4H, H-Ar of DMTr), 6.84 (m, 2H, H-Ar of Aq), 7.28 (m, 9H, H-Ar

of DMTr), 7.70-7.73 (m, 3H, H-Ar of Aq) 8.14-8.18 (m, 1H, H-Ar of Aq), 9.69 (s, 1H, base NH). $^{31}$P NMR (400 MHz, $CDCl_3$) δ (ppm) = 149.32-149.48.

### 3.5.8 *Oligonucleotides Synthesis.*

The oligonucleotides containing C-5 modified 2´-deoxyuridine and a dimethylsilylated pyrene at the 5´-terminus were synthesized on an automated DNA synthesizer (Applied Biosystems ABI-392) using standard protocol. The C-5 polyamine and/or anthraquinone bearing modified 2´-deoxyuridine analogs were incorporated into the oligomers in a manner similar to that reported previously [39-41]. The phosphoramidite derivative of dimethylsilylated pyrene was incorporated at 5´-termini of the oligomers using higher concentration of the amidite, as described previously [31]. After the assembly, the support bound modified oligoDNA was treated with concentrated ammonium hydroxide at 55 $^0$C for 12 hours. Thereafter the oligomer was purified by reversed-phase HPLC, ethanol precipitation and Sephadex G-25 gel filtration.

### 3.5.9 *Melting Temperature Analysis.*

A solution of either 3 µM oligonucleotide or its complex of 3 µM of each strand in a buffer of 10 mM sodium phosphate containing 100 mM NaCl was heated 90 ˚C for 3 minutes, cooled gradually to room temperature, and then used for the melting temperature study. UV absorbance was measured at 260 nm on a Shimadzu UV-2450 Spectrophotometer equipped with a temperature controller. The rate of heating was 0.1 $^o$C/min. $T_m$ values were determined from the first differentials of the absorbance versus temperature plot using Igor graphing and data analysis program (Wave Matrices, Inc.).

### 3.5.10 *Fluorescence Measurements.*

Fluorescence measurements were carried out in F-4500 Fluorescence Spectrophotometer and Fluoromax-4 Spectrofluorometer in a 3 ml cuvette with excitation at 350 nm and detection at 360-500 nm. All measurements were conducted in 10 mM sodium phosphate containing 100 mM sodium chloride with a concentration of 1.0 µM each strand.

## References


1. Wang, K.; Huang, J.; Yang, X.; He, X.; Liu, J. *Analyst,* 2013, **138**, 62.
2. Guo, J.; Ju, J.; Turro, N. J. *Anal. Bioanal. Chem.*, 2012, **402**, 3115.
3. Kobayashi, H.; Ogawa, M.; Alford, R.; Choyke, P. L.; Urano, Y. *Chem. Rev.*, 2010, **110**, 2620.
4. Matsuo, T. *Biochim. Biophys. Acta.*, 1998, **1379**, 178.
5. Marras, S. A. E.; Kramer, F. R.; Tyagi, S. *Genet. Anal.*, 1999, **14**, 151.
6. Bonnet, G.; Tyagi, S.; Libchabar, A.; Kramer, F. R. *Proc. Natl. Acad. Sci., USA* 1999, **96**, 6171.
7. Bratu, D. P.; Cha, B. J.; Mhlanga, M. M.; Kramer, F. R.; Tyagi, S. *Proc. Natl. Acad. Sci., USA* 2003, **100**, 13308.
8. Cui, Z. Q.; Zhang, Z. P.; Zhang, X. E.; Wen, J. K.; Zhou, Y. F.; Xie, W. H. *Nucl. Acids Res.*, 2005, **33**, 3245.
9. El-Hajj, H. H.; Marras, S. A. E.; Tyagi, S.; Shashkina, E.; Kamboj, M.; Kiehn, T. E.; Glickman, M. S.; Kramer, F. R.; Alland, D. *J. Clin. Microbiol*., 2009, **47**, 1190.
10. Chen, A. K.; Behlke, M. A.; Tsourkas, A. *Nucl. Acids Res.*, 2008, **36**, e69.
11. Hwang, G. T.; Seo, Y. J.; Kim, B. H. *J. Am. Chem. Soc.*, 2004, **126**, 6528.
12. Joshi, H. S.; Tor, Y. *Chem. Commun.*, 2001, 549.
13. Marras, S. A. E.; Kramer, F. R.; Tyagi, S. *Nucl. Acids Res.*, 2002, **30**, e122.

14. Dobson, N.; McDowell, D. G.; French, D. J.; Brown, L. J.; Mellor, J. M.; Brown, T. *Chem. Commun.*, 2003, 1234.

15. Ryu, J. H.; Seo, Y. J.; Hwang, G. T.; Lee, J. Y.; Kim, B. H. *Tetrahedron*, 2007, **63,** 3538.

16. Tan, W.; Wang, K.; Drake, T. J. *Curr. Opin. Chem. Biol.*, 2004, **8**, 547.

17. Venkatesan, N.; Seo, Y. J.; Kim, B. H. *Chem. Soc. Rev.*, 2008, **37**, 648.

18. Tyagi, S.; Kramer, F. R. *Nat. Biotechnol.*, 1996, **14**, 303.

19. Du, H.; Disney, M. D.; Miller, B. L.; Krauss, T. D. *J. Am. Chem. Soc.*, 2003, **125**, 4012.

20. Yang, C. J.; Lin, H.; Tan, W. *J. Am. Chem. Soc.*, 2005, **127**, 12772.

21. Stoermer, R. L.; Cederquist, K. B.; McFarland, S. K.; Sha, M. Y.; Penn, S. G.; Keating, C. D. *J. Am. Chem. Soc.*, 2006, **128**, 16892.

22. Cazzato, A.; Capobianco, M. L.; Zambianchi, M.; Favaretto, L.; Bettini, C.; Barbarella, G. *Bioconjug. Chem.*, 2007, **18**, 318.

23. Grossmann, T. N.; Roglin, L.; Seitz, O. *Angew. Chem., Int. Ed*., 2007, **46**, 5223.

24. Conlon, P.; Yang, C. J.; Wu, Y.; Chen, Y.; Martinez, K.; Kim, Y.; Stevens, N.; Marti, A. A.; Jockusch, S.; Turro, N. J.; Tan, W. *J. Am. Chem. Soc.*, 2008, **130**, 336.

25. Yi, J. W.; Park, J.; Singh, N. J.; Lee, I. J.; Kim, K. S.; Kim, B. H. *Bioorg. Med. Chem. Lett.*, 2011, **21**, 704.

26. Saito, Y.; Shinohara, Y.; Bag, S. S.; Takeuchi, Y.; Matsumoto, K.; Saito, I. *Nucleic Acids Symp. Ser.*, 2008, **52**, 361.

27. Østergaard, M. E.; Cheguru, P.; Papasani, M. R.; Hill, R. A.; Hrdlicka, P. J. *J. Am. Chem. Soc.*, 2010, **132**, 14221.

28. Fujimoto, K.; Shimizu, H.; Inouye, M. *J. Org. Chem.*, 2004, **69,** 3271.

29. Seo, Y. J.; Ryu, J. H.; Kim, B. H. *Org. Lett.*, 2005, **7,** 4931.

30. Seo, Y. J.; Hwang, G. T.; Kim, B. H. *Tetrahedron Lett.*, 2006, **47**, 4037.

31. Sekiguchi, T.; Ebara, Y.; Moriguchi, T.; Shinozuka, K. *Bioorg. Med. Chem. Lett.*, 2007, **17**, 6883.

32. Mogi, M.; Uddin, M. G.; Ichimura, M.; Moriguchi, T.; Shinozuka, K. *Chem. Lett.*, 2010, **39**, 1254.
33. Moriguchi, T.; Ichimura, M.; Kato, M.; Suzuki, K.; Takahashi, Y.; Shinozuka, K. *Bioorg. Med. Chem. Lett.*, 2014, **24**, 4372.
34. Moriguchi, T.; Hosaka, M.; Yoshinari, A.; Ozaki, A.; Takeuchi, T.; Shinozuka, K. *Chem. Lett.*, 2009, **38**, 966.
35. Kyusin, S.; Ikarugi, M.; Goto, M.; Hiratsuka, H.; Matsumoto, H. *Organometallics*, 1996, **15**, 1067.
36. Maeda, H.; Inoue, Y.; Ishida, H.; Mizuno, K. *Chem. Lett.*, 2001, 1224.
37. Moriguchi, T.; Hattori, M.; Sekiguchi, T.; Shinozuka, K. *Nucleic Acids Symp. Ser*., 2009, **53**, 31.
38. Chowdhury, J. A., Moriguchi, T.; Shinozuka, K. *Chem. Lett.*, 2014, **43**, 1915.
39. Sawai, H.; Nakamura, A.; Sekiguchi, S.; Yumoto, K.; Endo, M.; Ozaki, H. *J. Chem. Soc., Chem. Commun.*, 1994, 1997.
40. Ozaki, H.; Nakamura, A.; Arai, M.; Endo, M.; Sawai, H. *Bull. Chem. Soc. Jpn*., 1995, **68**, 1981.
41. Sato, Y.; Moriguchi, T.; Shinozuka, K. *Chem. Lett.*, 2012, **41**, 420.
42. Chowdhury, J. A., Moriguchi, T.; Shinozuka, K. *Bull. Chem. Soc. Jpn*., 2015, (Accepted for publication).
43. Matsukura, M.; Okamoto, T.; Miike, T.; Sawai, H.; Shinozuka, K. *Biochem. Biophys. Res. Commun.*, 2002, **293**, 1341.
44. Zafrul Azam, A. T. M.; Hasegawa, M.; Moriguchi, T.; Shinozuka, K. *Bioorg. Med. Chem. Lett.* 2004, **14**, 5747.